

See discussions, stats, and author profiles for this publication at: <https://www.researchgate.net/publication/289236519>

Hydrogeologic setting and groundwater flow simulation of the middle rio grande basin regional study area, New Mexico

Article in USGS professional paper · January 2011

CITATIONS

6

READS

263

5 authors, including:



Laura M Bexfield

United States Geological Survey

43 PUBLICATIONS 1,319 CITATIONS

[SEE PROFILE](#)



E. T. Vogler

16 PUBLICATIONS 227 CITATIONS

[SEE PROFILE](#)

Hydrogeologic Setting and Groundwater Flow Simulation of the Middle Rio Grande Basin Regional Study Area, New Mexico

By Laura M. Bexfield, Charles E. Heywood, Leon J. Kauffman, Gordon W. Rattray, and Eric T. Vogler

Section 2 of

Hydrogeologic Settings and Groundwater-Flow Simulations for Regional Investigations of the Transport of Anthropogenic and Natural Contaminants to Public-Supply Wells—Investigations Begun in 2004

Edited by Sandra M. Eberts

Professional Paper 1737–B

**U.S. Department of the Interior
U.S. Geological Survey**

U.S. Department of the Interior
KEN SALAZAR, Secretary

U.S. Geological Survey
Marcia K. McNutt, Director

U.S. Geological Survey, Reston, Virginia: 2011

For more information on the USGS—the Federal source for science about the Earth, its natural and living resources, natural hazards, and the environment, visit <http://www.usgs.gov> or call 1–888–ASK–USGS.

For an overview of USGS information products, including maps, imagery, and publications, visit <http://www.usgs.gov/pubprod>

To order this and other USGS information products, visit <http://store.usgs.gov>

Any use of trade, product, or firm names is for descriptive purposes only and does not imply endorsement by the U.S. Government.

Although this report is in the public domain, permission must be secured from the individual copyright owners to reproduce any copyrighted materials contained within this report.

Suggested citation:
Bexfield, L.M., Heywood, C.E., Kauffman, L.J., Rattray, G.W., and Vogler, E.T., 2011, Hydrogeologic setting and groundwater-flow simulation of the Middle Rio Grande Basin regional study area, New Mexico, section 2 of Eberts, S.M., ed., Hydrologic settings and groundwater flow simulations for regional investigations of the transport of anthropogenic and natural contaminants to public-supply wells—Investigations begun in 2004: Reston, Va., U.S. Geological Survey Professional Paper 1737–B, pp. 2-1–2-61.

Contents

| | |
|--|------|
| Abstract | 2-1 |
| Introduction..... | 2-1 |
| Purpose and Scope | 2-1 |
| Study Area Description..... | 2-2 |
| Topography and Climate | 2-2 |
| Surface-Water Hydrology | 2-2 |
| Land Use..... | 2-7 |
| Water Use | 2-7 |
| Conceptual Understanding of the Groundwater System | 2-9 |
| Geology..... | 2-9 |
| Groundwater Occurrence and Flow | 2-9 |
| Aquifer Hydraulic Properties | 2-12 |
| Water Budget | 2-17 |
| Groundwater Age..... | 2-18 |
| Groundwater Quality | 2-20 |
| Groundwater-Flow Simulations..... | 2-26 |
| Modeled Area and Spatial Discretization..... | 2-26 |
| Simulation-Code Modifications | 2-30 |
| Boundary Conditions and Model Stresses..... | 2-30 |
| Specified-Flow Boundaries..... | 2-30 |
| Subsurface, Mountain-Front, and Tributary Recharge..... | 2-30 |
| Seepage | 2-30 |
| Domestic Groundwater Withdrawals..... | 2-32 |
| Head-Dependent-Flow Boundaries | 2-32 |
| Reported Groundwater Withdrawals | 2-32 |
| Rivers | 2-32 |
| Drains | 2-33 |
| Lakes and Reservoirs | 2-33 |
| Riparian Evapotranspiration | 2-34 |
| Aquifer Hydraulic Properties | 2-34 |
| Model Evaluation | 2-43 |
| Simulated Hydraulic Heads..... | 2-43 |
| Model-Computed Water Budgets | 2-52 |
| Areas Contributing Recharge to Public-Supply Wells..... | 2-52 |
| Limitations and Appropriate Use of the Model..... | 2-54 |
| References Cited..... | 2-57 |

Figures

| | | |
|------------|---|------|
| 2.1. | Map showing location of the Middle Rio Grande regional study area relative to the Rio Grande aquifer system and the Basin and Range basin-fill aquifers | 2-2 |
| 2.2. | Map showing major cultural, geographic, and hydrologic features of the Middle Rio Grande Basin and the locations of public-supply wells in the Middle Rio Grande Basin regional study area, New Mexico..... | 2-4 |
| 2.3. | Map showing major structural features in the Middle Rio Grande Basin, New Mexico | 2-10 |
| 2.4. | Geologic section through Albuquerque, New Mexico..... | 2-11 |
| 2.5. | Map showing groundwater levels that represent predevelopment conditions, Middle Rio Grande Basin, New Mexico | 2-13 |
| 2.6. | Conceptual diagram of regional groundwater flow and budget components near Albuquerque, New Mexico under <i>A</i> , predevelopment and <i>B</i> , modern conditions. | 2-14 |
| 2.7. | Map showing water levels representing 1999–2002 conditions in the production zone in the Albuquerque area, New Mexico, and estimated water-level declines, 1960–2002 | 2-15 |
| 2.8. | Graph showing water levels in piezometers in the Garfield Park piezometer nest located in the Rio Grande inner valley, Albuquerque, New Mexico | 2-16 |
| 2.9. | Map showing estimated ages of groundwater in the Santa Fe Group aquifer system, Middle Rio Grande Basin, New Mexico..... | 2-19 |
| 2.10. | Map showing hydrochemical zones in the Middle Rio Grande Basin, New Mexico | 2-21 |
| 2.11A. | Map showing oxidation-reduction conditions for the upper 90 meters of the aquifer, Middle Rio Grande Basin regional study area, New Mexico. | 2-24 |
| 2.11B. | Map showing oxidation-reduction conditions for the deeper parts of the aquifer, Middle Rio Grande Basin regional study area, New Mexico | 2-25 |
| 2.12A. | Map showing revised groundwater-flow model showing groundwater-flow model domain and selected boundary conditions, Middle Rio Grande Basin, New Mexico | 2-27 |
| 2.12B. | Map showing revised groundwater-flow model showing water-distribution and sewer system, Middle Rio Grande Basin, New Mexico..... | 2-28 |
| 2.13. | Cross section showing configuration of layers in the revised groundwater-flow model, Middle Rio Grande Basin, New Mexico..... | 2-29 |
| 2.14A1–A2. | Map showing distribution of simulated horizontal hydraulic conductivity in the east-west direction for model layers 1–9, Middle Rio Grande Basin, New Mexico | 2-36 |
| 2.14A3–A4. | Map showing distribution of simulated horizontal hydraulic conductivity in the east-west direction for model layers 1–9, Middle Rio Grande Basin, New Mexico | 2-37 |
| 2.14A5–A6. | Map showing distribution of simulated horizontal hydraulic conductivity in the east-west direction for model layers 1–9, Middle Rio Grande Basin, New Mexico | 2-38 |
| 2.14A7–A8. | Map showing distribution of simulated horizontal hydraulic conductivity in the east-west direction for model layers 1–9, Middle Rio Grande Basin, New Mexico | 2-39 |

| | | |
|----------|---|------|
| 2.14A9. | Map showing distribution of simulated horizontal hydraulic conductivity in the east-west direction for model layers 1–9, Middle Rio Grande Basin, New Mexico | 2-40 |
| 2.14B. | Map showing simulated horizontal anisotropy for layers 1–2 and 3–8, Middle Rio Grande Basin, New Mexico | 2-41 |
| 2.14C. | Map showing simulated vertical anisotropy for layers 1–2 of the revised groundwater-flow model, Middle Rio Grande Basin, New Mexico | 2-42 |
| 2.15A. | Map showing simulated steady-state water table and hydraulic-head residual at each steady-state observation well, Middle Rio Grande Basin, New Mexico | 2-44 |
| 2.15B. | Map showing simulated March 2008 water table and maximum hydraulic-head residual for the period 1900–2008 at each transient observation well for the revised groundwater-flow model, Middle Rio Grande Basin, New Mexico..... | 2-45 |
| 2.16A–D. | Graphs showing measured and simulated hydraulic heads for selected wells in the revised groundwater-flow model, Middle Rio Grande Basin, New Mexico. Well locations are shown in figure 2.15B. A, San Felipe, model layers 3 and 4; B, Santa Ana 2, model layers 3 and 4; C, Tierra Mirage, model layers 4 and 5; D, Sandia ECW 2, model layer 2 | 2-46 |
| 2.16E–H. | Graphs showing measured and simulated hydraulic heads for selected wells in the revised groundwater-flow model, Middle Rio Grande Basin, New Mexico. Well locations are shown in figure 2.15B. E, Sandia ECW 1, model layer 2; F, West Mesa 2, model layer 5; G, Coronado 1, model layers 4 and 5; H, Volcano Cliffs 1, model layers 4 and 5 | 2-47 |
| 2.16I–L. | Graphs showing measured and simulated hydraulic heads for selected wells in the revised groundwater-flow model, Middle Rio Grande Basin, New Mexico. Well locations are shown in figure 2.15B. I, City Observation 3, model layers 3 and 4; J, City Observation 2, model layer 3; K, City Observation 1, model layer 3; L, Thomas 2, model layers 4 and 5 | 2-48 |
| 2.16M–P. | Graphs showing measured and simulated hydraulic heads for selected wells in the revised groundwater-flow model, Middle Rio Grande Basin, New Mexico. Well locations are shown in figure 2.15B. M, West Mesa 1A, model layers 3 and 4; N, Lomas 1, model layers 4 and 5; O, Sandia 2, model layers 4 and 5; P, Isleta ECW 3, model layers 2 and 3 | 2-49 |
| 2.16Q–T. | Graphs showing measured and simulated hydraulic heads for selected wells in the revised groundwater-flow model, Middle Rio Grande Basin, New Mexico. Well locations are shown in figure 2.15B. Q, Grasslands, model layer 3; R, Belen Airport, model layers 3 and 4; S, McLaughlin, model layers 2 and 3; T, Sevilleta, model layers 2 and 3..... | 2-50 |
| 2.17 | Graphs showing comparison of residuals and measured hydraulic heads, steady-state and transient simulations of the revised groundwater-flow model, Middle Rio Grande Basin, New Mexico | 2-51 |
| 2.18 | Graphs showing hydraulic-head residuals from the steady-state and transient stress periods of the revised groundwater-flow model, Middle Rio Grande Basin, New Mexico..... | 2-51 |
| 2.19. | Graphs showing median simulated distributions of traveltimes of groundwater to 59 public-supply wells under transient conditions with the revised groundwater-flow model, Middle Rio Grande Basin, New Mexico | 2-53 |

| | | |
|-------|--|------|
| 2.20. | Graphs showing distributions of measured and simulated <i>A</i> , trichlorotrifluoroethane (CFC-113) concentrations and <i>B</i> , carbon-14 values in public-supply wells simulated under transient conditions with the revised groundwater-flow model, Middle Rio Grande Basin, New Mexico..... | 2-55 |
| 2.21. | Maps showing areas contributing recharge and zones of contribution to 59 public-supply wells for effective porosities of <i>A</i> , 0.02, <i>B</i> , 0.08, <i>C</i> , 0.2, and <i>D</i> , 0.35 in the revised groundwater-flow model, regional study area, Middle Rio Grande Basin, New Mexico | 2-56 |

Tables

| | | |
|------|---|------|
| 2.1. | Summary of hydrogeologic and groundwater-quality characteristics for the Basin and Range basin-fill aquifers and the Middle Rio Grande Basin regional study area, New Mexico | 2-5 |
| 2.2. | Year-2000 water-use estimates for selected counties of the Middle Rio Grande Basin, New Mexico | 2-8 |
| 2.3. | Model-computed net annual groundwater budgets for steady-state conditions and year ending October 31, 1999, from the McAda and Barroll (2002) groundwater-flow model, Middle Rio Grande Basin, New Mexico | 2-17 |
| 2.4. | Median values of selected water-quality parameters by hydrochemical zone, Middle Rio Grande Basin, New Mexico | 2-22 |
| 2.4. | Median values of selected water-quality parameters by hydrochemical zone, Middle Rio Grande Basin, New Mexico | 2-23 |
| 2.5. | Model-computed net annual groundwater budgets for steady-state conditions and year ending October 31, 1999, for the revised groundwater-flow model , Middle Rio Grande Basin, New Mexico | 2-31 |
| 2.6. | Parameter values and sensitivities in the revised groundwater-flow model of the Middle Rio Grande Basin near Albuquerque, New Mexico..... | 2-35 |

Hydrogeologic Setting and Groundwater Flow Simulation of the Middle Rio Grande Basin Regional Study Area, New Mexico

By Laura M. Bexfield, Charles E. Heywood, Leon J. Kauffman, Gordon W. Rattray, and Eric T. Vogler

Abstract

The transport of anthropogenic and natural contaminants to public-supply wells was evaluated in the northern part of the Middle Rio Grande Basin near Albuquerque, New Mexico, as part of the U.S. Geological Survey National Water-Quality Assessment Program. The Santa Fe Group aquifer system in the Middle Rio Grande Basin regional study area is representative of the Basin and Range basin-fill aquifers of the southwestern United States, is used extensively for public water supply, and is susceptible and vulnerable to contamination in places. Conditions within the Santa Fe Group aquifer system, which reaches a thickness of about 4,500 meters in parts of the study area, are unconfined to semiconfined. Withdrawals from public-supply wells completed in about the upper 300 meters of the aquifer system have altered the natural groundwater-flow patterns. A nine-layer, steady-state and transient groundwater-flow model of the Santa Fe Group aquifer system near Albuquerque, New Mexico, was developed by revising an existing model, and it simulates groundwater conditions through the end of 2008. The revised groundwater-flow model and advective particle-tracking simulations were used to compute areas contributing recharge and traveltimes from recharge areas for 59 public-supply wells. Model results for a full year ending October 31, 1999, indicate that recharge from river, lake, reservoir, canal, and irrigation losses provided 75 percent of the total net inflow; 48, 33 and 19 percent of the total net groundwater outflow was to drains, groundwater withdrawals, or riparian evapotranspiration, respectively. Depending on well location, particle-tracking results indicate areas contributing recharge to public-supply wells extend toward the basin margins, which are areas of mountain-front recharge and subsurface inflow, the Rio Grande, and (or) the Jemez River. Traveltimes estimated with particle tracking ranged from less than 10 years to more than 10,000 years.

Introduction

The Middle Rio Grande Basin (MRGB) regional study area for the transport of anthropogenic and natural contaminants to public-supply wells (TANC) is in the Rio Grande valley near Albuquerque, New Mexico, and is part of the Rio Grande Valley study unit of the U.S. Geological Survey National Water-Quality Assessment (NAWQA) program (fig. 2.1). The study area is in the most populous alluvial basin in the Rio Grande Valley study unit, which extends from the Rio Grande headwaters in southern Colorado to El Paso, Texas, and includes much of the Rio Grande aquifer system (fig. 2.1). The MRGB regional study area, delineated to focus data-collection efforts and investigation of the transport of anthropogenic and natural contaminants to public-supply wells in the most populous part of the MRGB, covers about the northern half of the basin, which is where most of the population resides. However, the model used by the TANC study to simulate groundwater flow within the MRGB regional study area is a revised and updated version of an existing model covering essentially the entire MRGB. The aquifer of the MRGB is one of a network of basin-fill aquifers within the Rio Grande aquifer system, and is composed of Tertiary and Quaternary deposits that together are commonly known in the MRGB as the Santa Fe Group aquifer system.

Purpose and Scope

The purpose of this Professional Paper section is to present the hydrogeologic setting of the MRGB regional study area and to document revisions and updates to an existing transient groundwater-flow model for the entire MRGB. Groundwater-flow characteristics, groundwater-withdrawal information, and water-quality data were compiled from existing data to improve the conceptual understanding of

2-2 Hydrogeologic Settings and Groundwater-Flow Simulations for Regional TANC Studies Begun in 2004



EXPLANATION

- Middle Rio Grande Basin regional study area
- Rio Grande aquifer system
- Basin and Range basin-fill aquifers
- NAWQA study unit—Rio Grande Valley
- Middle Rio Grande Basin

Figure 2.1. Location of the Middle Rio Grande regional study area relative to the Rio Grande aquifer system and the Basin and Range basin-fill aquifers.

groundwater conditions in the MRGB regional study area. A nine-layer transient groundwater-flow model by McAda and Barroll (2002) of the Santa Fe Group aquifer system in the MRGB was revised and updated to simulate groundwater-flow conditions through the end of 2008. The revised groundwater-flow model and associated particle tracking were used to simulate advective groundwater-flow paths and to delineate areas contributing recharge and zones of contribution to selected public-supply wells. Groundwater traveltimes from recharge to public-supply wells, oxidation-reduction (redox) conditions along flow paths, and the presence of potential contaminant sources in areas contributing recharge were tabulated into a relational database described in Appendix 1 of Chapter A of this Professional Paper. This section, Section 2 of Chapter B, provides the foundation for future groundwater susceptibility and vulnerability analyses of the study area and comparisons among regional aquifer systems.

Study Area Description

The MRGB regional study area is located in central New Mexico near the City of Albuquerque and encompasses 4,486 square kilometers (km^2) in the northern part of the 7,922- km^2 MRGB (figs. 2.1 and 2.2). The Albuquerque metropolitan area is the most populous area in New Mexico, and it grew by more than 20 percent between 1990 and 2000, from about 589,000 to 713,000 people (U.S. Census Bureau, 2001a). Historically, groundwater has been essentially the sole source of public water supply in the metropolitan area. The groundwater-flow system in the study area is representative not only of other alluvial basins along the Rio Grande, but also of alluvial basins in the Basin and Range basin-fill aquifers of the southwestern United States (fig. 2.1; table 2.1). Both geologic sources of natural contaminants and a long history of agricultural and urban land uses in areas of intrinsic susceptibility contribute to groundwater vulnerability in the study area.

Topography and Climate

The MRGB is located primarily in the Basin and Range physiographic province (Fenneman, 1931) and is defined by the extent of Cenozoic deposits (fig. 2.2; table 2.1). The MRGB regional study area is bounded by the Jemez Mountains and the Nacimiento Uplift to the north and northwest, by the Sandia and Manzanita Mountains to the east, and by the Rio Puerco fault zone and San Juan structural basin to the west (fig. 2.2). The southern boundary was assigned to correspond with the southernmost extent of Bernalillo County, thereby defining the study area to include the two most populous counties within the basin, Bernalillo and Sandoval Counties, and the recharge areas for the groundwater used in those counties. Land-surface elevation within the study area ranges from about 1,485 meters (m) at the Rio Grande along the southern

edge of the study area to more than 2,000 m along the foothills of the Sandia and Jemez Mountains. The Rio Grande and Rio Puerco are located in terraced valleys.

Most of the MRGB regional study area is categorized as having a semiarid climate, characterized by abundant sunshine, low humidity, and a high rate of evaporation that substantially exceeds the low rate of precipitation. Precipitation shows relatively large spatial variation because of the range in land-surface elevation across the area. Mean annual precipitation for 1914–2005 at Albuquerque was 21.7 centimeters per year (cm/yr) (Western Regional Climate Center, 2006a), whereas mean annual precipitation for 1953–1979 at the crest of the Sandia Mountains that border the basin to the east was 57.4 cm/yr (Western Regional Climate Center, 2006b). Most precipitation at lower elevations falls between July and October as a result of localized, high-intensity thunderstorms of short duration; winter storms of lower intensity and longer duration make a greater contribution to annual precipitation at higher elevations.

Surface-Water Hydrology

The Rio Grande is a perennial stream and is the primary surface-water feature of the MRGB regional study area, with a mean annual discharge at Albuquerque of about 37 cubic meters per second (m^3/s) for 1974–2009 (U.S. Geological Survey, Water Resources, 2010). Although the Rio Grande primarily loses water to the aquifer system as it flows through the study area from north to south, some river sections in the northern part of the study area gain water (McAda and Barroll, 2002; Plummer and others, 2004a). A system of levees and jetty jacks directs the course of the Rio Grande through the study area, and an upstream series of dams, including the dam for Cochiti Lake at the northern end of the MRGB, affects the seasonal discharge patterns of the river. From May to October, substantial quantities of water are diverted north of Albuquerque from the Rio Grande into an extensive network of irrigation canals crisscrossing the historic flood plain, also known as the Rio Grande inner valley (fig. 2.2). Riverside and interior drains maintain the water table in the inner valley at a sufficient depth below land surface to allow sustained irrigated agriculture without damaging crops.

Tributaries that contribute water to the Rio Grande within the regional study area include the Jemez River, which drains areas west of the Rio Grande and is perennial through most of the study area, and several streams and arroyos that contribute ephemeral flow to the Rio Grande only during large storm events. Many of these streams and arroyos enter the MRGB along the eastern margin, where flow may be perennial or intermittent (McAda and Barroll, 2002). The groundwater-drain system and flood-diversion channels also contribute flow to the Rio Grande.

2-4 Hydrogeologic Settings and Groundwater-Flow Simulations for Regional TANC Studies Begun in 2004

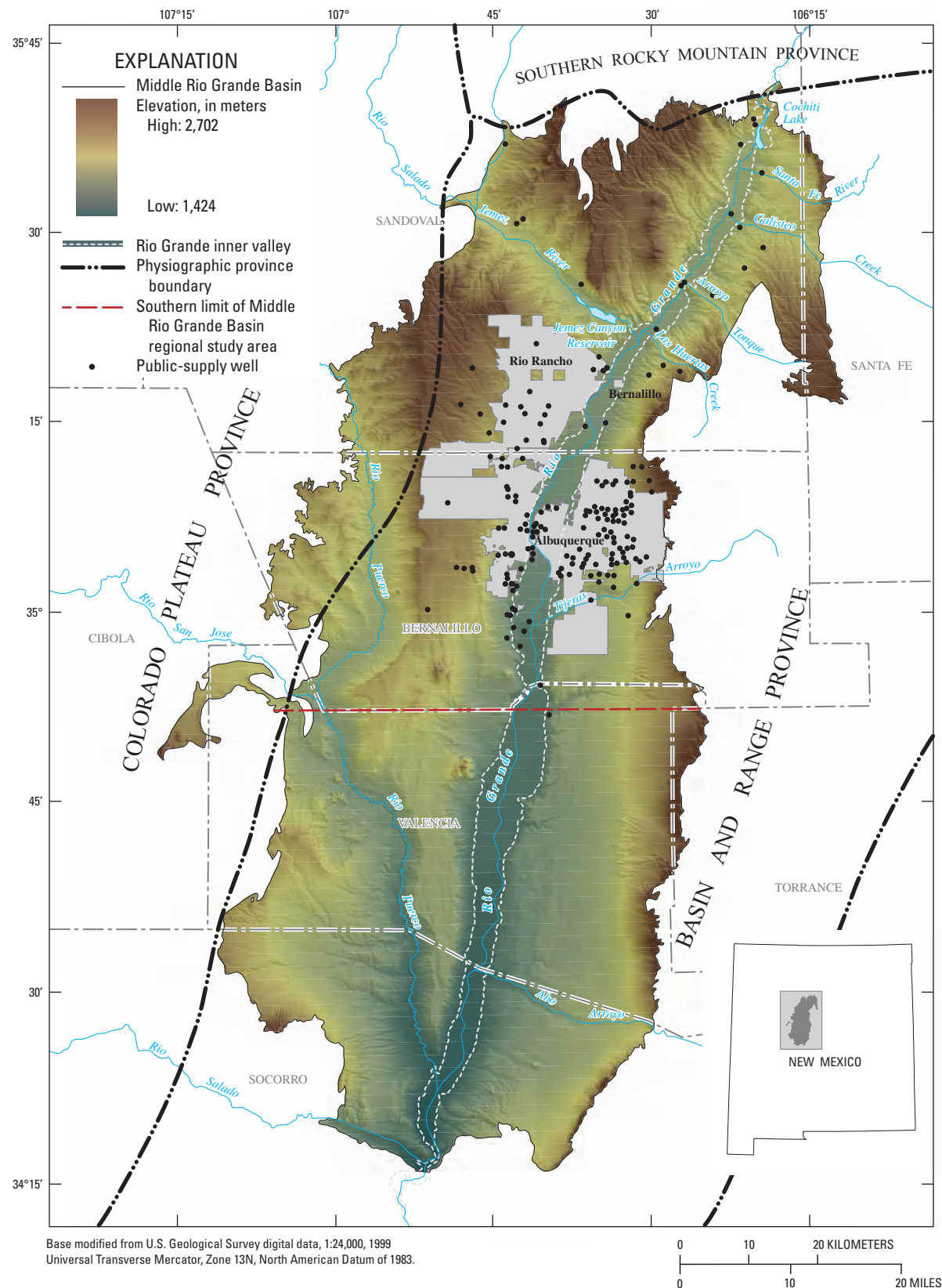


Figure 2.2. Major cultural, geographic, and hydrologic features of the Middle Rio Grande Basin and the locations of public-supply wells in the Middle Rio Grande Basin regional study area, New Mexico.

Table 2.1 Summary of hydrogeologic and groundwater-quality characteristics for the Basin and Range basin-fill aquifers and the Middle Rio Grande Basin regional study area, New Mexico.

[NAWQA, National Water-Quality Analysis; ft, feet; m, meters; in/yr, inches per year; cm/yr, centimeters per year; °C, temperature in degrees Celsius; °F, temperature in degrees Fahrenheit; m³/yr, cubic meters per year; acre-ft/year, acre-feet per year; ft/day, feet per day; ft²/day, square feet per day; m/d, meters per day; m²/day, square meters per day; µS/cm, microsiemens per centimeter at 25 °C; mg/L, milligrams per liter]

| Characteristic | NAWQA Principal Aquifer: Basin and Range | Middle Rio Grande Basin regional study area, New Mexico |
|-------------------------|---|--|
| Geography | | |
| Topography | Altitude ranges from about 46m (150 ft) at Yuma, Arizona to over 3,048 m (10,000 ft) at the crest of some mountain ranges (Robson and Banta, 1995). | Altitude of the Rio Grande ranges from about 1,485 m (4,870 ft) at the south end of the study area to about 1,650 m (5,400 ft) at the north end. Land-surface altitude exceeds 2,000 m (6,560 ft) along foothills of the Jemez and Sandia Mountains. |
| Climate | Arid to semiarid climate. Precipitation ranges from 10 to 20 cm/yr (4 to 8 in/yr) in basins and 40 to 76 cm/yr (16 to 30 in/yr) in mountains (Robson and Banta, 1995). | Semiarid climate. Annual precipitation is about 22 cm (8.7 in) in the valley (Western Regional Climate Center, 2006a) and approaches 60 cm (24 in) in the Sandia Mountains (Western Regional Climate Center, 2006b). Mean monthly temperatures in the valley range from about 1.8°C (35°F) in January to about 25.6°C (78°F) in July (Western Regional Climate Center, 2006a). |
| Surface-water hydrology | Streams drain from surrounding mountains into basins. Basins generally slope toward a central depression with a main drainage that is dry most of the time. Many basins have playas in their lowest depressions. Groundwater discharge to streams can occur in basin depressions. (Planert and Williams, 1995) | The Rio Grande is the major stream and alternately gains and loses flow. Water from the Rio Grande is diverted into canals to supply irrigated agriculture in the flood plain. The Jemez River is a major tributary. Arroyos originating in the eastern mountains convey substantial quantities of water to the Rio Grande during storm events. |
| Land use | Undeveloped basins are unused, grazing, and rural residential. Developed basins are urban, suburban and agricultural. | Urban, suburban, rural residential, agricultural, and grazing. |
| Water use | Groundwater withdrawals from wells supply water for agricultural irrigation and municipal use. Population increases since the 1960's have increased the percentage of water being used for municipal supply. | Groundwater was essentially the sole source of public supply through 2008. Ground-water withdrawals during 2000 were about 194 million m ³ /yr (157,000 acre-ft/yr) (Wilson and others, 2003). In 2000, surface-water withdrawals for agriculture nearly equaled groundwater withdrawals for public supply. |
| Geology | | |
| Surficial geology | Tertiary and Quaternary unconsolidated to moderately consolidated fluvial gravel, sand, silt and clay basin-fill deposits include alluvial fans, flood plain deposits, and playas. (Robson and Banta, 1995; Planert and Williams, 1995) | Tertiary and Quaternary unconsolidated to moderately consolidated basin-fill sediments up to about 4,500 m (15,000 ft) in thickness. Sediments include fluvial, piedmont-slope, eolian, and playa deposits. Volcanic flows and ash beds also are present. |
| Bedrock geology | Mountains surrounding basins are composed of Paleozoic to Tertiary bedrock formations. Tertiary volcanic and metamorphic rocks are in general impermeable. Paleozoic and Mesozoic carbonate rocks are cavernous allowing inter-basin flow in some areas. (Robson and Banta, 1995; Planert and Williams, 1995) | Most surrounding mountain ranges are composed of Precambrian plutonic and metamorphic rocks overlain by Paleozoic limestone, sandstone, and shale. Cenozoic volcanic rocks make up the Jemez Mountains. |

2-6 Hydrogeologic Settings and Groundwater-Flow Simulations for Regional TANC Studies Begun in 2004

Table 2.1 Summary of hydrogeologic and groundwater-quality characteristics for the Basin and Range basin-fill aquifers and the Middle Rio Grande Basin regional study area, New Mexico.—Continued

[NAWQA, National Water-Quality Analysis; ft, feet; m, meters; in/yr, inches per year; cm/yr, centimeters per year; °C, temperature in degrees Celsius; °F, temperature in degrees Fahrenheit; m³/yr, cubic meters per year; acre-ft/year, acre-feet per year; ft/day, feet per day; ft²/day, square feet per day; m/d, meters per day; m³/day, square meters per day; µS/cm, microsiemens per centimeter at 25 °C; mg/L, milligrams per liter]

| Characteristic | NAWQA Principal Aquifer: Basin and Range | Middle Rio Grande Basin regional study area, New Mexico |
|------------------------------|---|--|
| Groundwater hydrology | | |
| Aquifer conditions | Unconfined basin-fill aquifers surrounded by relatively impermeable bedrock mountains and foothills. Basin groundwater-flow systems are generally isolated and not connected with other basins except in some locations where basins are hydraulically connected via cavernous carbonate bedrock. | Unconfined basin-fill aquifer surrounded by relatively impermeable uplifts. Conditions are semiconfined at depth. Groundwater flow through the central part of the basin is primarily north to south. Along basin margins, flow is directed generally toward the central part of the basin. |
| Hydraulic properties | Transmissivity ranges from less than 93 m ² /day (1,000 ft ² /day) to greater than 2,790 m ² /day (30,000 ft ² /day). In general, alluvial fan deposits near basin margins are more conductive than flood plain and lacustrine deposits near basin centers. (Robson and Banta, 1995; Planert and Williams, 1995) | Transmissivity estimates range from less than 65 m ² /day (700 ft ² /day) to about 7,430 m ² /day (80,000 ft ² /day) (Thorn and others, 1993). Horizontal hydraulic conductivity ranges from about 2×10^{-2} to 1×10^2 m/day (5×10^{-2} to 3×10^2 ft/day), whereas vertical hydraulic conductivity ranges from about 9×10^{-5} to 1×10^1 m/day (3×10^{-4} to 4×10^1 ft/day) (CH2MHill, 1999; McAda and Barroll, 2002; this report). |
| Groundwater budget | Recharge to basin fill deposits is from surface-water runoff in mountains where precipitation is highest. Ground-water discharges naturally as evapotranspiration to playas and stream channels in basin depressions. Groundwater withdrawal from wells is largest component of discharge from Basin and Range aquifers. (Robson and Banta, 1995) | Recharge is primarily from mountain-front processes; seepage from the Rio Grande, tributary streams and arroyos, irrigation canals, and crop irrigation; and subsurface inflow from adjacent basins. Discharge is mostly to groundwater withdrawal, groundwater evapotranspiration, drains, and streams (the Rio Grande). |
| Groundwater residence times | No regional information. | Modern to more than 30,000 years. |
| Groundwater quality | | |
| | Water quality varies between basins. Total dissolved solids can range from less than 500 mg/L to over 35,000 mg/L. Generally, water that has low concentrations of total dissolved solids and is oxic occurs near recharge areas of basin margins. Water with high concentrations of total dissolved solids and that is anoxic can occur with depth or near basin centers and playa lakes. (Robson and Banta, 1995; Planert and Williams, 1995) | Total dissolved solids are lowest (specific conductance less than 400 µS/cm) in water recharged along the northern and eastern mountain fronts and the Rio Grande. Calcium-bicarbonate or calcium-sodium-bicarbonate type water dominates in these areas, where pH is typically 7 to 8. Groundwater inflow from the Jemez Mountain region is sodium-bicarbonate type water and generally has pH greater than 8. Total dissolved solids are highest (specific conductance exceeding 1,000 µS/cm) where groundwater inflow or arroyo infiltration dominate recharge. Groundwater is oxic, except at shallow depths, within the Rio Grande flood plain. |

Land Use

Prior to substantial urbanization of the MRGB regional study area, land outside the Rio Grande inner valley was almost exclusively rangeland. For 83 percent of the regional study area, rangeland has remained the dominant land-use type according to the National Land Cover Database (NLCD) dataset for 2001 (<http://www.mrlc.gov/>; Homer and others, 2004). In the northern part of the study area, much of this land is within American Indian reservations.

Within the inner valley—an area that is intrinsically susceptible to groundwater contamination because of depths to groundwater generally less than about 7.6 m (Anderholm, 1997)—agriculture was practiced as early as the 1700s, and grew rapidly during the mid- to late-1800s (Bartolino and Cole, 2002). Mapping of 1935 Albuquerque urban areas indicates that the city was first urbanized primarily within the inner valley (Bartolino and Cole, 2002), where industry was developed by the 1950s (U.S. Environmental Protection Agency, 2005). Population growth in the Albuquerque area since about 1940 has led to extensive urbanization of upland areas, in addition to urbanization of irrigated agricultural land in the inner valley (Bartolino and Cole, 2002). Irrigated agriculture makes up only about 3.5 percent of land in the regional study area, as shown by the 2001 NLCD dataset, probably because of urbanization and the narrow width of the inner valley. In Bernalillo County in 1992, alfalfa was the most abundant crop type based on planted acreage (Kinkel, 1995, appendix 4), and urban turf grass was the second most abundant (Bartolino and Cole, 2002). The 2001 NLCD dataset classified about 11 percent of land in the regional study area as urban. In 2000, population density within the City of Albuquerque was about 960 persons per km², compared with less than 6 persons per km² for New Mexico as a whole (U.S. Census Bureau, 2006).

Water Use

Despite urbanization, irrigated agriculture remains a large water user within the MRGB regional study area. Estimates of water use in Bernalillo and Sandoval Counties (table 2.2)

by Wilson and others (2003) indicate that 43.8 percent of the total surface-water and groundwater withdrawals of nearly 360,000 thousand m³ in these two counties in 2000 was for irrigated agriculture. However, only 28.7 percent of the total water depletion, which is defined as the part of withdrawal that is lost to the local water resource for future use because of consumption, evapotranspiration, or other processes, of nearly 160,000 thousand m³ was associated with irrigated agriculture. Almost 97 percent of the water used for irrigated agriculture was surface water, primarily diverted from the Rio Grande and delivered to areas within the inner valley. Bernalillo and Sandoval Counties extend outside the regional study area, but combined estimates of water use for these counties are expected to approximate use within the study area, where most of the population and irrigated agriculture are located.

Water use for public supply in Bernalillo and Sandoval Counties in 2000 accounted for 44.9 percent of total water withdrawals (table 2.2)—just slightly more than the use for irrigated agriculture—and about 48.9 percent of total water depletion. Essentially all the water used for public supply was groundwater (table 2.2), withdrawn primarily from the Santa Fe Group aquifer system. Most (87.6 percent) of groundwater used for public supply in 2000 was withdrawn by the City of Albuquerque (now the Albuquerque Bernalillo County Water Authority), which began diverting surface water from the Rio Grande in 2008 with the intent eventually to meet most demand; this change in water-supply strategy is largely the result of concerns about declining water levels in the aquifer (City of Albuquerque, 2003). Files of the City of Albuquerque and the Albuquerque Bernalillo County Water Authority indicate the 4 months of June through September have historically accounted for about 46 percent of annual groundwater withdrawals, and the Albuquerque Bernalillo County Water Authority plans to continue withdrawing groundwater to supplement supplies during this summer peak-demand period and during drought. Wilson and others (2003) estimated groundwater withdrawn by private domestic wells to be only about 5.3 percent of groundwater use in 2000 (table 2.2); self-supplied commercial and industrial withdrawals combined were about 7.4 percent of groundwater use.

2-8 Hydrogeologic Settings and Groundwater-Flow Simulations for Regional TANC Studies Begun in 2004

Table 2.2 Year-2000 water-use estimates for selected counties of the Middle Rio Grande Basin, New Mexico.

| Water-use category | Surface-water withdrawal (thousands of cubic meters) | Groundwater withdrawal (thousands of cubic meters) | Total withdrawal (thousands of cubic meters) | Total depletion ¹ (thousands of cubic meters) |
|---|---|---|---|---|
| Bernalillo County | | | | |
| Public water supply | 82.19 | 145,933.11 | 146,015.30 | 64,764.36 |
| Domestic | .00 | 6,874.00 | 6,874.00 | 6,874.00 |
| Irrigated agriculture | 76,392.00 | 4,075.42 | 80,467.42 | 22,485.14 |
| Livestock | 25.78 | 990.25 | 1,016.03 | 1,016.03 |
| Commercial and industrial | .00 | 7,259.29 | 7,259.29 | 5,756.51 |
| Mining and power generation | .00 | 1,601.34 | 1,601.34 | 1,121.62 |
| Reservoir evaporation | .00 | .00 | .00 | .00 |
| County totals: | 76,499.96 | 166,733.42 | 243,233.38 | 102,017.66 |
| Sandoval County | | | | |
| Public water supply | 196.32 | 15,072.89 | 15,269.21 | 12,281.66 |
| Domestic | .00 | 3,490.56 | 3,490.56 | 3,490.56 |
| Irrigated agriculture | 75,875.17 | 1,016.39 | 76,891.56 | 22,721.97 |
| Livestock | 152.98 | 165.99 | 318.97 | 318.97 |
| Commercial and industrial | 12.33 | 7,019.68 | 7,032.02 | 3,390.18 |
| Mining and power generation | .00 | 540.64 | 540.64 | 432.18 |
| Reservoir evaporation | 12,791.21 | .00 | 12,791.21 | 12,791.21 |
| County totals: | 89,028.01 | 27,306.14 | 116,334.15 | 55,426.70 |
| Total estimated water use for Bernalillo and Sandoval Counties | | | | |
| Public water supply | 278.51 | 161,006.00 | 161,284.51 | 77,046.01 |
| Domestic | .00 | 10,364.55 | 10,364.55 | 10,364.55 |
| Irrigated agriculture | 152,267.17 | 5,091.81 | 157,358.98 | 45,207.11 |
| Livestock | 178.76 | 1,156.24 | 1,335.00 | 1,335.00 |
| Commercial and industrial | 12.33 | 14,278.97 | 14,291.31 | 9,146.69 |
| Mining and power generation | .00 | 2,141.98 | 2,141.98 | 1,553.79 |
| Reservoir evaporation | 12,791.21 | .00 | 12,791.21 | 12,791.21 |
| Total for both counties: | 165,527.97 | 194,039.56 | 359,567.53 | 157,444.36 |

¹ Depletion is the part of withdrawal that is lost to the local water resource for future use because of consumption, evapotranspiration, or other processes.

Conceptual Understanding of the Groundwater System

The conceptual understanding of groundwater flow for the MRGB, and consequently of the MRGB regional study area, has been developed through investigations of the geology, hydrology, and water chemistry of the basin spanning the past 100 years. Lee (1907) conducted the first detailed reconnaissance of water resources in the Rio Grande valley. Early studies focusing on groundwater resources within the MRGB were published by Meeks (1949), Bjorklund and Maxwell (1961), and Titus (1961). The first three-dimensional groundwater-flow model of the basin was constructed by Kernodle and Scott (1986), and the first detailed study of groundwater chemistry was conducted by Anderholm (1988). Detailed investigations of the hydrogeology of the basin by Hawley and Haase (1992) and of hydrologic conditions in the basin by Thorn and others (1993) demonstrated that the extent and thickness of highly productive parts of the aquifer in the area were substantially smaller than previously believed. The need for improved knowledge of the availability of groundwater resources in the MRGB led to an intensive 6-year, multidisciplinary group of studies by Federal, State, and local agencies and universities during 1995–2001. Results of the numerous investigations included in this effort are summarized in Bartolino and Cole (2002), were incorporated into the groundwater-flow model by McAda and Carroll (2002), and are selectively discussed in the following sections.

Geology

The MRGB is located along the Rio Grande Rift, which is a generally north-south trending area of Cenozoic crustal extension, and is hydraulically connected to the Espanola Basin on the north and the Socorro Basin on the south. Three subbasins (fig. 2.3) that are separated by bedrock structural highs and contain alluvial fill up to about 4,500 m thick (fig. 2.4) are included within the overall MRGB (Grauch and others, 1999); the regional study area entirely encompasses the northern two subbasins. Relatively shallow benches on the east and west bound the deeper parts of the basin. In addition to major faults that juxtapose alluvium and bedrock along uplifts and benches near the basin margins, numerous other primarily north-south trending faults have caused offsets within the alluvial fill (Grauch and others, 2001; Connell, 2006) (fig. 2.3). The uplifts on the east and the Nacimiento Uplift on the northwest are composed of Precambrian plutonic and metamorphic rocks, generally overlain by Paleozoic and (or) Mesozoic sedimentary rocks (Hawley and Haase, 1992; Hawley and others, 1995). The Jemez Mountains on the north are a major Cenozoic volcanic center.

The alluvial fill of the MRGB is composed primarily of the unconsolidated to moderately consolidated Santa Fe Group deposits of late Oligocene to middle Pleistocene age, which

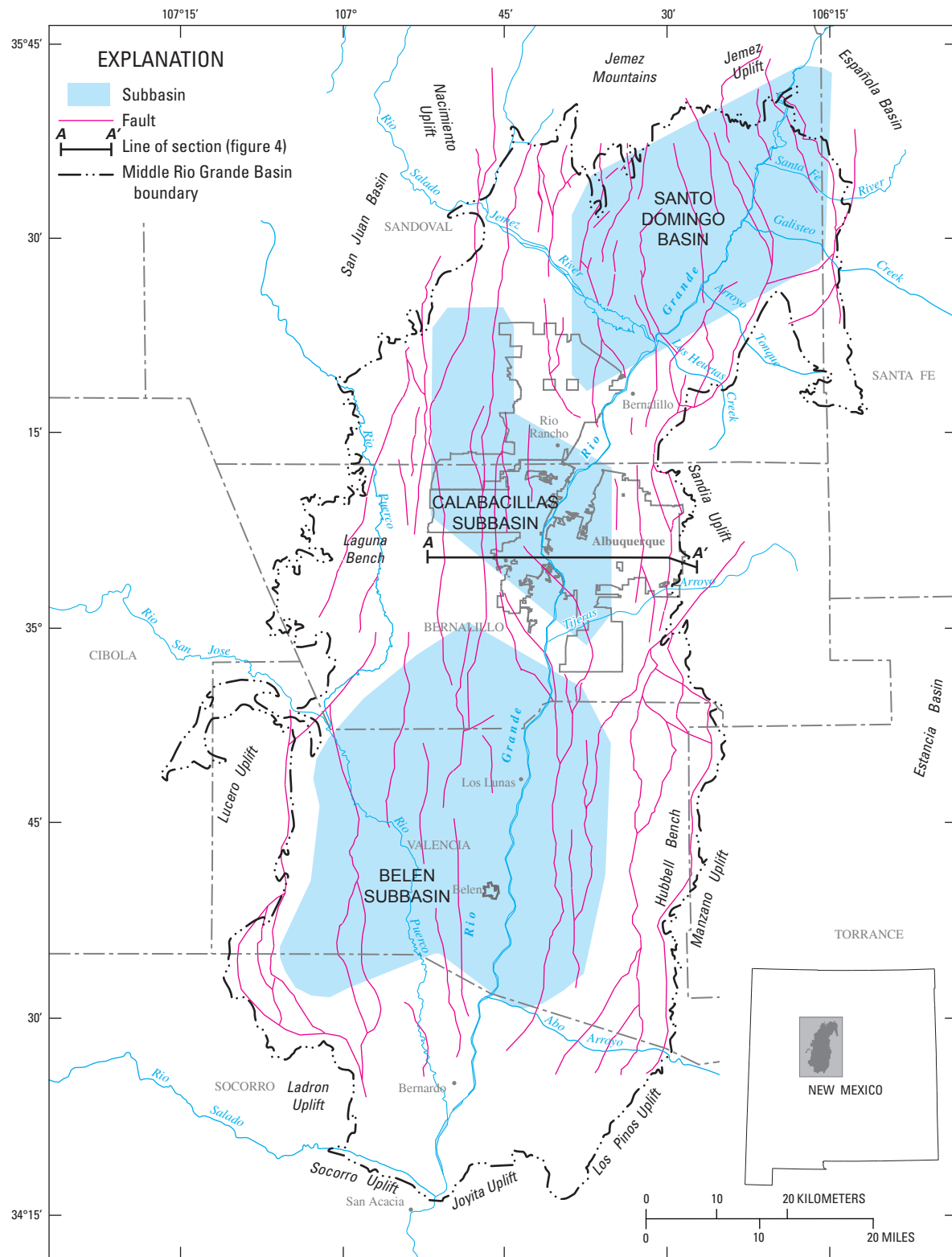
overlie lower and middle Tertiary rocks in the central part of the basin and Mesozoic, Paleozoic, and Precambrian rocks near the basin margins (McAda and Barrell, 2002). Post-Santa Fe Group valley and basin-fill deposits of Pleistocene to Holocene age typically are in hydraulic connection with the Santa Fe Group deposits; in combination, these deposits form the Santa Fe Group aquifer system (Thorn and others, 1993). The sediments in the basin consist generally of sand, gravel, silt, and clay that were deposited in fluvial, lacustrine, or piedmont-slope environments.

Hawley and Haase (1992) defined broad lower, middle, and upper parts of the Santa Fe Group based on both the timing and environment of deposition, as described here. Sediments of the lower Santa Fe Group, which may be more than 1,000 m thick in places, were deposited about 30 to 15 million years ago in a shallow, internally drained basin. Along with piedmont-slope and eolian deposits, the lower unit includes extensive basin-floor playa deposits that have low hydraulic conductivity. The middle Santa Fe Group ranges from about 75 to 2,700 m thick and was deposited about 15 to 5 million years ago, during a time when major fluvial systems from the north, northeast, and southwest transported large quantities of sediment into the basin. In addition to piedmont-slope deposits, the middle unit consists largely of basin-floor fluvial deposits in the north and playa deposits in the south, where the fluvial systems terminated. Within the Ceja Formation, a red-brown clay layer named the Atrisco Member by Connell and others (1998), and shown on the sections in Connell (1997 and 2006) and figure 2.4, marks the top of the middle Santa Fe Group. The upper unit generally is less than about 300 m thick and was deposited about 5 to 1 million years ago during development of the ancestral Rio Grande system. The axial-channel deposits of this high-energy fluvial system include thick zones of clean sand and gravel that compose the most productive aquifer materials in the basin. Most public-supply wells in the study area are completed in the upper and (or) middle units east of the Rio Grande, and in the middle and (or) lower units west of the Rio Grande.

Post-Santa Fe Group valley-fill sediments generally are less than about 40 m thick and were deposited during the most recent (10,000- to 15,000-year) partial backfilling sequence of the Rio Grande and Rio Puerco, following earlier incision (Hawley and Haase, 1992). These sediments provide a connection between the surface-water system and the underlying Santa Fe Group deposits. Relatively young basin-fill materials also include eolian and fan deposits, along with volcanics that were emplaced during the middle to late Pleistocene.

Groundwater Occurrence and Flow

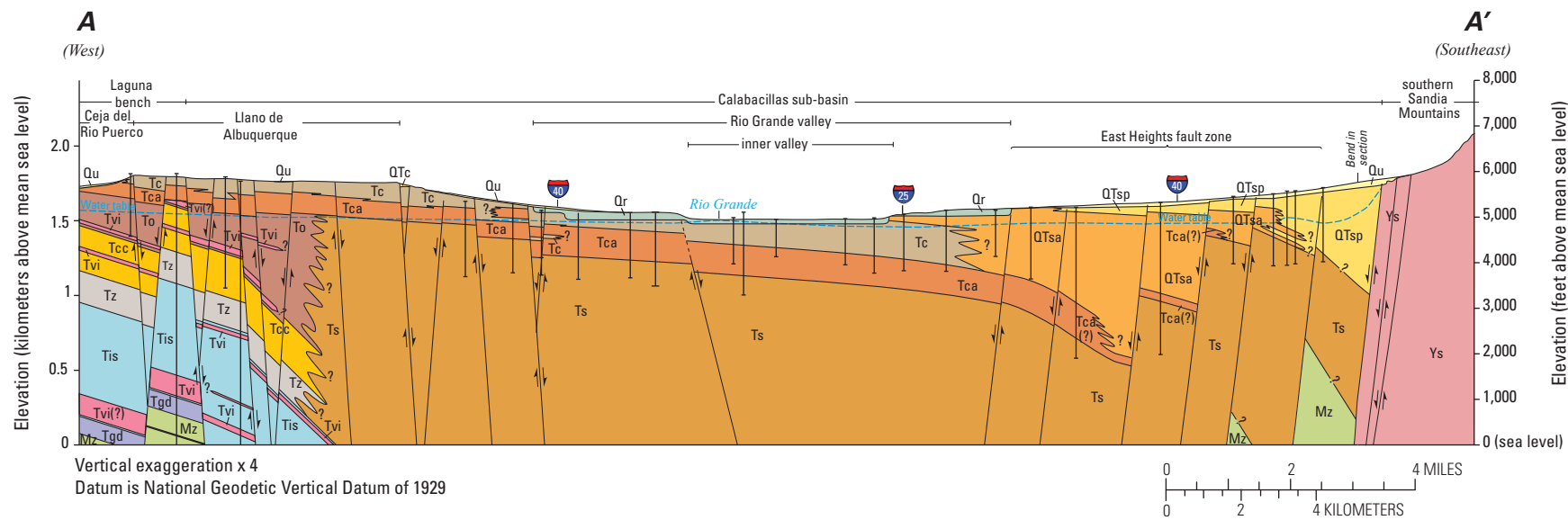
Conditions within the Santa Fe Group aquifer system of the MRGB regional study area generally are unconfined, but are semiconfined at depth. Water-level maps of predevelopment (generally pre-1960) conditions in the study area (Meeks, 1949; Bjorklund and Maxwell, 1961; Titus, 1961; Bexfield



Base modified from U.S. Geological Survey digital data, 1:24,000, 1999
Universal Transverse Mercator Zone 13N, North American Datum of 1983.

Faults modified from Mark Hudson and Scott Minor,
U.S. Geological Survey, written commun., 1999

Figure 2.3. Major structural features in the Middle Rio Grande Basin, New Mexico.



Post-Santa Fe Group deposits

| | |
|--------------------------------|---|
| Qu | Pleistocene and Holocene sediments, undivided |
| Qr | Rio Grande fluvial deposits, undivided (modern-middle Pleistocene) |
| Santa Fe Group deposits | |
| Ts | Rio Grande fluvial deposits, undivided lower and middle subgroups (upper Oligocene-upper Miocene) |
| QTsa | Sierra Ladrones Formation, axial-fluvial member (Pliocene-lower Pleistocene) |
| QTsp | Sierra Ladrones Formation, upper piedmont member (Pliocene-lower Pleistocene) |
| Tc | Ceja Formation, undivided (Pliocene-lower Pleistocene(?) |

EXPLANATION

| | |
|------------------------------------|--|
| QTc | Calabacillas Formation (upper Pliocene(?) |
| Tca | Ceja Formation, Atrisco Member (Pliocene) |
| To | Arroyo Ojito Formation, undivided (middle-upper Miocene) |
| Tcc | Cerro Conejo Formation (middle Miocene) |
| Tz | Zia Formation, undivided (upper Oligocene-lower Miocene) |
| Pre-Santa Fe Group deposits | |
| Tis | Unit of Isleta well #2 (upper Eocene-Oligocene) sandstone, mudstone, and interbedded volcanic rocks described by Lozinsky (1994) in subsurface |
| Tvi | Interbedded volcanic rocks of Tertiary age. |
| Tgd | Diamond Tail and Galisteo Formations, undivided. |
| Mz | Mesozoic sedimentary rocks, undivided. |
| Crystalline rocks | |
| Ys | Sandia granite. |
| ← | Fault—Arrows indicate direction of movement. |
| ? | Contact—Queried where uncertain. |
| ↓ | Deep well in geologic cross section. |

Figure 2.4. Geologic section through Albuquerque, New Mexico (modified from Connell, 1997). See figure 2.3 for section location. Formations and member names usage from the New Mexico Bureau of Geology and Mineral Resources (Connell, 1997).

and Anderholm, 2000) indicate that the principal direction of groundwater flow was north to south through the center of basin, with greater components of east-to-west flow near the basin margins (fig. 2.5). This general flow pattern reflects not only sedimentation patterns in the basin, but also the areal distribution of groundwater recharge and discharge (fig. 2.6). Mountain-front processes (shallow subsurface groundwater inflow and infiltration through mountain stream channels) contribute recharge along the northern and eastern basin margins, where deep subsurface inflow through mountain blocks also occurs. The San Juan Basin contributes subsurface groundwater inflow along the western margin of the MRGB. Along most of its length, the Rio Grande leaks water to the aquifer system, as do some tributary streams and arroyos. Before the arrival of irrigated agriculture and a substantial population, most discharge occurred through riparian evapotranspiration (fig. 2.6A) (McAda and Barroll, 2002), defined for this study as evapotranspiration from the water table in riparian areas along the Rio Grande inner valley and the Jemez River. Since development of irrigated agriculture and urbanized areas, water also recharges the aquifer system through seepage from irrigation canals, irrigated agricultural fields, and septic systems (fig. 2.6B); although not specifically addressed by previous groundwater budgets for the MRGB, irrigated urban landscaping and leaky sewer and (or) water-distribution lines also are likely to contribute recharge in some areas. Water now also discharges from the system through groundwater drains (riverside and interior) and groundwater withdrawals for public supply.

Predevelopment water-level maps indicate the presence of depressions—or “water-level troughs”—in the water-level surface both east and west of the Rio Grande (fig. 2.5). Highly permeable channel gravels west of the Rio Grande in the far north part of the basin (Smith and Kuhle, 1998) and east of the Rio Grande near Albuquerque (Hawley and Haase, 1992) support the hypothesis of high permeability pathways as the most probable explanation for the groundwater troughs in these areas (McAda and Barroll, 2002). Kernodle and others (1995) also hypothesized the presence of a relatively thick sequence of permeable material in the area of the trough west of the Rio Grande near Albuquerque, but detailed lithologic information subsequently obtained from wells in the area generally do not appear to support this hypothesis (Hawley, 1996; Stone and others, 1998; Tiedeman and others, 1998). Based on groundwater chemistry, Plummer and others (2004a, b, c) hypothesized that this trough may be a transient feature that reflects changes in the quantity and spatial distribution of recharge through time. The transient paleohydrologic model of Sanford and others (2004a, b) indicates that recharge quantities probably have changed through time and that low rates of recharge along basin margins have contributed to trough formation. Horizontal anisotropy and faults acting as flow barriers also have been proposed as factors contributing to the existence of the trough west of Albuquerque (McAda and Barroll, 2002).

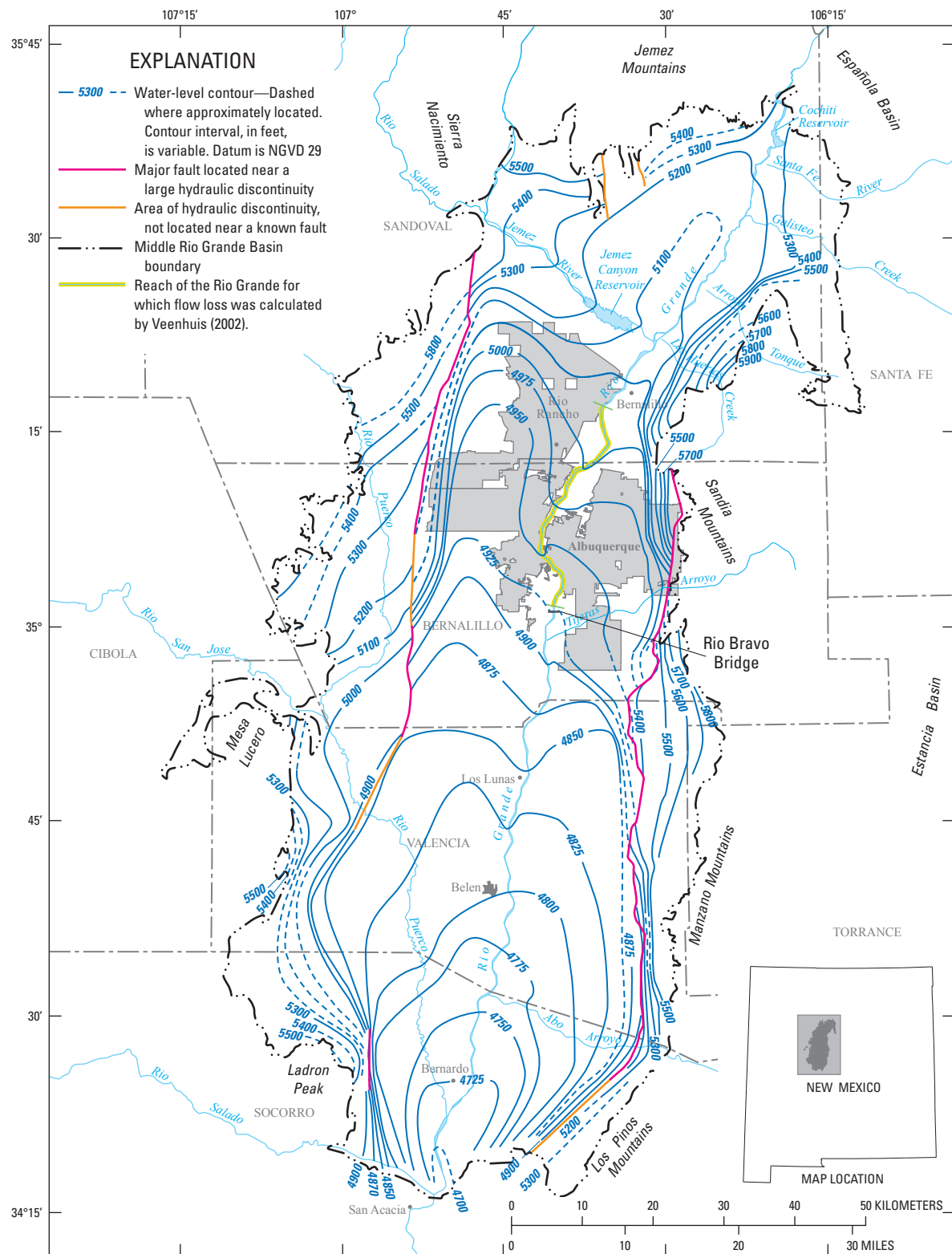
Large and extensive water-level declines from sustained groundwater withdrawals in urbanized areas have substantially altered the direction of groundwater flow in the regional

study area, particularly in and around Albuquerque (Bexfield and Anderholm, 2002a) (fig. 2.7). Water-level declines since predevelopment in the production zone (the depth interval from which most supply-well withdrawals occur—typically from less than about 60 m to 275 m or more below the water table) have exceeded 30 m across broad areas east of the Rio Grande and 20 m across smaller areas west of the Rio Grande. Consequently, groundwater now flows into the major pumping centers from all directions (fig. 2.7). Also, water-level declines in the aquifer have induced additional inflow from the surface-water system compared with predevelopment conditions.

Water-level data from deep piezometer nests across the Albuquerque area indicate that vertical gradients generally are downward in the Rio Grande inner valley and areas to the west, and upward in areas east of the inner valley, except in close proximity to the mountain front (Bexfield and Anderholm, 2002b). These deep nests typically include three piezometers with relatively short screened intervals (on the order of a few meters) located near the water table (shallow), the middle of the production zone (middle), and the bottom of the production zone (deep). Using data from continuous water-level monitors for 1997–1999, Bexfield and Anderholm (2002b) found that water levels in the middle and deep zones tend to respond in a similar manner to seasonal changes in groundwater withdrawals (fig. 2.8), with seasonal water-level variations in individual piezometers ranging from less than 0.3 m to more than 6 m. Water levels at the water table (where the storage coefficient is largest) change the least from seasonal changes in groundwater withdrawals. For the Garfield Park nest in the Rio Grande inner valley, the water table shows seasonal variations apparently associated with seepage of irrigation water through canals and (or) turf areas. In some nests, the time lag between water-level changes in different zones was shorter than in other nests, indicating a better hydraulic connection (Bexfield and Anderholm, 2002b). Vertical gradients between individual zones in the nests generally were smallest east of the inner valley, and they ranged in magnitude from about 0.002 (upward) to 0.080 (downward) overall. In most nests, water levels appeared to be declining at an annual rate of about 0.3 m or less (Bexfield and Anderholm, 2002b).

Aquifer Hydraulic Properties

Horizontal hydraulic conductivities for the Santa Fe Group aquifer system have mostly been estimated from aquifer-test data in long-screened wells (Thorn and others, 1993) and slug-test data in piezometers (Thomas and Thorn, 2000). For the upper Santa Fe Group, estimates generally range from about 1.2 to 46 meters per day (m/d) (Thorn and others, 1993), although smaller conductivities have been estimated for discrete fine-grained zones (Thomas and Thorn, 2000). Estimates at the higher end of the range for the upper Santa Fe Group typically come from wells located east of the Rio Grande that are completed in axial-channel deposits of the ancestral river. For the middle and lower parts of the Santa



Base modified from U.S. Geological Survey digital data, 1:24,000, 1999
Universal Transverse Mercator, Zone 13N, NGVD 1929.

Figure 2.5. Groundwater levels that represent predevelopment conditions, Middle Rio Grande Basin, New Mexico (modified from Bexfield and Anderholm, 2000). The unit of measurement for contour interval (feet) and the use of the National Geodetic Vertical Datum of 1929 have been retained from the source illustration (Bexfield and Anderholm, 2000).

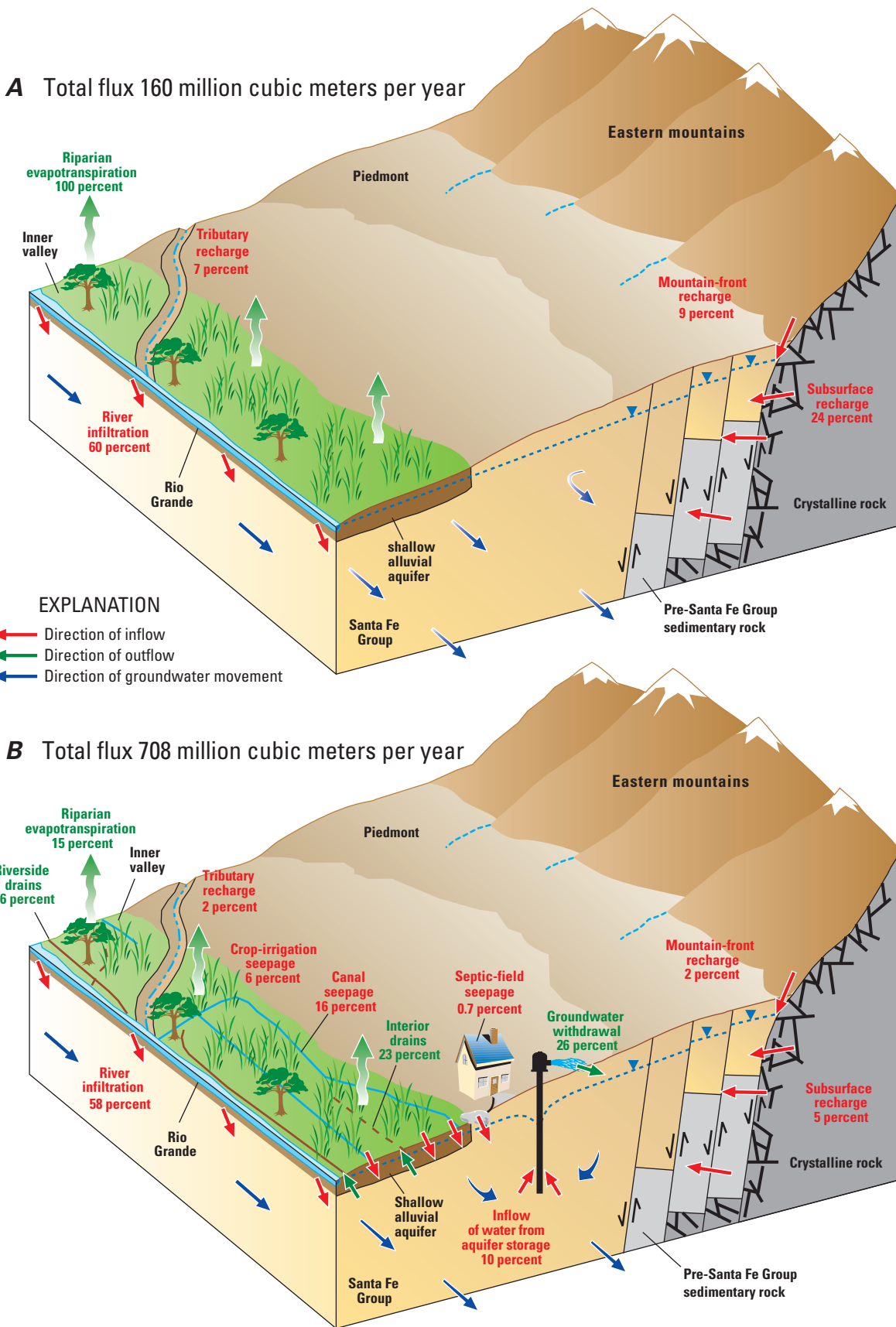
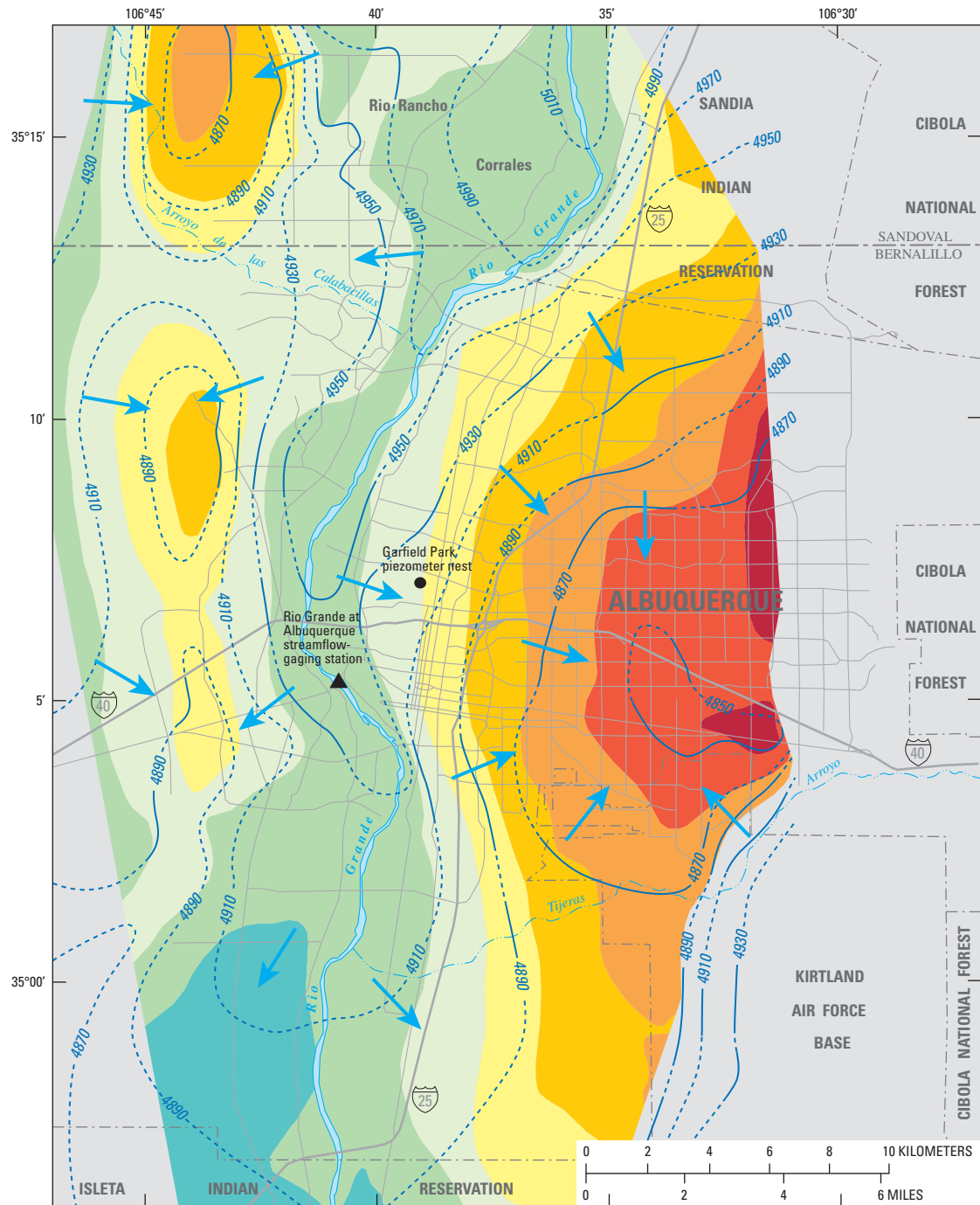


Figure 2.6. Conceptual diagram of regional groundwater flow and budget components near Albuquerque, New Mexico under A, predevelopment and B, modern conditions. Details of the water budget are provided in table 2.3.



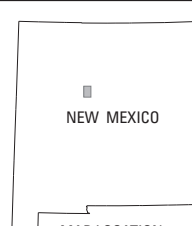
EXPLANATION

Estimated water-level decline, in feet, 1960 to 2002

| | | |
|------------|-----------|-----------------------|
| No decline | 40 to 60 | 100 to 120 |
| 0 to 20 | 60 to 80 | More than 120 |
| 20 to 40 | 80 to 100 | Decline not estimated |

— 4890 - Water-level contour—Interval 20 feet (6.1 meters). Dashed where approximately located. Datum is NGVD 29

→ Generalized direction of groundwater flow



NEW MEXICO

Figure 2.7. Water levels representing 1999–2002 conditions in the production zone in the Albuquerque area, New Mexico, and estimated water-level declines, 1960–2002 (modified from Bexfield and Anderholm, 2002a). The unit of measurement for estimated water-level decline (feet) and the use of the National Geodetic Vertical Datum of 1929 have been retained from the source illustration (Bexfield and Anderholm, 2002a).

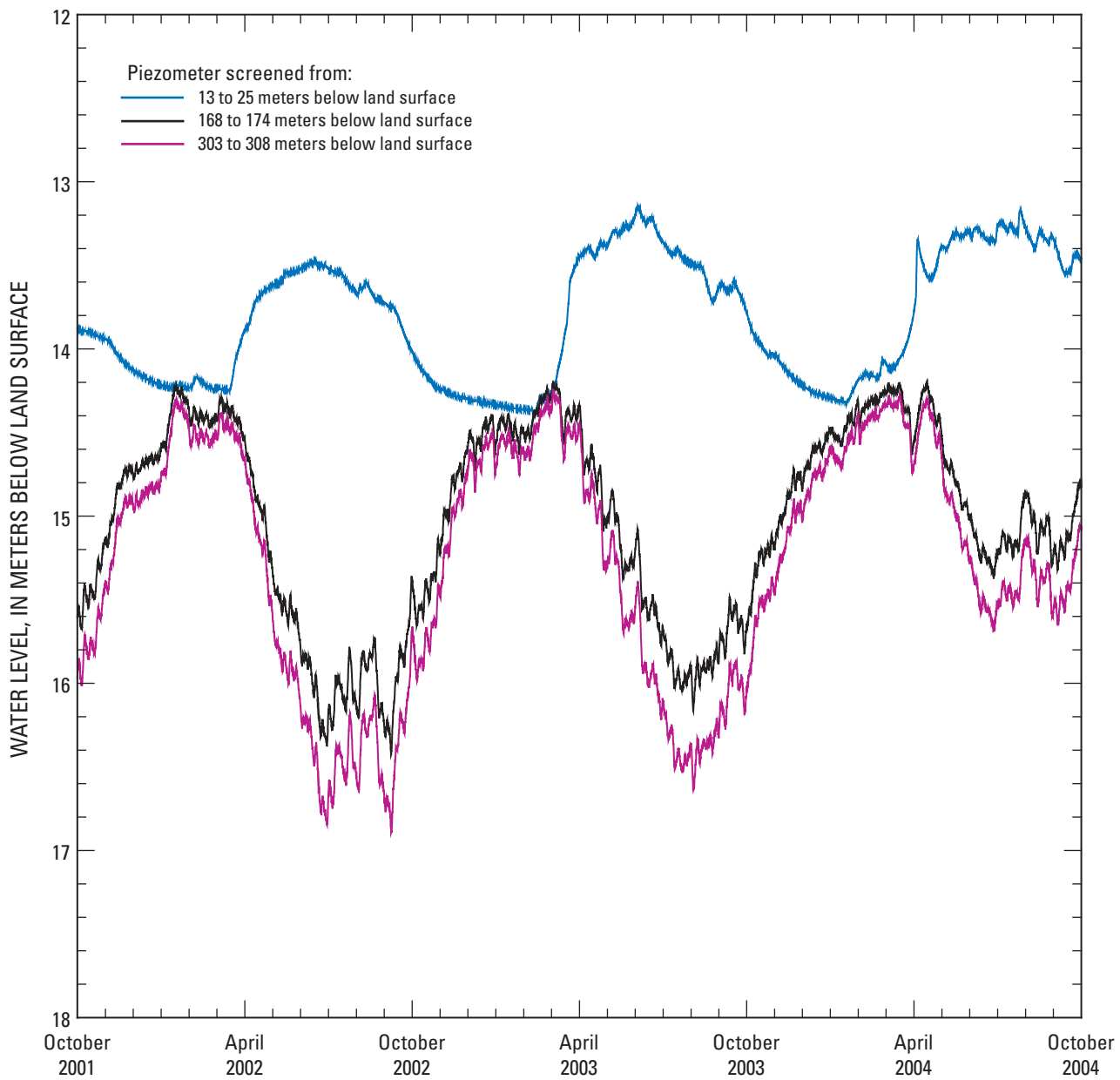


Figure 2.8. Water levels in piezometers in the Garfield Park piezometer nest located in the Rio Grande inner valley, Albuquerque, New Mexico. The location of the piezometer nest is shown on figure 2.7.

Fe Group, estimated hydraulic conductivities tend to be about 3.4 m/d or smaller (McAda and Barroll, 2002). Studies of the post-Santa Fe Group alluvium along the Rio Grande resulted in a wide range of hydraulic-conductivity determinations, from less than 0.1 m/d for silty clays to more than 100 m/d for coarse materials (McAda and Barroll, 2002). For a model simulation of an aquifer test in a public-supply well located in the inner valley in the Albuquerque area, McAda (2001) found a hydraulic conductivity of about 14 m/d to be appropriate for the river alluvium.

No specific yield data were found for the Santa Fe Group aquifer system (Kernodle and others, 1995), but specific yields

of about 0.15 to 0.20 have been used in groundwater-flow models in the MRGB, because these values are considered to be in a range typical of basin fill (McAda and Barroll, 2002). Using data from an extensometer in the Albuquerque area, Heywood (1998; 2001) calculated the elastic specific storage of Santa Fe Group sediments to be 6×10^{-7} per m, equal to that used in models by Kernodle and others (1995) and McAda and Barroll (2002). Unpublished USGS bulk-density and moisture-content data for saturated sediments collected at various depths from a borehole in the upper Santa Fe Group indicate 0.3 to 0.4 as a reasonable range of porosity.

Table 2.3. Model-computed net annual groundwater budgets for steady-state conditions and year ending October 31, 1999, from the McAda and Barroll (2002) groundwater-flow model, Middle Rio Grande Basin, New Mexico.

[m³/yr; cubic meters per year; —, not applicable]

| Water-budget component | Steady state | | | | Year ending October 31, 1999 | | | |
|---|---|--|---|-------------------------------------|---|--|--|-------------------------------------|
| | Specified net flow (10 ⁶ m ³ /yr) | Computed net flow (10 ⁶ m ³ /yr) | Total net flow (10 ⁶ m ³ /yr) | Percentage of net inflow or outflow | Specified net flow (10 ⁶ m ³ /yr) | Computed net flow (10 ⁶ m ³ /yr) | Net flow rate (10 ⁶ m ³ /yr) | Percentage of net inflow or outflow |
| Model inflow (recharge) | | | | | | | | |
| Mountain-front recharge | 15 | — | 15 | 9 | 15 | — | 15 | 2 |
| Tributary recharge | 11 | — | 11 | 7 | 11 | — | 11 | 2 |
| Subsurface inflow | 38 | — | 38 | 24 | 38 | — | 38 | 5 |
| Canal seepage | 0 | — | 0 | 0 | 111 | — | 111 | 16 |
| Crop-irrigation seepage | 0 | — | 0 | 0 | 43 | — | 43 | 6 |
| Rio Grande and Cochiti Lake ¹ | — | 78 | 78 | 49 | — | 390 | 390 | 55 |
| Jemez River and Jemez Canyon Reservoir ¹ | — | 18 | 18 | 11 | — | 21 | 21 | 3 |
| Septic-field seepage | 0 | — | 0 | 0 | 5 | — | 5 | 1 |
| Aquifer storage ² | — | 0 | 0 | 0 | — | 74 | 74 | 10 |
| Total inflow³ | — | — | 160 | 100 | — | — | 708 | 100 |
| Model outflow (discharge) | | | | | | | | |
| Riverside drains | — | 0 | 0 | 0 | — | 256 | 256 | 36 |
| Interior drains | — | 0 | 0 | 0 | — | 164 | 164 | 23 |
| Groundwater withdrawal ⁴ | 0 | — | 0 | 0 | 185 | — | 185 | 26 |
| Riparian evapotranspiration | — | 159 | 159 | 100 | — | 104 | 104 | 15 |
| Total outflow³ | — | — | 159 | 100 | — | — | 709 | 100 |

¹ Cochiti Lake and Jemez Canyon Reservoir were not present during steady-state conditions.

² Net inflow of water from aquifer storage reflects loss of water from aquifer storage to the groundwater system (that is, a decline in aquifer storage).

³ Due to flow rate rounding, budget discrepancies in the table differ from the corresponding model output. Model-computed volumetric budget discrepancies are 0.02 percent for the steady-state stress period and 0.07 percent for the stress period ending October 31, 1999.

⁴ Includes withdrawals for domestic, municipal, commercial, and industrial uses.

Patterns in faulting and sedimentation in the MRGB led McAda and Barroll (2002) to use horizontal-anisotropy ratios (defined as ratios of hydraulic conductivity along model columns to hydraulic conductivity along model rows) of 1:1, 2:1, and 5:1 in selected areas of their model of the basin.

McAda and Barroll (2002) state that vertical anisotropy ratios (defined as ratios of horizontal hydraulic conductivity to vertical hydraulic conductivity) used in models of the basin have ranged between about 80:1 and 1,000:1; as a result of calibration, the ratio used throughout their model was 150:1. Using detailed profiles of temperature with depth, Reiter (2001) estimated a vertical (downward) specific discharge of about 0.12 meters per year (m/yr) in the 157-m deep Rio Bravo Park well located adjacent to the Rio Grande near the southern part of Albuquerque. Water-level data for two depths at the Rio Bravo Park location (about 6.7 and 157 m) (DeWees, 2003) indicate

a downward vertical gradient of about 0.011. By use of these data and the estimated horizontal hydraulic conductivity of 2.4 m/d at corresponding depths in this area (McAda and Barroll, 2002), a vertical hydraulic conductivity of about 0.03 m/d and vertical anisotropy ratio of 80:1 was estimated for this site.

Water Budget

Conceptual water budgets have been developed for the MRGB in association with previous groundwater-flow models. Because the McAda and Barroll (2002) model incorporated the latest estimates of various budget components resulting from the 1995–2001 intensive multidisciplinary group of studies of hydrogeology in the basin (Cole, 2001b), this model budget (table 2.3) provides the basis for most of the discussion in this section.

As a result of high evaporation rates and generally large depths to groundwater, areal recharge to the Santa Fe Group aquifer system of the MRGB from precipitation is believed to be minor (Anderholm, 1988). Instead, groundwater recharge occurs primarily along surface-water features and basin margins. Using the chloride-balance method, Anderholm (2001) calculated mountain-front recharge along the entire eastern margin of the basin to total about 14×10^6 cubic meters per year (m^3/yr), although other methods have indicated this value might be as high as about $47 \times 10^6 \text{ m}^3/\text{yr}$ (Anderholm, 2001). The McAda and Barroll (2002) model uses a value totaling $15 \times 10^6 \text{ m}^3/\text{yr}$ along all basin margins (table 2.3), including areas along the Jemez Mountains on the north and Ladron Peak on the southwest, where mountain-front recharge has not been quantified. Subsurface recharge occurring as groundwater inflow from adjacent basins has been estimated through groundwater-flow modeling, using supporting evidence from studies of hydrogeology (Smith and Khule, 1998; Grant, 1999) and groundwater ages (Sanford and others, 2004a, b). McAda and Barroll (2002) use a total of $38 \times 10^6 \text{ m}^3/\text{yr}$ of subsurface recharge for the basin.

Within the MRGB, most recharge to the aquifer system occurs as seepage of surface water along the Rio Grande and the Jemez River, as well as (in modern times) along features of their associated irrigation systems (table 2.3). By comparison, tributary recharge is small along the Rio Puerco in the west, the Rio Salado in the south, and streams and arroyos entering the basin from the east (which generally do not contain persistent flow more than a few hundred meters from the mountain front). Based partly on streamflow losses estimated by Thomas and others (2000) for the Santa Fe River in the northeast, tributary recharge in the McAda and Barroll (2002) model totals $11 \times 10^6 \text{ m}^3/\text{yr}$. Even prior to large-scale declines in groundwater levels associated with withdrawals for public supply, the Rio Grande, which is in hydraulic connection with the Santa Fe Group aquifer system along its entire length through the basin, is thought to have lost water to the aquifer system. The McAda and Barroll (2002) model simulates the net magnitude of these losses under steady-state conditions to be $78 \times 10^6 \text{ m}^3/\text{yr}$. Along the Jemez River, which is in hydraulic connection with the aquifer system through most of its length within the basin, these net losses are simulated to be $18 \times 10^6 \text{ m}^3/\text{yr}$ under steady-state conditions and only slightly higher ($21 \times 10^6 \text{ m}^3/\text{yr}$) in modern times, including after commencement of Jemez Reservoir operation in 1979.

Seepage of water to the aquifer system in the Rio Grande inner valley has increased since urbanization and the development of large-scale irrigation systems in the MRGB, as simulated by the water budget of McAda and Barroll (2002) for the year starting on November 1, 1998, and ending on October 31, 1999 (table 2.3). The model simulates seepage from irrigation canals, including some along the Jemez River, as contributing $111 \times 10^6 \text{ m}^3/\text{yr}$ of water to the aquifer system. By applying an estimated average recharge rate of 0.15 m/yr to all agricultural cropland along the Rio Grande and Jemez River, recharge through crop-irrigation seepage is estimated to

total $43 \times 10^6 \text{ m}^3/\text{yr}$. Because of declines in groundwater levels and commencement of Cochiti Lake operations in 1973, seepage along the Rio Grande is simulated to be $390 \times 10^6 \text{ m}^3/\text{yr}$, or five times the seepage simulated under steady-state conditions. Another source of recharge resulting from urbanization is septic-field seepage, which occurs both within and outside the Rio Grande inner valley and is estimated by McAda and Barroll (2002) to total about $5 \times 10^6 \text{ m}^3/\text{yr}$ for the year ending on October 31, 1999, based on census data and an estimated seepage rate of $0.23 \text{ cubic meters per day (m}^3/\text{d}\text{)}$ per person. Leakage of water from sewer and (or) water-distribution pipes is a potential source of recharge from urbanization, but it was not included in the McAda and Barroll (2002) model.

Under steady-state conditions, groundwater discharged from the aquifer system primarily through evapotranspiration from riparian vegetation and wetlands in the Rio Grande inner valley (Kernodle and others, 1995). Groundwater withdrawals for public supply and construction of an extensive groundwater drainage system in the inner valley have lowered the water table and resulted in reduced riparian evapotranspiration to $104 \times 10^6 \text{ m}^3/\text{yr}$ for the year ending on October 31, 1999, in comparison to $159 \times 10^6 \text{ m}^3/\text{yr}$ under steady-state conditions, as simulated by McAda and Barroll (2002). The largest component of outflow from the aquifer system currently is discharge to the groundwater drain system, which the McAda and Barroll (2002) model simulated to total $420 \times 10^6 \text{ m}^3/\text{yr}$ (table 2.3), with slightly more than 60 percent of this discharge being to the riverside drains, as opposed to interior drains located farther from the Rio Grande. Much of the groundwater discharging to the drain system is water that infiltrated from the Rio Grande or seeped from irrigation canals and irrigated fields (McAda and Barroll, 2002). Groundwater likely also discharges directly to the Rio Grande in some reaches, particularly in the northern part of the basin (Trainer and others, 2000; McAda and Barroll, 2002), and it leaves the MRGB in relatively small quantities as underflow at the southern end (Sanford and others, 2004b). Groundwater withdrawals currently are a major component of the water budget (26 percent of total discharges), discharging an estimated $185 \times 10^6 \text{ m}^3/\text{yr}$ from the aquifer system during the year ending on October 31, 1999 (table 2.3), and resulting in the simulated removal of $74 \times 10^6 \text{ m}^3/\text{yr}$ from aquifer storage during the same year.

Groundwater Age

The age of most groundwater in the Santa Fe Group aquifer system of the MRGB, as estimated using carbon-14 (^{14}C), is on the order of thousands of years (fig. 2.9) (Plummer and others, 2004a, b, c). Groundwater less than 2,000 years in age typically is found only near known areas of recharge—primarily basin margins and surface-water features. Chlorofluorocarbons and tritium—indicators of the presence of young (post-1950s) recharge—were most common at relatively shallow depths within the Rio Grande inner valley (Plummer and others, 2004a). However, chlorofluorocarbons and tritium

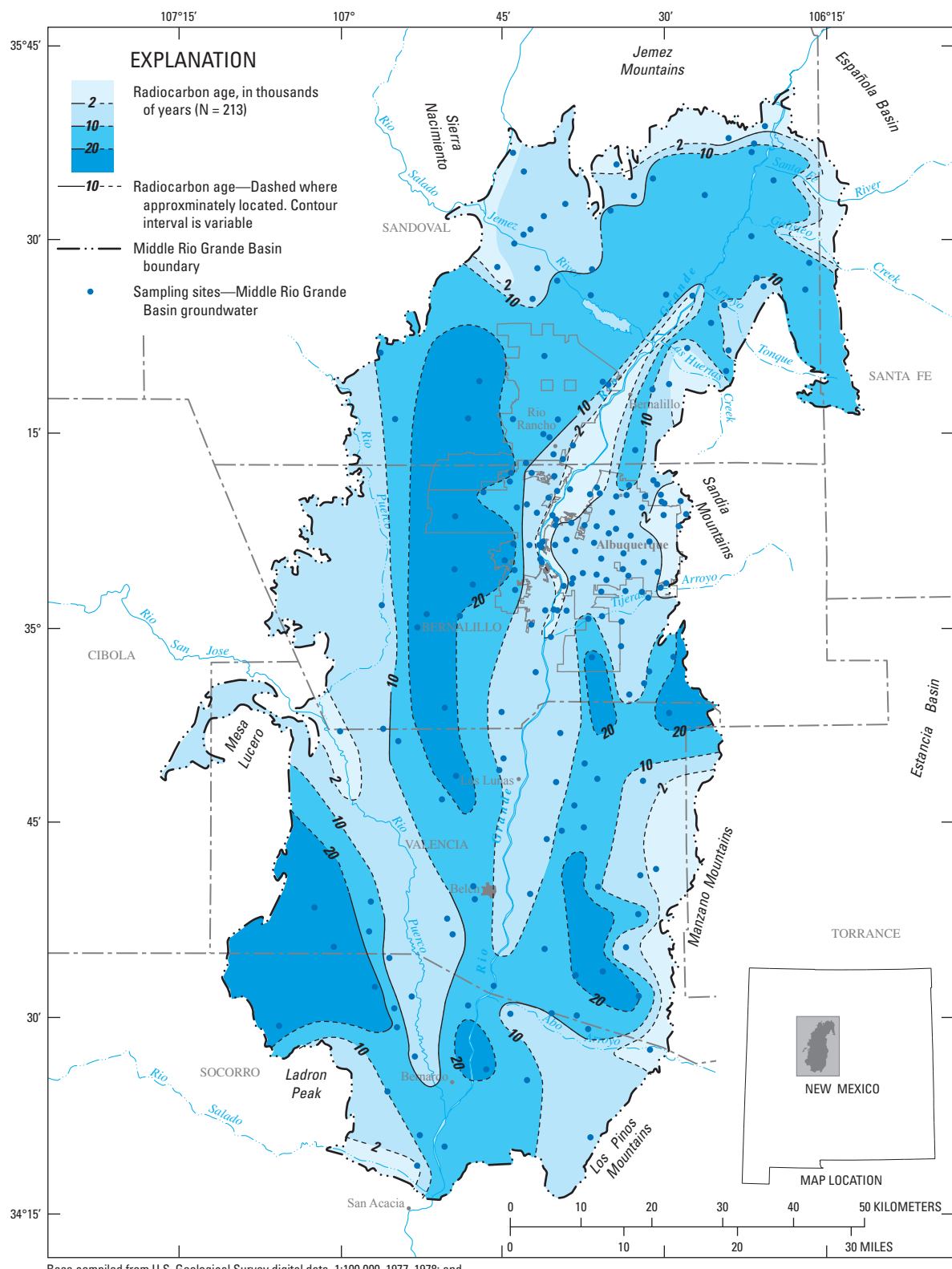


Figure 2.9. Estimated ages of groundwater in the Santa Fe Group aquifer system, Middle Rio Grande Basin, New Mexico (modified from Plummer and others, 2004a).

were detected in some samples from the water table beneath upland areas, indicating the potential presence of recharge sources in these areas that have not been well characterized. Spatial patterns in groundwater ages indicate that the residence time of much of the groundwater in the basin exceeds 10,000 years (fig. 2.9), thereby illustrating that water flux through the basin is relatively small given the basin's size. Simulation of paleorecharge conditions in the basin using a transient groundwater-flow model calibrated to ^{14}C activities (Sanford and others, 2004a, b) indicates that flux might have been as much as 10 times larger during the last glacial maximum, which occurred approximately 21,500 years ago.

Groundwater Quality

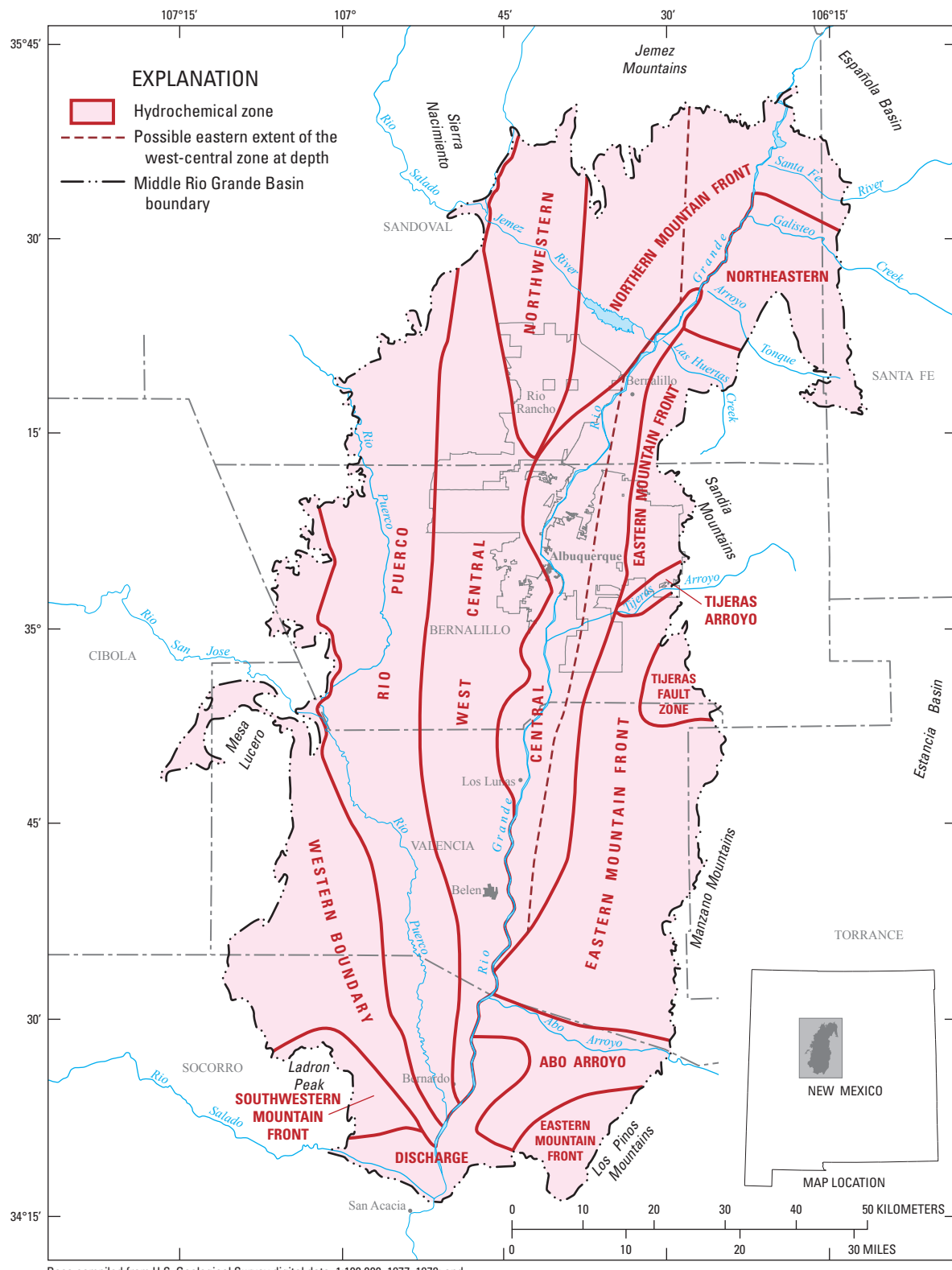
Because sediments of the Santa Fe Group aquifer system are relatively unreactive, groundwater quality in the MRGB regional study area is determined primarily by the source of recharge rather than by processes occurring within the aquifer (Plummer and others, 2004a). Studies by Anderholm (1988), Logan (1990), Bexfield and Anderholm (2002b), and Plummer and others (2004a, b) have illustrated spatial patterns in water chemistry across the Albuquerque area and (or) the MRGB. Based primarily on hydrochemical patterns in data from hundreds of wells of various types (public supply, monitoring, domestic, and other), Plummer and others (2004a, b) delineated individual hydrochemical zones throughout the MRGB (fig. 2.10 and table 2.4), each with relatively homogeneous groundwater chemistry that is distinct from other zones. These zones represent individual sources of recharge to the basin and are used to facilitate this discussion of water chemistry within the MRGB regional study area. To further enhance this discussion, groundwater chemistry data collected for the TANC study (as described in Section 1 of this chapter, Chapter B, and Section 1 of Chapter A) were incorporated, as were data obtained from various sources for additional wells within the regional study area that were sampled between 2000 and 2004.

Groundwater along the Jemez and Sandia mountain fronts has some of the smallest dissolved-solids concentrations found in the MRGB. The Northern Mountain Front and Eastern Mountain Front zones of Plummer and others (2004a, b), which delineate areas where relatively high-elevation mountain-front recharge processes dominate, include most of the wells located along these mountain fronts and groundwater in those zones has specific-conductance values that commonly are less than 400 microsiemens per centimeter at 25 degrees Celsius ($\mu\text{S}/\text{cm}$) (table 2.4). Groundwater in these zones typically is of the calcium-bicarbonate type, although sodium is the dominant cation in places. The groundwater generally has pH between 7 and 8 and is well oxidized as indicated by dissolved-oxygen concentrations (fig. 2.11). In the Northwestern zone, which delineates groundwater believed to have recharged at relatively low elevations along the Jemez mountain front (Plummer and others, 2004a), dissolved-solids concentrations, sodium concentrations, and pH values typically

are slightly higher than those found in the Northern Mountain Front zone. Similar to the Northern and Eastern Mountain Front zones, groundwater of the Northwestern zone also is generally well oxidized, with the exception of a relatively small area in the far northwestern corner (fig. 2.11A). In fact, in most areas of the MRGB, groundwater continues to be well oxidized even far from sources of recharge and at depths of nearly 100 m, probably because of a general paucity of organic carbon in aquifer materials (Plummer and others, 2004a).

Groundwater in the Central zone (fig. 2.10), representing recharge from the Rio Grande and its associated irrigation system, has relatively small dissolved-solids concentrations, indicated by specific-conductance of generally less than 600 $\mu\text{S}/\text{cm}$ (table 2.4). Bicarbonate is the dominant anion in groundwater of this zone; the cation content is dominated by calcium and (or) sodium. The pH generally is between 7 and 8, but exceeds 8 in places—particularly at depth—likely in association with cation exchange on clays that allows increased dissolution of calcium carbonate where present (Plummer and others, 2004a). Unlike the oxidized redox conditions observed for groundwater in most of the basin, conditions at shallow depths within the Central zone tend to be manganese or iron reducing (fig. 2.11), probably reflecting greater organic-carbon content for sediments within the Rio Grande inner valley. At some sites in the Central zone, elevated dissolved-solids concentrations, indicated by specific-conductance values greater than 800 $\mu\text{S}/\text{cm}$, at shallow depths might be indicative of recent recharge of irrigation water, septic-tank effluent, or other sources associated with anthropogenic activity.

The West-Central zone extends southward from the Jemez Mountain area through much of the western half of the MRGB (fig. 2.10) and extends at depth beneath adjacent hydrochemical zones to the east. The West-Central zone represents groundwater inflow that entered at depth along the northern margin the basin. Dissolved-solids concentrations are moderate throughout much of this zone, where specific-conductance values generally are less than 600 $\mu\text{S}/\text{cm}$ (table 2.4), despite estimates of groundwater age on the order of tens of thousands of years (fig. 2.9). Most groundwater in the zone is of the sodium-bicarbonate type, although sulfate is the dominant anion in places. The groundwater is generally well oxidized (fig. 2.11); pH exceeds 8 over broad areas, and approach or exceed 9 in places. Groundwater of the West-Central zone commonly has arsenic concentrations greater than the U.S. Environmental Protection Agency drinking-water standard of 10 micrograms per liter (U.S. Environmental Protection Agency, 2006). The elevated arsenic concentrations in this zone generally are associated with silicic volcanism in the Jemez Mountains and with desorption from metal oxides, especially in areas where pH exceeds about 8.5 (Bexfield and Plummer, 2003; Plummer and others, 2004a). Elevated arsenic concentrations in groundwater in other areas of the MRGB typically are associated with deep mineralized water that appears to upwell along major structural features, also resulting in elevated concentrations of chloride and other elements (Bexfield and Plummer, 2003; Plummer and others, 2004a).



Base compiled from U.S. Geological Survey digital data, 1:100,000, 1977, 1978; and City of Albuquerque digital data, 1:2,400, 1994; North American Datum of 1983.

Figure 2.10. Hydrochemical zones in the Middle Rio Grande Basin, New Mexico (modified from Plummer and others, 2004a).

2-22 Hydrogeologic Settings and Groundwater-Flow Simulations for Regional TANC Studies Begun in 2004

Table 2.4. Median values of selected water-quality parameters by hydrochemical zone, Middle Rio Grande Basin, New Mexico.

[—, no data; $\mu\text{S}/\text{cm}$, microsiemens per centimeter at 25 degrees Celsius; deg. C, degrees Celsius; mg/L, milligrams per liter; $\mu\text{g}/\text{L}$, micrograms per liter; pmC, percent modern carbon]

| Hydrochemical zone | Specific conductance ($\mu\text{S}/\text{cm}$) | Field pH | Water temperature (deg. C) | Dissolved oxygen (mg/L) | Calcium (mg/L) | Magnesium (mg/L) | Sodium (mg/L) | Potassium (mg/L) |
|-----------------------------|--|----------|----------------------------|-------------------------|----------------|------------------|---------------|------------------|
| Northern Mountain Front | 340 | 7.49 | 18.9 | 5.12 | 38.5 | 6.1 | 20.0 | 4.9 |
| Northwestern | 400 | 7.84 | 20.6 | 6.68 | 33.9 | 4.2 | 49.9 | 5.7 |
| West Central | 535 | 8.22 | 23.8 | 3.00 | 12.0 | 2.5 | 103 | 4.2 |
| Western Boundary | 4,572 | 7.70 | 22.0 | 4.09 | 135 | 56.4 | 589 | 15.2 |
| Rio Puerco | 2,731 | 7.50 | 20.0 | 3.73 | 135 | 42.7 | 290 | 10.4 |
| Southwestern Mountain Front | 462 | 8.11 | 19.1 | 4.43 | 52.6 | 13.5 | 27.8 | 2.5 |
| Abo Arroyo | 1,055 | 7.45 | 20.7 | 6.23 | 92.5 | 34.4 | 49.2 | 3.1 |
| Eastern Mountain Front | 382 | 7.67 | 22.0 | 5.16 | 45.0 | 5.1 | 29.2 | 2.2 |
| Tijeras Fault Zone | 1,406 | 7.42 | 18.5 | 4.66 | 171 | 36.0 | 95.0 | 6.1 |
| Tijeras Arroyo | 677 | 7.39 | 16.1 | 6.97 | 89.4 | 24.5 | 29.3 | 3.8 |
| Northeastern | 1,221 | 7.50 | 19.4 | 6.44 | 141 | 29.5 | 81.8 | 4.8 |
| Central | 436 | 7.74 | 18.1 | 0.12 | 42.9 | 8.0 | 31.0 | 6.4 |
| Discharge | 1,771 | 7.70 | 20.6 | 0.08 | 93.0 | 31.0 | 190 | 10.5 |

| Hydrochemical zone | Barium (mg/L) | Boron (mg/L) | Chromium ($\mu\text{g}/\text{L}$) | Copper ($\mu\text{g}/\text{L}$) | Iron (mg/L) | Lead ($\mu\text{g}/\text{L}$) | Lithium (mg/L) | Manganese (mg/L) |
|-----------------------------|---------------|--------------|-------------------------------------|-----------------------------------|-------------|---------------------------------|----------------|------------------|
| Northern Mountain Front | 0.062 | 0.043 | 1.2 | 0.8 | 0.060 | 0.20 | 0.058 | 0.005 |
| Northwestern | 0.056 | 0.118 | 2.0 | 0.4 | 0.030 | 0.10 | 0.068 | 0.002 |
| West Central | 0.032 | 0.239 | 5.7 | 0.5 | 0.028 | 0.11 | 0.045 | 0.002 |
| Western Boundary | 0.014 | 0.900 | 10.6 | 3.0 | 0.213 | 0.12 | 0.251 | 0.041 |
| Rio Puerco | 0.014 | 0.291 | 3.0 | 3.4 | 0.130 | 0.10 | 0.253 | 0.015 |
| Southwestern Mountain Front | 0.045 | 0.094 | 1.9 | 9.3 | 0.030 | 0.41 | 0.041 | 0.007 |
| Abo Arroyo | 0.017 | 0.130 | 4.4 | 2.0 | 0.105 | 0.10 | 0.031 | 0.004 |
| Eastern Mountain Front | 0.084 | 0.050 | 1.0 | 1.7 | 0.031 | 0.27 | 0.020 | 0.003 |
| Tijeras Fault Zone | 0.046 | 0.347 | 1.7 | 4.3 | 0.111 | 0.34 | 0.227 | 0.023 |
| Tijeras Arroyo | 0.057 | 0.060 | 1.1 | 1.0 | 0.050 | 0.10 | 0.017 | 0.005 |
| Northeastern | 0.018 | 0.215 | 3.2 | 3.7 | 0.170 | 0.11 | 0.040 | 0.004 |
| Central | 0.083 | 0.085 | 1.0 | 0.8 | 0.041 | 0.10 | 0.040 | 0.015 |
| Discharge | 0.030 | 0.630 | 10.2 | 1.7 | 0.080 | 0.15 | 0.326 | 0.010 |

Table 2.4. Median values of selected water-quality parameters by hydrochemical zone, Middle Rio Grande Basin, New Mexico.—Continued

[—, no data; $\mu\text{S}/\text{cm}$, microsiemens per centimeter at 25 degrees Celsius; deg. C, degrees Celsius; mg/L, milligrams per liter; $\mu\text{g}/\text{L}$, micrograms per liter; pmC, percent modern carbon]

| Hydrochemical zone | Alkalinity (mg/L as sodium bicarbonate) | Sulfate (mg/L) | Chloride (mg/L) | Fluoride (mg/L) | Bromide (mg/L) | Silica (mg/L) | Nitrate (mg/L as N) | Aluminum ($\mu\text{g}/\text{L}$) | Arsenic ($\mu\text{g}/\text{L}$) |
|-----------------------------|--|-------------------|--------------------|--------------------|-------------------|------------------|------------------------|--|---------------------------------------|
| Northern Mountain Front | 137 | 19.5 | 5.6 | 0.35 | 0.08 | 53.3 | 0.56 | — | 3.2 |
| Northwestern | 160 | 44.8 | 8.5 | 0.61 | 0.07 | 30.1 | 2.44 | — | 9.8 |
| West Central | 174 | 92.0 | 13.4 | 0.99 | 0.11 | 34.5 | 1.24 | 6.76 | 23.2 |
| Western Boundary | 300 | 793 | 820 | 1.64 | 0.38 | 22.5 | 0.86 | 5.00 | 1.8 |
| Rio Puerco | 190 | 1,080 | 185.8 | 0.63 | 0.64 | 21.8 | 0.88 | 5.00 | 1.0 |
| Southwestern Mountain Front | 202 | 53.0 | 15.0 | 1.02 | 0.21 | 17.6 | 1.12 | 3.31 | 0.2 |
| Abo Arroyo | 148 | 346 | 25.9 | 0.90 | 0.17 | 24.0 | 1.40 | 4.14 | 5.2 |
| Eastern Mountain Front | 157 | 31.0 | 10.5 | 0.60 | 0.17 | 28.4 | 0.31 | 5.56 | 2.0 |
| Tijeras Fault Zone | 599 | 100 | 139 | 1.27 | 0.69 | 18.9 | 1.09 | 5.22 | 2.2 |
| Tijeras Arroyo | 240 | 115 | 56.6 | 0.60 | 0.35 | 19.5 | 3.79 | 4.09 | 1.0 |
| Northeastern | 208 | 390 | 22.7 | 0.51 | 0.19 | 38.5 | 0.64 | 4.34 | 2.7 |
| Central | 158 | 66.0 | 16.6 | 0.44 | 0.09 | 47.0 | 0.08 | 6.00 | 5.4 |
| Discharge | 157 | 290 | 280 | 1.40 | 0.47 | 39.0 | 0.42 | 4.50 | 9.9 |

| Hydrochemical zone | Molybdenum ($\mu\text{g}/\text{L}$) | Strontium (mg/L) | Uranium ($\mu\text{g}/\text{L}$) | Vanadium ($\mu\text{g}/\text{L}$) | Zinc ($\mu\text{g}/\text{L}$) | Delta deuterium (δD) (per mil) | Delta oxygen-18 ($\delta^{18}\text{O}$) (per mil) | Delta carbon-13 ($\delta^{13}\text{C}$) (per mil) | Carbon-14 (^{14}C) (pmC) |
|-----------------------------|--|---------------------|---------------------------------------|--|------------------------------------|--|---|---|---|
| Northern Mountain Front | 1.7 | 0.31 | 1.0 | 6.4 | 258. | -77.7 | -10.9 | -8.50 | 33.4 |
| Northwestern | 3.4 | 0.57 | 2.7 | 15.6 | 9.0 | -64.7 | -8.73 | -6.93 | 29.6 |
| West Central | 8.2 | 0.20 | 3.7 | 27.9 | 5.0 | -96.7 | -12.7 | -7.18 | 8.80 |
| Western Boundary | 9.9 | 2.09 | 4.4 | 5.7 | 118 | -64.4 | -9.12 | -4.70 | 6.19 |
| Rio Puerco | 7.0 | 3.92 | 6.0 | 3.4 | 117 | -61.6 | -8.51 | -7.65 | 36.4 |
| Southwestern Mountain Front | 3.0 | 0.86 | 0.9 | 1.0 | 252 | -53.5 | -7.74 | -5.76 | 40.0 |
| Abo Arroyo | 3.4 | 1.48 | 5.4 | 9.5 | 8.1 | -65.2 | -9.05 | -6.72 | 24.1 |
| Eastern Mountain Front | 2.0 | 0.32 | 3.6 | 7.5 | 6.7 | -81.0 | -11.4 | -8.70 | 47.2 |
| Tijeras Fault Zone | 3.7 | 1.11 | 7.3 | 6.3 | 61.5 | -74.2 | -10.3 | -0.98 | 9.70 |
| Tijeras Arroyo | 1.9 | 0.47 | 3.7 | 3.0 | 4.5 | -75.7 | -10.3 | -6.80 | 72.8 |
| Northeastern | 6.7 | 1.72 | 8.5 | 3.8 | 99.5 | -68.6 | -9.72 | -6.40 | 28.5 |
| Central | 5.0 | 0.40 | 3.6 | 9.3 | 5.0 | -95.4 | -12.8 | -8.87 | 61.0 |
| Discharge | 10.3 | 3.02 | 3.9 | 7.1 | 16.2 | -90.8 | -12.1 | -7.00 | 10.8 |

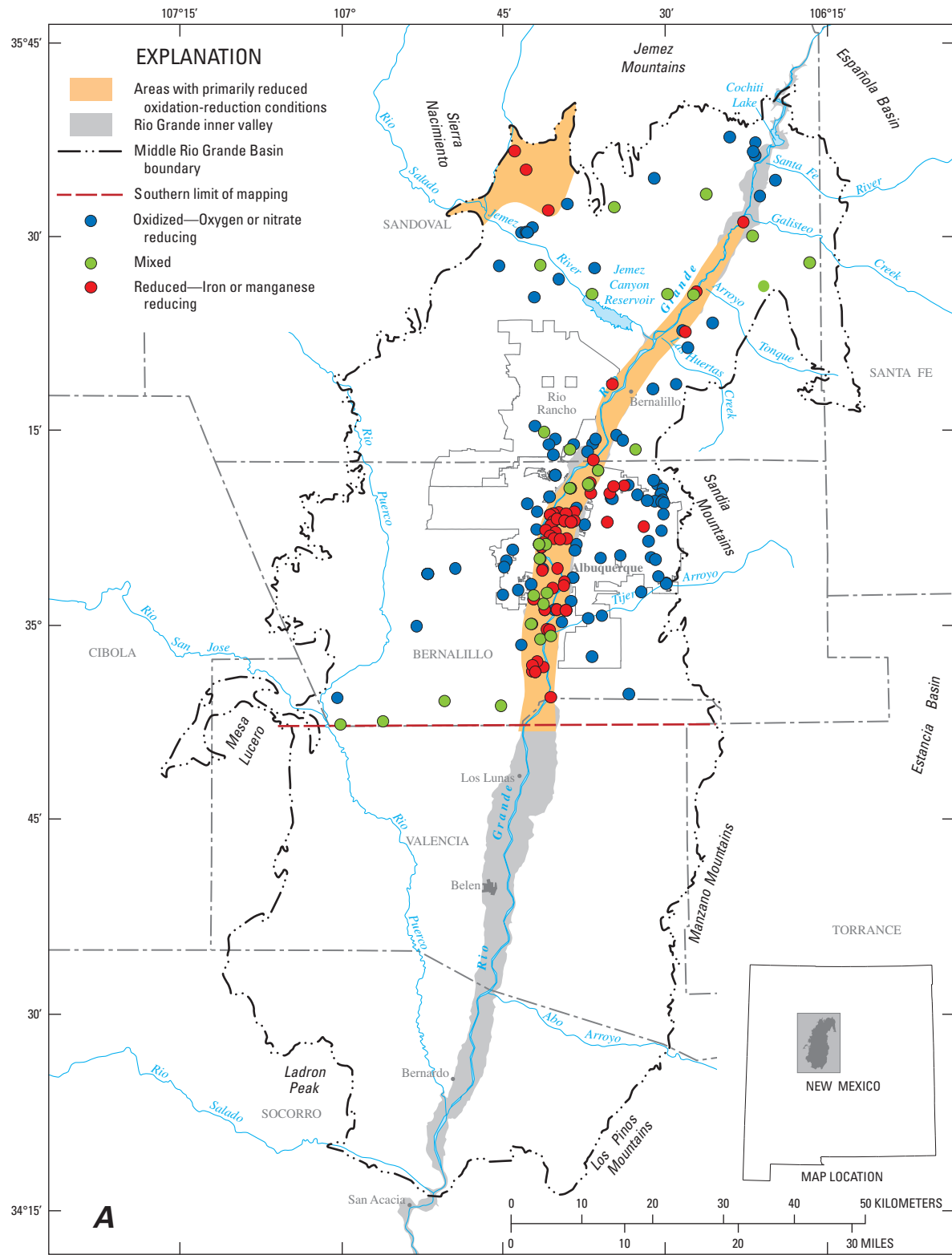
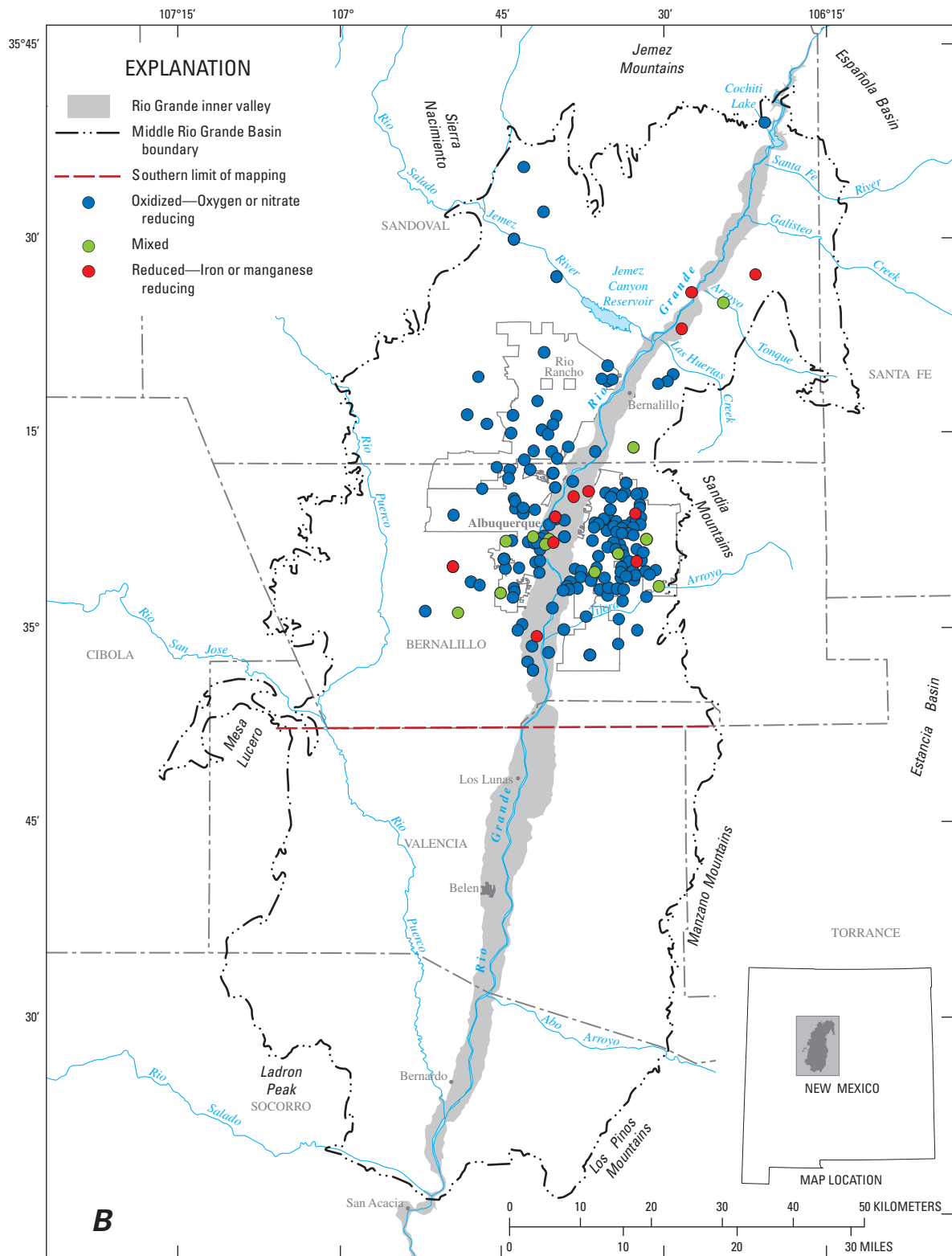


Figure 2.11A. Oxidation-reduction conditions for the upper 90 meters of the aquifer, Middle Rio Grande Basin regional study area, New Mexico.



Base modified from U.S. Geological Survey digital data, 1:24,000, 1999
Universal Transverse Mercator Zone 13N, North American Datum of 1983.

Figure 2.11B. Oxidation-reduction conditions for the deeper parts of the aquifer, Middle Rio Grande Basin regional study area, New Mexico.

The MRGB regional study area also includes part or all of five other hydrochemical zones defined by Plummer and others (2004a, b): the Western Boundary, Rio Puerco, North-eastern, Tijeras Fault Zone, and Tijeras Arroyo zones. These zones are dominated by groundwater inflow along basin margins or major fault systems and (or) by arroyo recharge. With the exception of the Tijeras Arroyo zone, groundwater in these zones has relatively large dissolved-solids concentrations, indicated by specific-conductance values generally greater than 1,000 $\mu\text{S}/\text{cm}$ (table 2.4), and is not typically used for public water supply. Groundwater in the Tijeras Arroyo zone is partly characterized by elevated concentrations of nitrate, calcium, magnesium, sulfate, and chloride relative to the Eastern Mountain Front zone. Similar to the Eastern Mountain Front zone, groundwater in the Tijeras Arroyo zone is well oxidized and has pH between 7 and 8 (fig. 2.11).

Groundwater-Flow Simulations

A MODFLOW (Harbaugh, 2005) model was constructed and calibrated to simulate groundwater flow in a 6,077- km^2 area of the MRGB (fig. 2.12A). This model (subsequently referred to as the “revised model”) simulates conditions in a different area than the previously defined MRGB regional study area, because it is based on the groundwater-flow model documented by McAda and Barroll (2002), which simulated conditions through March 2000. Relative to the McAda and Barroll (2002) model, the revised model incorporates 8.8 additional years of groundwater withdrawal data (through December, 2008), finer horizontal spatial discretization, leakage from the water-distribution and sewer systems in the greater Albuquerque metropolitan area, and simulation of reported withdrawals with the Multi-Node Well (MNW1) Package (Halford and Hanson, 2002). Model-input files were constructed for compatibility with MODFLOW-2005 (Harbaugh, 2005), and some parameter values were adjusted by model calibration with PEST (Doherty, 2005). Changes to most conceptual aspects of the McAda and Barroll (2002) model, such as the hydrogeologic framework and boundary-condition specifications, were minimized.

Conditions prior to 1900 are represented by a steady-state stress period, which provides the initial conditions for subsequent transient stress periods simulating 109 years, from 1900 through December 31, 2008. Time discretization is similar to that used in the McAda and Barroll (2002) model. Stress periods simulating time from 1900 to 1974 and 1975 through 1989, are 5 and 1 years long, respectively. Seasonal stress periods used after January 1, 1990, simulate both irrigation seasons that extend from March 16 through October 31 and winter seasons that extend from November 1 through March 15. Significant changes to surface-water features, such as the construction of riverside drains on either side of the Rio Grande, Cochiti Lake, and Jemez Canyon Reservoir, are simulated at representative stress periods by changes to boundary-condition specifications with the River and Drain Packages

of MODFLOW (Harbaugh, 2005). The riverside and interior drain cell locations changed during the course of the transient simulation.

Modeled Area and Spatial Discretization

The model domain, which includes the metropolitan area of Albuquerque, is somewhat smaller than the MRGB and is bounded on the eastern and western sides by normal faults that are thought to form distinct hydrologic boundaries (Kernodle and others, 1995) (fig. 2.3). The northern and southern boundaries correspond to the MRGB boundaries located at Cochiti Lake and San Acacia (fig. 2.12A), respectively. The model domain incorporates the Cenozoic Rio Grande Rift deposits, which range in thickness from 4 m on the basin margins to approximately 4,600 m and 5,300 m in the deepest parts of the Belen and Calabacillas subbasins, respectively, and includes the Santa Fe Group aquifer system.

The revised model grid is comprised of 9 layers, each containing 312 rows and 160 columns of finite-difference cells that have uniform horizontal dimensions of 0.5 by 0.5 km, which is finer than the 1.0- by 1.0-km cell dimensions of the McAda and Barroll (2002) model. There are a maximum of 24,305 active cells per layer, with the most active cells located in layer 1 and a progressive decrease to 18,944 active cells in layer 9. The simulated direction of anisotropy is aligned with the model grid, corresponding to the general north-south strike of major faults in the basin (Mark Hudson and Scott Minor, U.S. Geological Survey, written commun., 1999). The top four layers are convertible from confined to unconfined conditions.

Although nine model layers (fig. 2.13) represent the Santa Fe Group aquifer system within the MRGB, they do not represent particular lithologic units, with the exception of layers 1 and 2, which represent post-Santa-Fe-Group alluvium within the Rio Grande inner valley. The bases of model layers 1 through 7 tilt upward from south to north, such that they each maintain a consistent depth beneath the Rio Grande. The thickness of model layers 1 through 5 increases with distance perpendicular from the Rio Grande, as do the model-layer-bottom elevations of layers 1 through 4. The thickness of the unsaturated zone in model layer 1 increases away from the Rio Grande to a maximum of 585 m. For simulated steady-state hydraulic heads, the saturated thickness in layer 1 is up to 14 m thick. The steady-state saturated thickness of layers 2, 3, 4, and 5 ranges between 15–23, 30–47, 65–103, and 118–184 m, respectively. The base of layer 5 is at an elevation 244 m below the Rio Grande, and it maintains that elevation perpendicular to the trend of the river except where basement rock is at a higher elevation near the basin perimeter. Layers 6 and 7 have constant thicknesses of 183 and 305 m, respectively. The top of layer 8 is at an elevation 732 m below the Rio Grande, except near the basin perimeter, where the base rises, and ranges in thickness from 18 to 1,175 m. The thickness of layer 9 ranges from 153 to 2,350 m. Cells in layers 1–9 are active where the base of the cell is higher than the base of the Santa Fe Group basin fill.

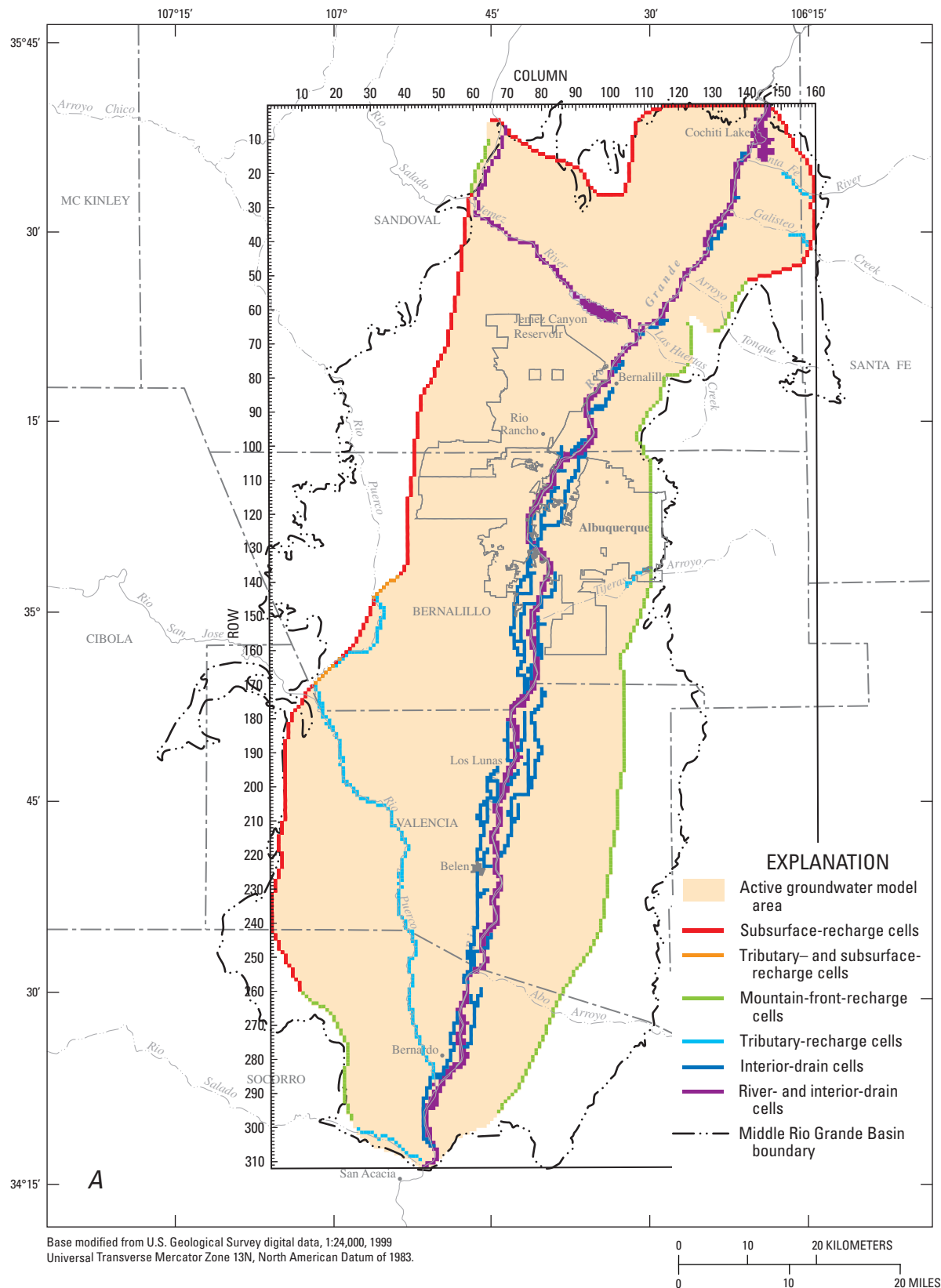


Figure 2.12A. Revised groundwater-flow model showing groundwater-flow model domain and selected boundary conditions, Middle Rio Grande Basin, New Mexico. With the exception of subsurface recharge, applied to model layers 1–3, boundary conditions are applied to the uppermost active model finite-difference cell. For all deeper layers and where no boundary condition is shown, the lateral boundary is no-flow. Depicted drain-boundary locations (A) are those simulated for the period from Nov. 1, 1991, through the end of the simulation in 2008.

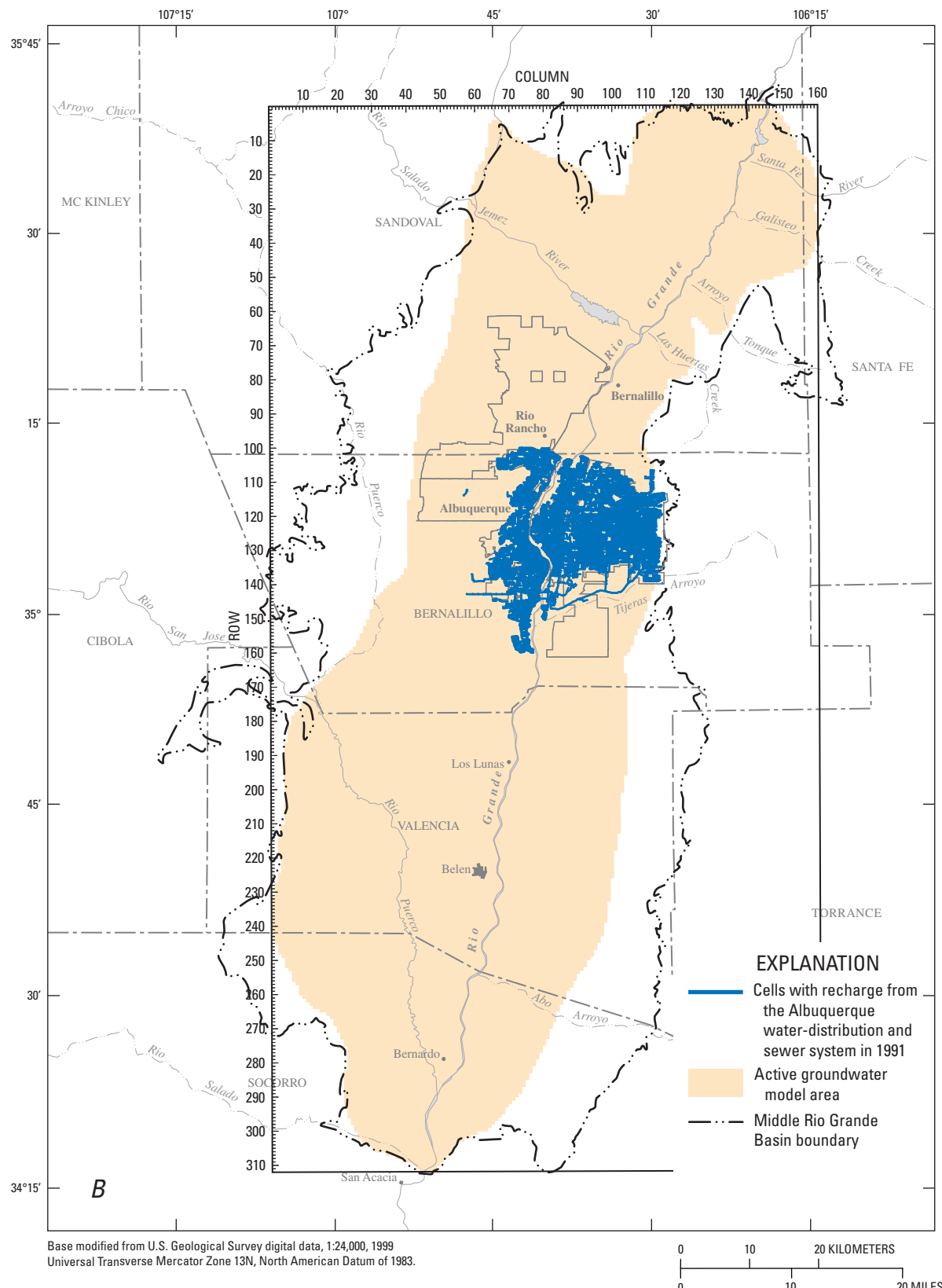


Figure 2.12B. Revised groundwater-flow model showing water-distribution and sewer system, Middle Rio Grande Basin, New Mexico. With the exception of subsurface recharge, applied to model layers 1–3, boundary conditions are applied to the uppermost active model finite-difference cell. For all deeper layers and where no boundary condition is shown, the lateral boundary is no-flow. Depicted drain-boundary locations (A) are those simulated for the period from Nov. 1, 1991, through the end of the simulation in 2008.

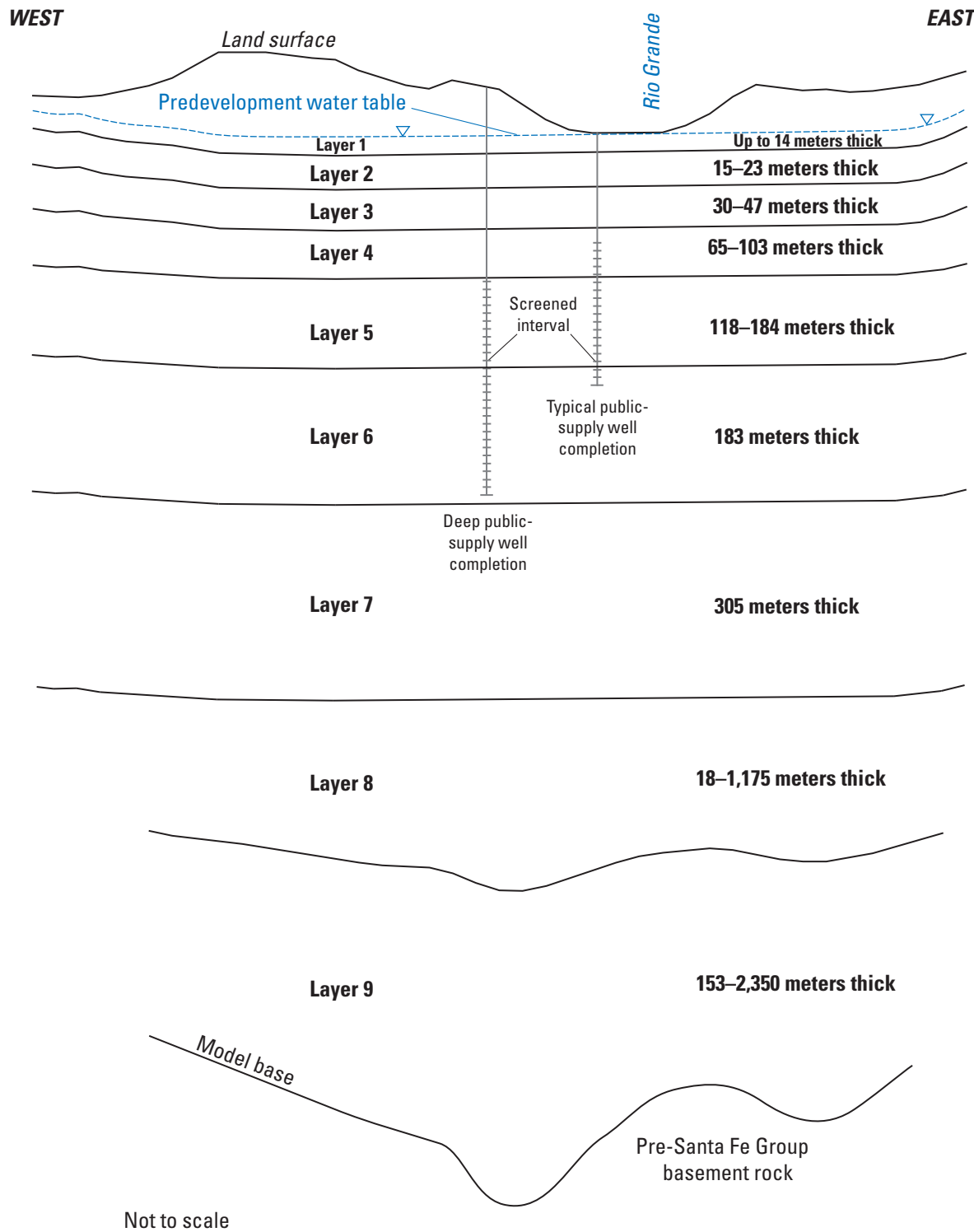


Figure 2.13. Configuration of layers in the revised groundwater-flow model, Middle Rio Grande Basin, New Mexico (modified from McAda and Barroll, 2002).

Simulation-Code Modifications

Modifications to the Well Package, which were previously documented by McAda and Barroll (2002), and that reassign specified flows in cells that dry out to successively deeper model layers, were made to the MODFLOW-2005 version of the source code. A version of the executable code that runs under Windows® operating systems was compiled with double precision, which reduced mass-balance errors during simulation time steps when cells dry out. Use of the NOCV-CORRECTION option in the Layer Property Flow Package (Harbaugh, 2005) was required for model convergence.

Boundary Conditions and Model Stresses

The top of the groundwater model corresponds to the land surface. The bottom of the groundwater model is a no-flow boundary that corresponds to the base of the Santa Fe Group aquifer system. The perimeter of the model domain is simulated with specified-flow boundary conditions. Other features within the model domain are simulated with either specified-flow or head-dependent-flow boundary conditions, as described below.

Specified-Flow Boundaries

Flows representing mountain-front and tributary recharge, seepages from canals, irrigated areas, and septic systems, and leakage from the sewer/water collection/distribution systems for the greater Albuquerque metropolitan area were specified into the uppermost active finite-difference cells in each model layer (figs. 2.12A and B). Flows representing subsurface underflow from outside the perimeter of the model domain and domestic groundwater withdrawals from within the MRGB were specified as described below.

Subsurface, Mountain-Front, and Tributary Recharge

Specified flows to layers 1 through 3 along most of the western and northern model boundaries simulate underflow (subsurface recharge) into the basin based on information described in McAda and Barroll (2002), the total of which was $37 \times 10^6 \text{ m}^3/\text{yr}$ (table 2.5).

A total of $15 \times 10^6 \text{ m}^3/\text{yr}$ of mountain front recharge was specified into the uppermost active model layer along the northern, eastern, and southwestern boundaries of the model (table 2.5) as described in McAda and Barroll (2002). Recharge rates calculated by Anderholm (2001) along the Sandia, Manzanita, Manzano, and Los Pinos Mountains are included in the total value.

The total of $11.1 \times 10^6 \text{ m}^3/\text{yr}$ (table 2.5) of tributary recharge estimated by McAda and Barroll (2002) was specified with the Recharge Package (Harbaugh, 2005). Simulated recharge from tributaries along the southern and western model boundaries, which correspond to the Rio Salado and Rio Puerco, respectively, accounts for $3.0 \times 10^6 \text{ m}^3/\text{yr}$ of this

total. In the northeastern part of the MRGB, specified recharge from Galisteo Creek and the Santa Fe River was 2.2×10^6 and $4.3 \times 10^6 \text{ m}^3/\text{yr}$, respectively. On the eastern side of the MRGB, a portion ($0.9 \times 10^6 \text{ m}^3/\text{yr}$) of the total recharge calculated by Anderholm (2001) in the area of Tijeras Arroyo has been simulated as tributary recharge, and the remainder has been simulated as mountain-front recharge. Recharge specified from the Rio Puerco was $0.7 \times 10^6 \text{ m}^3/\text{yr}$.

Seepage

Canal seepage was simulated within the Rio Grande inner valley for a network that also includes laterals, feeder canals, and ditches. A Geographic Information System (GIS) database (R.A. Durall, U.S. Geological Survey, written commun., 2001) that contains width and depth data was used to define the canal network. Where data were unavailable, characteristics were based on average conditions for the same feature class. Canal seepage was not explicitly specified prior to 1930 due to a lack of data, but it was considered part of the specified crop-irrigation seepage. Because canals were both constructed and abandoned between 1900 and 2000, the locations of specified canal seepage change between stress periods. Canal seepage was not simulated for the 4.5-month long stress periods after 1989 because canals were not operated during the winter. Using the method and equation described in McAda and Barroll (2002), recharge specified into the aquifer from canal seepage for the year ending on October 31, 1999, was calculated to be $115 \times 10^6 \text{ m}^3/\text{yr}$ (table 2.5).

Specification of the spatial distribution of crop-irrigation seepage was based upon GIS data of land use in the Rio Grande inner valley for 1935 (National Biological Service, undated) and for 1955, 1975, and 1992 (Bureau of Reclamation, undated). Specification of crop-irrigation seepage along the Jemez River Valley was based upon the Bureau of Reclamation data from 1955 and 1975. McAda and Barroll (2002) calculated an average recharge rate (weighted by crop types) of $0.21 \text{ m}/\text{yr}$ for 1991 and 1993 that was reduced to $0.15 \text{ m}/\text{yr}$ to account for the rotation of crops and fallow land (McAda and Barroll, 2002). The specified crop-irrigation flux rate was the product of $0.15 \text{ m}/\text{yr}$ with the fraction of cropland area in a model cell. Because crop irrigation occurs mainly during the irrigation season, it was not included in winter-season stress periods, simulated after 1989. Total specified recharge from crop-irrigation seepage for the year ending on October 31, 1999, was $41 \times 10^6 \text{ m}^3/\text{yr}$ (table 2.5).

Septic-field seepage originates from septic tanks and leach fields in populated areas that are not connected to sewage collection systems. Specification of septic-field seepage with the Recharge Package for stress periods after 1960 was based on population density. Prior to 1960, most of the population in unsewered areas lived in the Rio Grande inner valley, where septic-return flows were considered to be volumetrically insignificant compared with other components of the Rio Grande surface-water system. Population density was determined using U.S. Census Bureau tract data from 1970

Table 2.5. Model-computed net annual groundwater budgets for steady-state conditions and year ending October 31, 1999, for the revised groundwater-flow model, Middle Rio Grande Basin, New Mexico.

[m³/yr; cubic meters per year; —, not applicable]

| Water-budget component | Steady state | | | | Year ending October 31, 1999 | | | |
|---|---|--|---|-------------------------------------|---|--|--|-------------------------------------|
| | Specified net flow (10 ⁶ m ³ /yr) | Computed net flow (10 ⁶ m ³ /yr) | Total net flow (10 ⁶ m ³ /yr) | Percentage of net inflow or outflow | Specified net flow (10 ⁶ m ³ /yr) | Computed net flow (10 ⁶ m ³ /yr) | Net flow rate (10 ⁶ m ³ /yr) | Percentage of net inflow or outflow |
| Model inflow (recharge) | | | | | | | | |
| Mountain-front recharge | 15 | — | 15 | 10 | 15 | — | 15 | 3 |
| Tributary recharge | 11 | — | 11 | 7 | 11 | — | 11 | 2 |
| Subsurface inflow | 37 | — | 37 | 25 | 37 | — | 37 | 6 |
| Canal seepage | 0 | — | 0 | 0 | 115 | — | 115 | 20 |
| Crop-irrigation seepage | 0 | — | 0 | 0 | 41 | — | 41 | 7 |
| Rio Grande and Cochiti Lake ¹ | — | 74 | 74 | 49 | — | 264 | 264 | 45 |
| Jemez River and Jemez Canyon Reservoir ¹ | — | 14 | 14 | 9 | — | 16 | 16 | 3 |
| Septic-field seepage | 0 | — | 0 | 0 | 3 | — | 3 | 1 |
| Sewer- and distribution-system leakage | 0 | — | 0 | 0 | 14 | — | 14 | 2 |
| Aquifer storage ² | — | 0 | 0 | 0 | — | 67 | 67 | 11 |
| Total inflow³ | — | — | 151 | 100 | — | — | 583 | 100 |
| Model outflow (discharge) | | | | | | | | |
| Riverside drains | — | 0 | 0 | 0 | — | 148 | 148 | 25 |
| Interior drains | — | 0 | 0 | 0 | — | 132 | 132 | 23 |
| Groundwater withdrawal ⁴ | 0 | — | 0 | 0 | 191 | — | 191 | 33 |
| Riparian evapotranspiration | — | 152 | 152 | 100 | — | 112 | 112 | 19 |
| Total outflow³ | — | — | 152 | 100 | — | — | 583 | 100 |

¹ Cochiti Lake and Jemez Canyon Reservoir were not present during steady-state conditions.

² Net inflow of water from aquifer storage reflects loss of water from aquifer storage to the groundwater system (that is, a decline in aquifer storage).

³ Due to flow rate rounding, budget discrepancies in the table differ from the corresponding model output. Model-computed volumetric budget discrepancies are 0.2 percent for the steady-state stress period and 0.07 percent for the stress period ending October 31, 1999.

⁴ Includes withdrawals for domestic, municipal, commercial, and industrial uses.

through 2000 (U.S. Census Bureau, 1970; 1980; 1990; 2001b). The amount of septic-field seepage applied to a model cell was calculated as the product of the population in the cell with the rate of septic-field seepage per person (McAda and Barroll, 2002). Assuming that 90 to 95 percent of indoor water use was not consumed (McAda and Barroll, 2002), and that average indoor water use is approximately 0.24 m^3 per person per day (Wilson, 1992), the average seepage rate was 0.23 m^3 per person per day. Specified recharge from septic field seepage for the year ending on October 31, 1999, totaled $3 \times 10^6 \text{ m}^3/\text{yr}$.

Water-level drawdowns simulated by the McAda and Barroll (2002) model were greater than drawdowns observed under Albuquerque east of the Rio Grande. McAda and Barroll (2002) noted that water-distribution and sewer system leakages, which were not simulated in their model, should decrease water-level drawdowns. Water-distribution-system losses, which were primarily attributed to leakage, metering inaccuracies, and unauthorized consumption during the years 2004 to 2007, ranged from 9.9 percent to 15.4 percent (City of Albuquerque, 2009). Because the quantity of leakage from the Albuquerque water-distribution and sewer systems has been uncertain, leakage was assumed to be 10 percent of the City of Albuquerque annual groundwater withdrawals for each stress period of this simulation. GIS databases of the extent of the Albuquerque Metropolitan area in the years 1935, 1951, 1973, and 1991 (Feller and Hester, 2001) were intersected with GIS databases of the City of Albuquerque water-distribution and sewage-pipe systems to generate geospatial data of the areas susceptible to pipe leakage at those times. Although the spatial distributions of water-pipe leaks (New Mexico Environmental Finance Center, 2006) and sewer-pipe leaks (Camp Dresser & McKee, 1998) have been correlated with material pipe types, the leaky-pipe recharge flux was homogeneously specified over areas designated as susceptible to pipe leakage in each stress period (fig. 2.12B). Simulated recharge to the aquifer from sewer and water collection/distribution losses for the year ending on October 31, 1999, was $14 \times 10^6 \text{ m}^3/\text{yr}$.

Domestic Groundwater Withdrawals

Withdrawals of groundwater from domestic wells were simulated with a modified version of the Well Package beginning with the 1960–64 stress period. Domestic-well withdrawals were assigned to model cells based on population densities from U.S. Census Bureau tract data from 1970, 1980, 1990, and 2000 (U.S. Census Bureau, 1970; 1980; 1990; 2001b). A per-person withdrawal rate of 0.38 m^3 per day (for indoor and outdoor purposes) was used based on a study by Wilson (1992). The total domestic-well withdrawal from a model cell was calculated as the product of this rate times the population density times the cell area. Because domestic-well construction data were lacking, layer assignments for domestic wells were based on the steady-state water table depth: layer 1 for water-table depths of less than 15.24 m, layer 2 for depths 15.24 to 91.44 m, and layer 3 for depths greater than 91.44 m. The modified version of the Well Package transfers

withdrawals in cells that become dry to the next lower active cell, thereby preventing exclusion of domestic-well withdrawals when the water table declines below the bottom of the specified model layer. Specified domestic-well withdrawals for the year ending on October 31, 1999, totaled $8.2 \times 10^6 \text{ m}^3/\text{yr}$.

Head-Dependent-Flow Boundaries

Reported groundwater withdrawals, the Rio Grande and Jemez River, riverside and interior drains, Jemez Canyon Reservoir and Cochiti Lake, and evapotranspiration were simulated as head-dependent-flow boundaries (fig. 2.12A).

Reported Groundwater Withdrawals

Reported withdrawals of groundwater from production wells serving municipal, commercial, and industrial purposes were simulated with the Multi-Node Well Package (Halford and Hanson, 2002). For each stress period, the total withdrawal from each well was specified based on monthly or annual withdrawal reports that were adjusted to the stress period timing. The simulated layer-by-layer distribution of the total withdrawal specified for the well depends largely on the specified hydraulic conductivities in each of the finite-difference cells penetrated by the well-screen interval and on differences in simulated head between the withdrawal well and the heads in each of those cells. Although hydraulic heads in production wells are also affected by turbulent-flow head losses near the well and flow through drilling-damaged formation, gravel pack, or the well screen, these effects were not directly simulated.

Groundwater-withdrawal records were obtained from the New Mexico Office of the State Engineer, the City of Albuquerque, and Bjorklund and Maxwell (1961). Because groundwater-withdrawal data prior to the 1960s were limited, many earlier withdrawal rates for the City of Albuquerque, the University of New Mexico, Kirtland Air Force Base, and two local power-plant supply wells were extrapolated from later records (Kernodle and others, 1995). For wells not operated by these entities, withdrawals were specified only in years for which records were available. Consequently, model-simulated withdrawals may under-represent actual withdrawals.

Rivers

Seepage between the Rio Grande and the underlying Santa Fe Group aquifer system was simulated with the River Package (Harbaugh, 2005). The simulated conductance between a river boundary and an underlying finite-difference cell is the product of the riverbed hydraulic conductivity with the riverbed area in the model cell, divided by the riverbed thickness. McAda and Barroll (2002) estimated a riverbed hydraulic conductivity of 0.03 m per day by calibration of simulated river seepage to an independent flow loss calculation for the Rio Grande and riverside drains (Veenhuis, 2002). The riverbed area varies depending on the geometry of the Rio

Grande within individual model cells, and riverbed thickness was assumed to be 0.3 m (Kernodle and others, 1995).

Riverbed areas within each model cell were calculated using the National Biological Service GIS databases for 1935 and 1989 (Roelle and Hagenbuck, 1994), which provided information about perennially and seasonally flooded areas. The specified riverbed areas for the revised model differ from the McAda and Barroll (2002) model because they include exposed sandbars. McAda and Barroll (2002) used measurements of historically low flows in October and high flows in May to estimate average conditions from 1900 through 1989. The Rio Grande stage during this time period was determined from USGS topographic maps. For the seasonal stress periods beginning in 1990, riverbed area within each model cell was adjusted based on average seasonal flow conditions at USGS streamflow-gaging station 08330000 (fig. 2.7). McAda and Barroll (2002) calculated percentages of seasonally flooded areas to add to perennially flooded areas to yield riverbed areas for each model cell at various times. They also derived a relation between river-stage change and the ratio of perennially to seasonally flooded channel areas that was used to specify the stage for each model cell during post-1989 stress periods in the revised model.

Like the Rio Grande, the Jemez River is in hydraulic connection with the aquifer system and was simulated with the River Package. Unlike the Rio Grande, however, only limited descriptive information was available for the Jemez River. The riverbed hydraulic conductance was specified as the product of the length of the river in a model cell and a parameter that incorporated river-bed width, thickness, and hydraulic conductivity. This parameter was specified as 75 and 25 m/d for the upper and lower reaches of the river, respectively. According to McAda and Barroll (2002): “The upper reach has a steeper gradient and a higher flow energy than the lower reach, resulting in a greater proportion of coarse material in the riverbed; therefore the upper reach was assumed to have a relatively larger riverbed hydraulic conductivity than the lower reach.”

Drains

McAda and Barroll (2002) classified drains in the Rio Grande valley into two types: “riverside drains” and “interior drains.” Beginning in the late 1920s, riverside drains were constructed on either side of the Rio Grande in the MRGB to mitigate water logging of agricultural land near the Rio Grande, and to enable water to be returned to the Rio Grande. Riverside drains can either gain or lose water, depending upon the drain stage and drain-bed altitude with respect to the water table, and were therefore simulated with the River Package. A GIS database (R.A. Durall, U.S. Geological Survey, written commun., 2001) was used to specify the locations, areas, and bed elevations of the drains. Following McAda and Barroll (2002), all drain-bed conductances were calculated by assuming the existence of “drain beds” with a hydraulic conductivity of 0.3 m/d and a thickness of 0.3 m. Riverside drains

simulated 148×10^6 m³/yr of net outflow from the aquifer during the year ending on October 31, 1999.

Interior drains were also installed during the late 1920s and early 1930s to intercept canal and crop-irrigation seepage in the inner valley. Water captured by interior drains from the shallow part of the aquifer system is discharged to the riverside drains. Because interior drains are thought to only intercept and convey water, they were simulated using the Drain Package (Harbaugh, 2005). Drain stages were specified for each cell as the land surface elevation at the center of the cell minus the average drain-stage depth below land surface. Interior drains simulated a net outflow of 132×10^6 m³/yr from the aquifer during the year ending on October 31, 1999.

Lakes and Reservoirs

The Jemez Canyon Reservoir was constructed along the lower reach of the Jemez River above its confluence with the Rio Grande to trap sediment. Prior to 1979, the reservoir stored water for short periods that were not simulated. For simulation stress periods beginning in 1979 and continuing through October 2000, after which the reservoir was completely drained, the reservoir was simulated with the River Package. Average annual stages were used for all stress periods; no attempt was made to simulate seasonal changes in reservoir stage. The reservoir bottom area was estimated for each stage using USGS 30-meter 1:24,000 Digital Elevation Models (DEMs). Because information on the hydraulic conductivity of the reservoir bed was not available, McAda and Barroll (2002) estimated the reservoir bed hydraulic conductance during model calibration. Their factor of 0.0015 per day (representing hydraulic conductivity divided by bed thickness) was applied to the reservoir area for 1979–1984; this value was reduced to 0.001 per day for 1985–2001 to account for the accumulation of fine-grained sediment. Simulated combined seepage from Jemez Canyon Reservoir and the Jemez River to the aquifer was 16×10^6 m³/yr during the year ending on October 31, 1999; for steady state, simulated recharge from the Jemez River alone was 14×10^6 m³/yr.

Cochiti Lake is located along the upper reach of the Rio Grande, and it began storing water in November 1973. Because the model uses a 5-year stress period for 1970–1974, simulation of Cochiti Lake with the River Package commences with the model stress period that begins in 1975. McAda and Barroll (2002) adjusted the Cochiti Lake bed hydraulic conductance to calibrate simulated seepage to measurement-based seepage estimates. Their factors, which represent hydraulic conductivity divided by bed thickness and range from 0.001 to 0.0027 per day, were applied to the reservoir area for simulated annual-average reservoir stages obtained from USGS Water-Data Reports for New Mexico (various years). The steep topography near Cochiti Lake required USGS 10-meter DEMs for lake-bed-area calculations. Simulated combined seepage from Cochiti Lake and the Rio Grande to the aquifer was 264×10^6 m³/yr during the

year ending on October 31, 1999; for steady state, simulated recharge from the Rio Grande alone was $74 \times 10^6 \text{ m}^3/\text{yr}$.

Riparian Evapotranspiration

Evapotranspiration from the riparian corridors that border the Rio Grande and Jemez River was simulated with the Evapotranspiration Segments Package (Banta, 2000). Simulated evapotranspiration rates decrease in linear segments from 1.5 m/yr where the water table is at land surface, to 0.6 m/yr where the water table is 2.7 m below land surface, to 0.2 m/yr where the water table is 4.9 m below land surface, and finally to zero where the water table is 9.1 m below land surface. The depths delineating these linear segments and associated rates correspond to the rooting depths of salt cedar (Bureau of Reclamation, 1973), willow (Robinson, 1958), and cottonwood trees (Robinson, 1958), respectively. The 1935 Rio Grande riparian corridor delineation (National Biological Service GIS data, undated) was used to specify evapotranspiration areas for stress periods from 1900 through 1944. Additional GIS data for Rio Grande riparian corridor delineations for 1955, 1975, and 1992 (Bureau of Reclamation, undated) were used for the remaining simulated periods. To specify riparian evapotranspiration areas along the Jemez River, stress periods from 1900 to 1964 utilized 1955 land-use data, and stress periods after 1965 utilized 1975 land-use data. Simulated evapotranspiration from the area under Jemez Canyon Reservoir was discontinued for stress periods after the reservoir was filled. For seasonal stress periods after 1989, evapotranspiration was simulated only during the summer stress periods. Simulated outflow from the aquifer due to riparian evapotranspiration was $152 \times 10^6 \text{ m}^3/\text{yr}$ for the steady-state stress period and $112 \times 10^6 \text{ m}^3/\text{yr}$ for the stress periods representing the year ending on October 31, 1999.

Aquifer Hydraulic Properties

McAda and Barroll (2002) based their distribution of zones of simulated hydraulic conductivity upon a three-dimensional digital geologic model of the hydrostratigraphic units (Cole, 2001a), with modifications based on findings of Hawley and Haase (1992), Hawley and others (1995), Connell and others (1998), and Smith and Kuhle (1998). Based partly on further work by Connell (2006), this zone distribution was modified in model layer 4 to simulate higher hydraulic conductivities in an area previously zoned for silt. The hydraulic-property parameter values documented by McAda and Barroll (2002) were used as starting values for model calibration by

nonlinear regression with PEST (Doherty, 2005), and they are tabulated with the corresponding calibrated parameter values in table 2.6. Parameters representing aquifer storage properties and various recharge fluxes were not modified in the PEST calibration. The calibrated horizontal hydraulic conductivities specified in the revised model range from 0.02 to 15.5 m/d in the east-west direction along model rows (fig. 2.14A1–A9). Horizontal anisotropy, which is expressed as the ratio of north-south to east-west hydraulic conductivity, in model layers 3 through 8 ranges from 5:1 along a naturally occurring groundwater trough (Meeks, 1949; Bjorklund and Maxwell, 1961; Bexfield and Anderholm, 2000) located in the west-central portion of the MRGB (fig. 2.14B1) to 1.5:1 throughout most of the central portion of the MRGB, and is isotropic in the northern and peripheral areas of the MRGB. The pattern of horizontal anisotropy for model layers 1 and 2 is similar, but isotropic in the post-Santa Fe Group alluvium within the Rio Grande inner valley (fig. 2.14B2). Horizontal hydraulic conductivity in model layer 9 is isotropic. The finite-difference model grid is aligned with an assumed north-south principal direction of anisotropy that corresponds to the north-south orientation of major faults in the basin, some of which are thought to impede groundwater flow. Major faults that McAda and Barroll (2002) determined were likely to act as “significant flow barriers” were simulated to vertically penetrate all nine model layers with the Horizontal Flow Barrier (HFB) package (figs. 2.14B1 and 2.14B2).

Vertical hydraulic conductivity is represented as a fraction of the horizontal hydraulic conductivity in two zones in model layers 1 and 2; one zone represents axial-river and alluvium deposits in the inner valley, where the ratio of horizontal to vertical hydraulic conductivity is 1.06:1, and the second zone represents the remainder of the model domain, outside of the inner valley, where the ratio of horizontal to vertical hydraulic conductivity ratio is 132:1 (fig. 2.14C). The vertical anisotropy ratio of 132:1 was also used throughout layers 3–9 and is similar to that simulated by other models of the MRGB (McAda and Barroll, 2002; McAda, 2001; Tiedeman and others, 1998); however, the vertical anisotropy representing the axial-river and alluvium deposits in the inner valley is significantly lower than the values used in previous models.

Specific storage was specified at 6.6×10^{-6} per meter based on water-level-change and associated extensometric-strain measurements (Heywood, 2001, 1998). Specific yield was specified at 0.20 for all zones representing different lithologies in the model, as was done by McAda and Barroll (2002).

Table 2.6. Parameter values and sensitivities in the revised groundwater-flow model of the Middle Rio Grande Basin near Albuquerque, New Mexico.

[Calibrated values of parameters with names shown in italic type did not differ from initial values]

| Parameter description | Parameter name | Relative sensitivity | Calibrated value | Initial value | Composite sensitivity |
|--|------------------|----------------------|------------------|---------------|-----------------------|
| Horizontal hydraulic conductivity of medium sand | Ksdm | 0.172 | 0.43 | 0.46 | 0.403 |
| Horizontal hydraulic conductivity of axial channel deposits | <i>Kaxial1</i> | .141 | 9.14 | 9.14 | .015 |
| Horizontal hydraulic conductivity of Santo Domingo subbasin | Ksdmc | .141 | 2.23 | 2.44 | .064 |
| Horizontal hydraulic conductivity of buffer area around axial channel deposits | <i>Kaxial2</i> | .131 | 2.96 | 4.57 | .044 |
| Horizontal hydraulic conductivity of eolian sand deposits | Ksdeo | .073 | 1.52 | 2.44 | .048 |
| Horizontal hydraulic conductivity of inner valley alluvium | Kalluv | .068 | 12.50 | 13.72 | .005 |
| Horizontal hydraulic conductivity of fine-medium sand deposits | <i>Ksdfm</i> | .050 | .02 | .02 | 3.297 |
| Horizontal hydraulic conductivity of silty deposits | Ksilts | .050 | 2.13 | .61 | .023 |
| Horizontal hydraulic conductivity of sediment in new zone | Kdirt | .049 | 15.54 | .61 | .003 |
| Horizontal hydraulic conductivity of piedmont sediments | Kpdmt | .042 | 3.66 | .15 | .011 |
| Horizontal hydraulic conductivity of western Santo Domingo subbasin and south | <i>Ksdmcwest</i> | .040 | 2.44 | 2.44 | .016 |
| Horizontal hydraulic conductivity of NW part of Santo Domingo subbasin | <i>Knw</i> | .026 | .15 | .15 | .169 |
| Horizontal hydraulic conductivity of coarse sand and gravel deposits | Kcgsv | .013 | 3.66 | .15 | .004 |
| Horizontal hydraulic conductivity of intrusives | <i>Kintr</i> | .005 | .30 | .30 | .017 |
| Horizontal hydraulic conductivity of volcanics | <i>Kvolc</i> | .003 | 2.44 | 2.44 | .001 |
| Anisotropy of horizontal hydraulic conductivity | HANIyes | .942 | 1.52 | 2 | .620 |
| Isotropy of horizontal hydraulic conductivity in areas defined as horizontally isotropic | <i>HANIno</i> | .543 | 1 | 1 | .543 |
| Anisotropy of horizontal hydraulic conductivity in "trough area" | <i>HANItrf</i> | .188 | 5 | 5 | .038 |
| Ratio of horizontal to vertical hydraulic conductivity | VANI2 | .711 | 132 | 150 | .005 |
| Ratio of horizontal to vertical hydraulic conductivity | VANI1 | .010 | 1.06 | 150 | .009 |

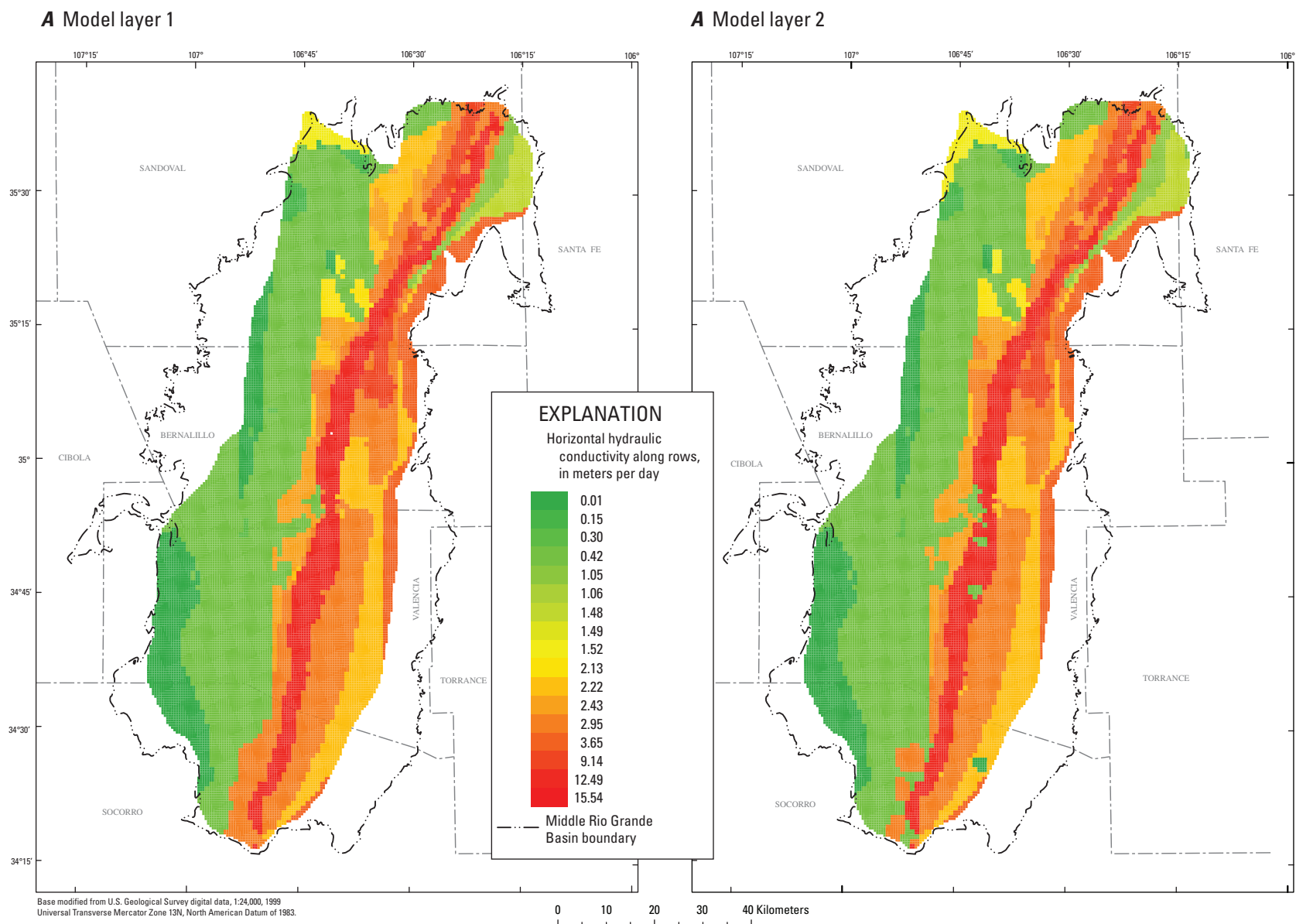


Figure 2.14A1–A2. Distribution of simulated horizontal hydraulic conductivity in the east-west direction for model layers 1–9, Middle Rio Grande Basin, New Mexico.

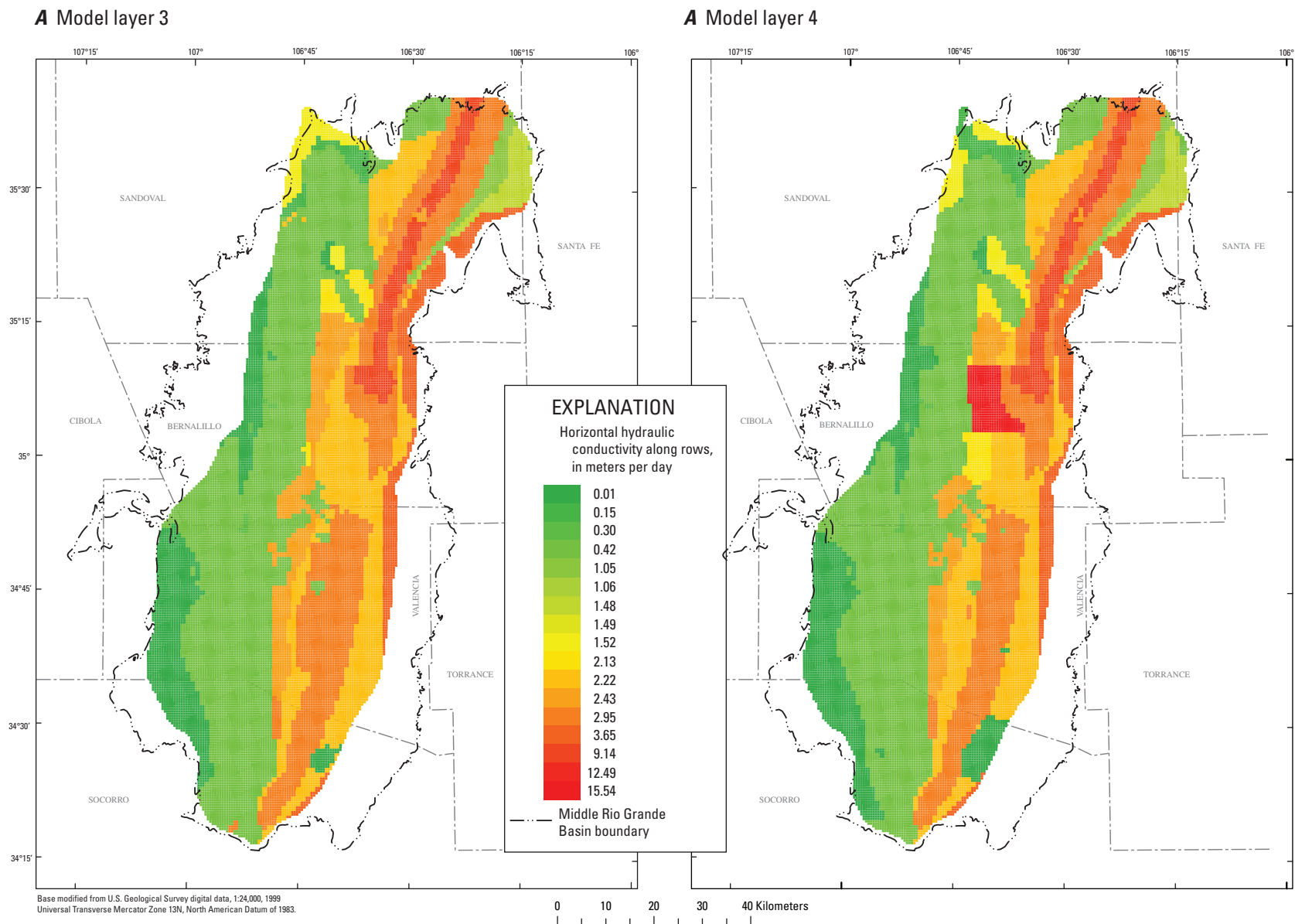


Figure 2.14A3–A4. Distribution of simulated horizontal hydraulic conductivity in the east-west direction for model layers 1–9, Middle Rio Grande Basin, New Mexico.

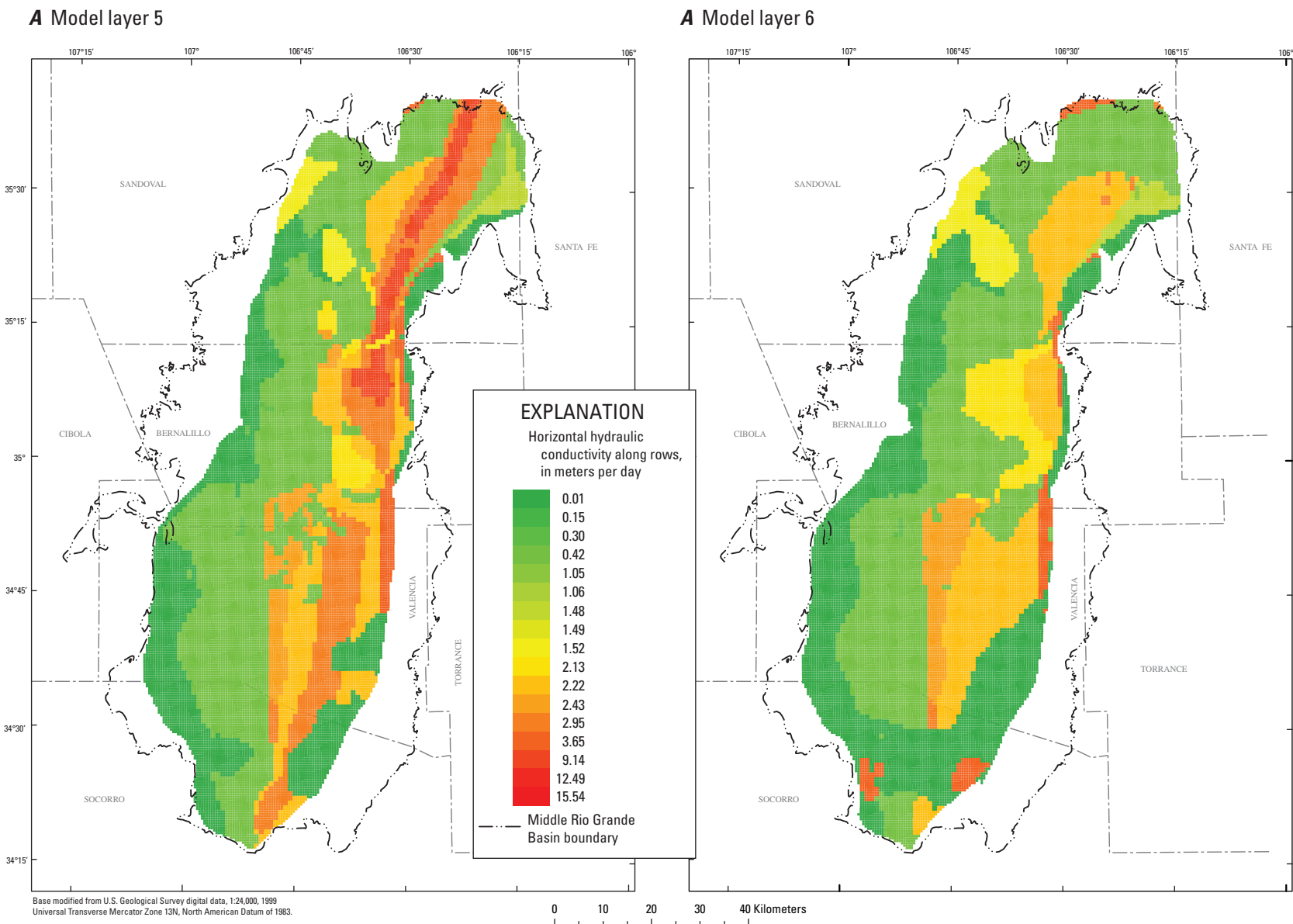


Figure 2.14A5–A6. Distribution of simulated horizontal hydraulic conductivity in the east-west direction for model layers 1–9, Middle Rio Grande Basin, New Mexico.

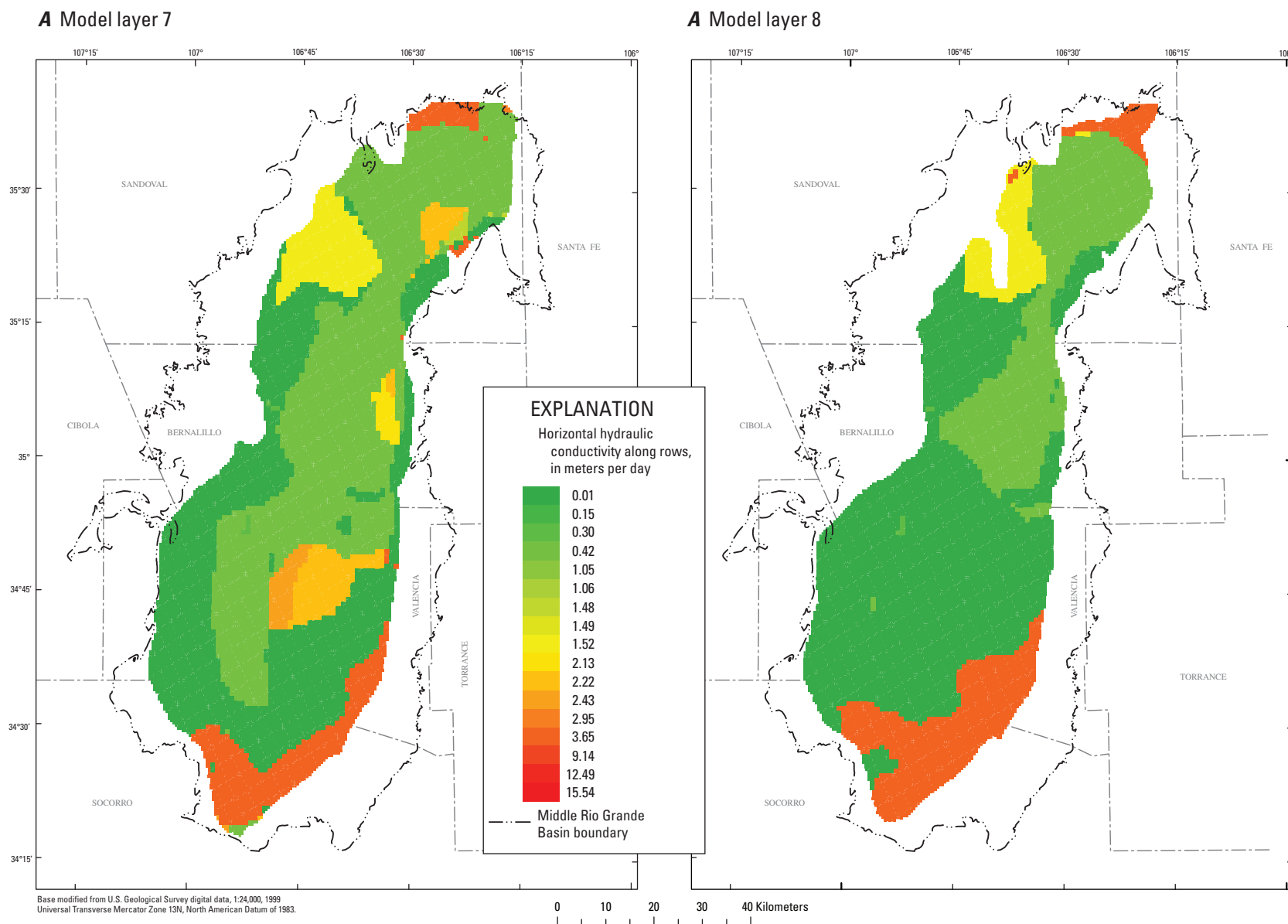


Figure 2.14A7–A8. Distribution of simulated horizontal hydraulic conductivity in the east-west direction for model layers 1–9, Middle Rio Grande Basin, New Mexico.

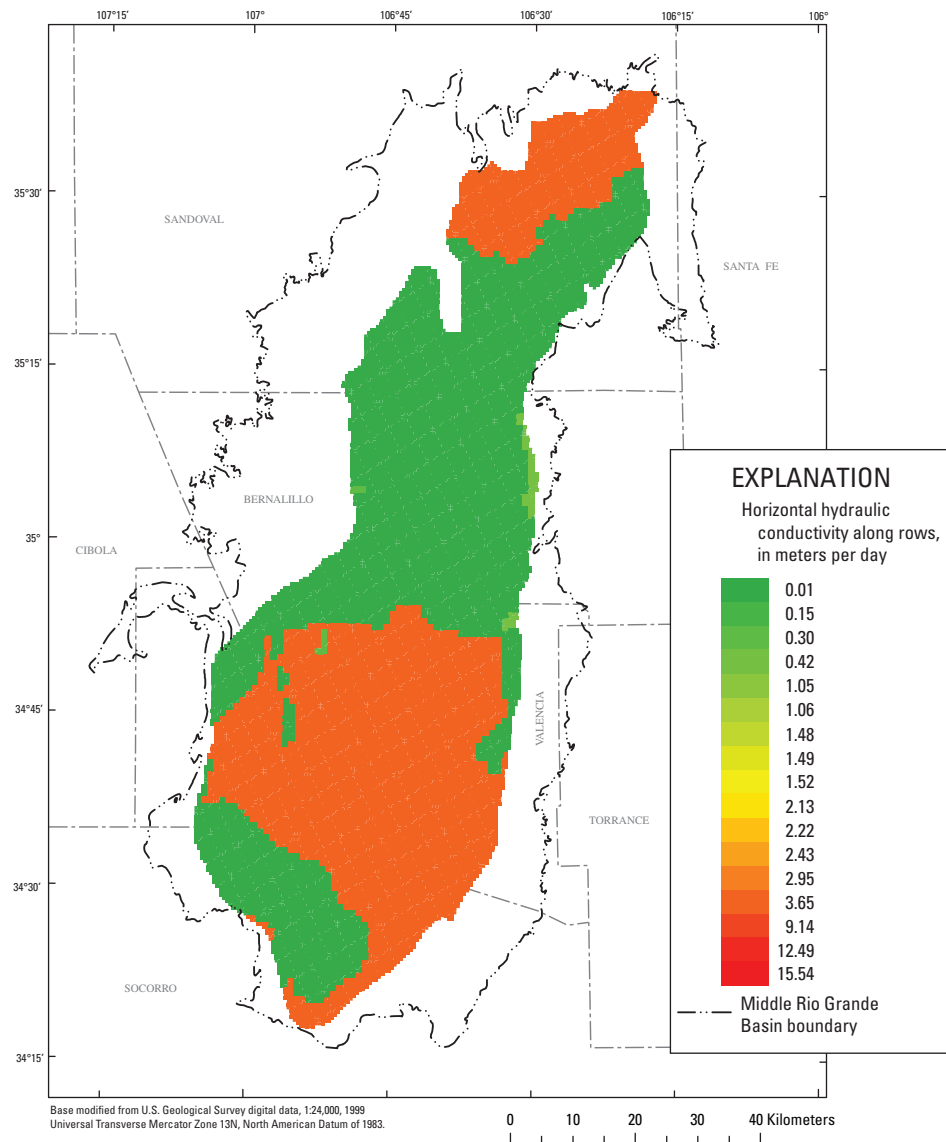
A Model layer 9

Figure 2.14A9. Distribution of simulated horizontal hydraulic conductivity in the east-west direction for model layers 1–9, Middle Rio Grande Basin, New Mexico.

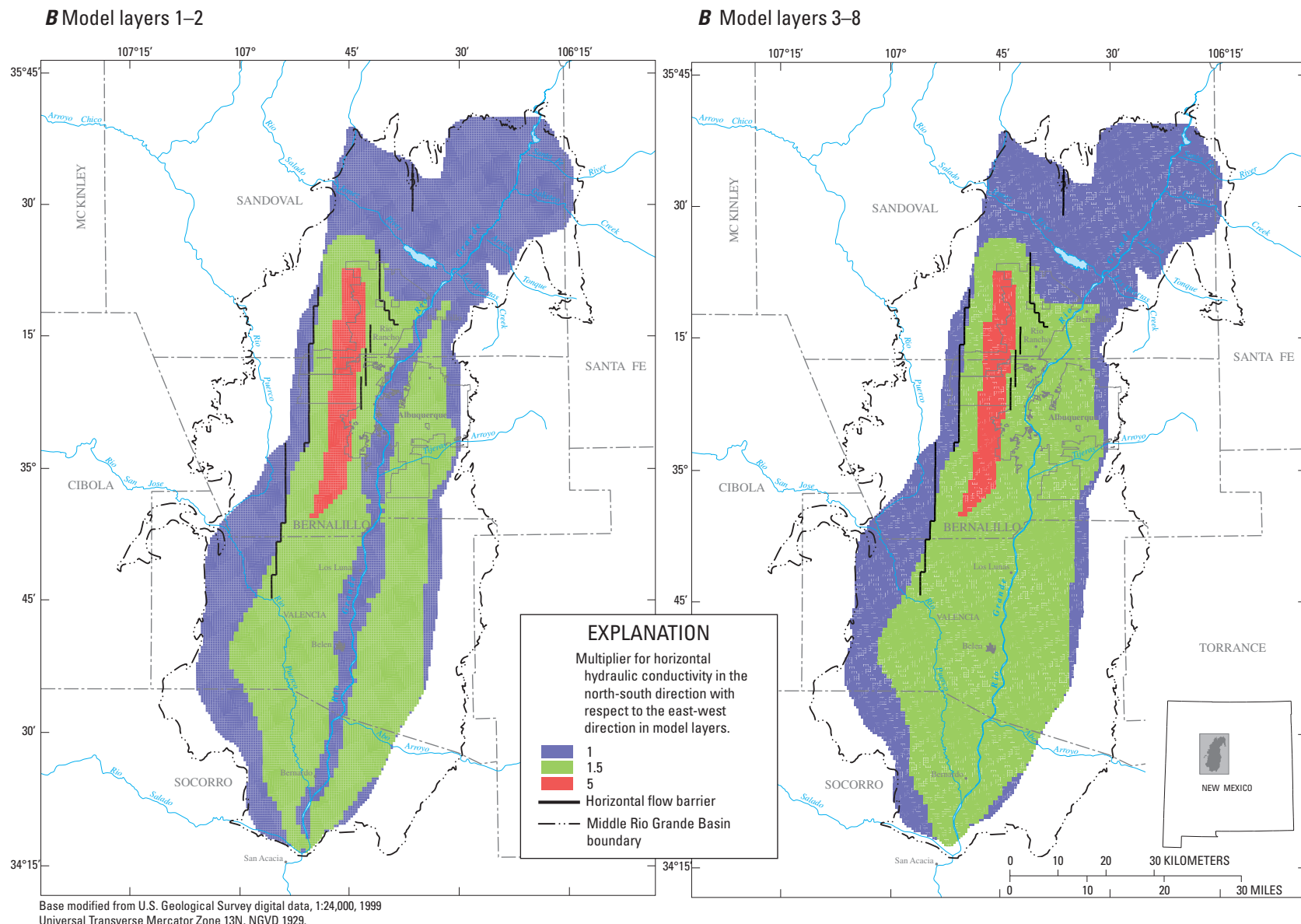


Figure 2.14B. Ssimulated horizontal anisotropy for layers 1–2 and 3–8, Middle Rio Grande Basin, New Mexico.

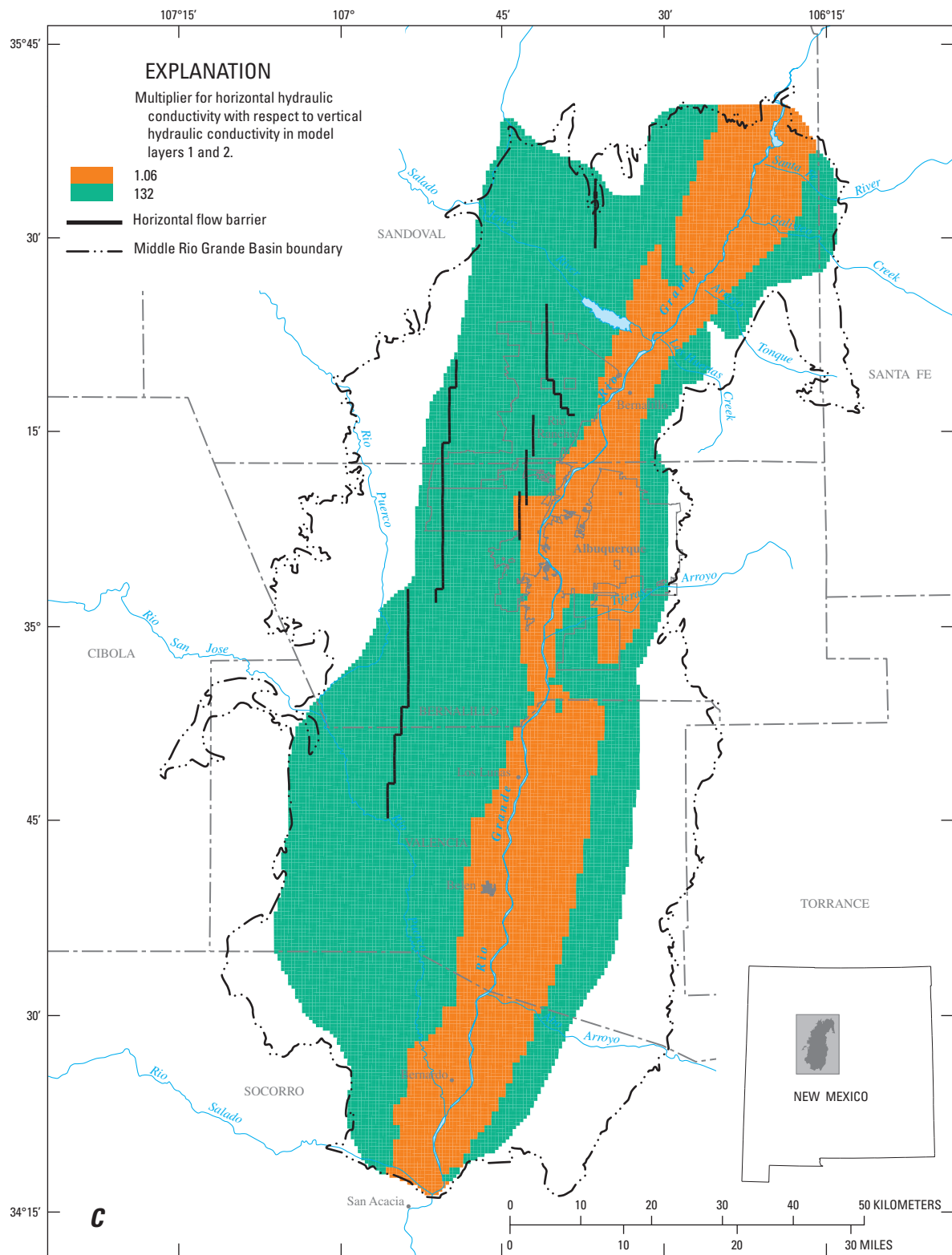


Figure 2.14C. Simulated vertical anisotropy for layers 1–2 of the revised groundwater-flow model, Middle Rio Grande Basin, New Mexico.

Model Evaluation

McAda and Barroll (2002) used a trial-and-error approach to calibrate their MRGB model to 344 reconstructed predevelopment hydraulic heads (Bexfield and Anderholm, 2000), 984 measured hydraulic heads, estimated seepage loss from Cochiti Lake, and a flow-loss measurement (Veenhuis, 2002) along the reach of the Rio Grande between Bernalillo and the Rio Bravo Bridge south of Albuquerque. In addition to head observations utilized by McAda and Barroll (2002), 490 additional head observations (DeWees, 2006) were utilized for calibration of the revised MRGB model by nonlinear regression with PEST. The values of parameters representing horizontal and vertical hydraulic conductivities were estimated by minimizing the objective function:

$$\sum_{i=1}^N (\omega_i h_i - \omega_i h'_i)^2$$

where h is the measured head for observation i , h' is the simulated-equivalent head to observation i , ω_i is the weight applied to observation i and its simulated equivalent, and N is the number of head observations used in the regression, which is 1,818. The head-observation weights (ω_i) utilized by McAda and Barroll (2002), applied as the inverse of the estimated variance in the measurements, were also used for the PEST calibration. Parameter adjustment during PEST calibration caused additional finite-difference cells to “go dry,” which occasionally prevented computation of simulated-equivalent heads at observed locations and times by the Head-Observation Package of MODFLOW. To allow the PEST calibration to proceed under these circumstances, it was necessary to substitute alternative heads for these observations utilizing the program SIM ADJUST (Poeter and Hill, 2008).

PEST computes a “composite sensitivity” (Doherty, 2005) of each model parameter with respect to all the weighted simulated heads ($\omega_i h'_i$). The relative composite sensitivities of parameters included in the regression were calculated by multiplying the composite sensitivities computed at the final parameter values with their corresponding final parameter value, and are summarized in table 2.6.

The head observations common to both the McAda and Barroll (2002) model and the revised model were used to compare overall fit between the two models. For each model, the sum-of-squared unweighted residuals (SSE) were calculated for this observation subset using the equation:

$$SSE = \sum_{i=1}^N (h_i - h'_i)^2$$

where N is the number of head observations common to both models, which is 1,328. The SSE of the revised model is about 82 percent of the SSE of McAda and Barroll (2002) model, indicating a slightly improved overall fit for the revised model.

Simulated Hydraulic Heads

Steady-state hydraulic heads simulated with the revised model of the MRGB generally are within 10 m of reconstructed predevelopment hydraulic heads (Bexfield and Anderholm, 2000) in the vicinity of Albuquerque, along the Rio Grande, and in the southern part of the basin. Eighty-nine percent of the simulated transient hydraulic heads are within 10 m of the measured heads, and the smallest residuals occur in the area described above for the steady-state observations. The largest residuals occur near the lateral model boundaries in the same locations as large residuals discussed by McAda and Barroll (2002) and likely are due to structural-model error, which may include the possible existence of nonsimulated “perched” conditions, uncertainty of recharge, and heterogeneity of hydraulic conductivity in various forms, including faults. Bexfield and Anderholm (2000) also discussed possible causes of observed “hydraulic discontinuities” located near major faults in these areas.

Simulated heads in the area of the water-level trough noted by McAda and Barroll (2002) are as much as 48 m higher than reconstructed steady-state (Bexfield and Anderholm, 2000) heads and water levels measured at observation wells (fig. 2.15). The similar residual magnitude and construction of both models suggests that this misfit is due to similar, yet unknown, structural-model error as discussed by McAda and Barroll (2002).

The locations of 20 observation wells for which McAda and Barroll (2002) also simulated hydrographs are shown in figure 2.15B. Hydrographs simulated with the revised model (figure 2.16) are very similar to those presented by McAda and Barroll (2002), but an improved fit to the observed heads is apparent for five of the wells. For example, heads simulated for the Tierra Mirage observation well (fig. 2.16C) northeast of Albuquerque are lower and closer to observed heads than those simulated with the McAda and Barroll (2002) model. Heads simulated for four observation wells (figures 2.16I–L) in the Albuquerque area better represent drawdown than corresponding heads simulated by the McAda and Barroll (2002) model, which increasingly under predict head through the period of record. The higher hydraulic heads simulated for these observation wells in the revised model probably result from larger simulated vertical hydraulic conductivity and (or) simulated recharge from the water-distribution system in the Albuquerque area.

Residuals of model-simulated hydraulic heads (calculated as measured minus simulated head) are plotted against their corresponding measured values for both the steady-state and all transient stress periods in figure 2.17. Measured hydraulic heads of approximately 1,625 m have the largest residuals, which, as described above, are located south of Albuquerque along the western and eastern model boundaries (fig. 2.15). A histogram of the residual magnitudes (fig. 2.18) illustrates that most are less than 5 m. The largest negative and positive residuals are -48 and 155 m, respectively, with a median of -1.18 m, and a mean of -0.76 m. This negative model bias reflects

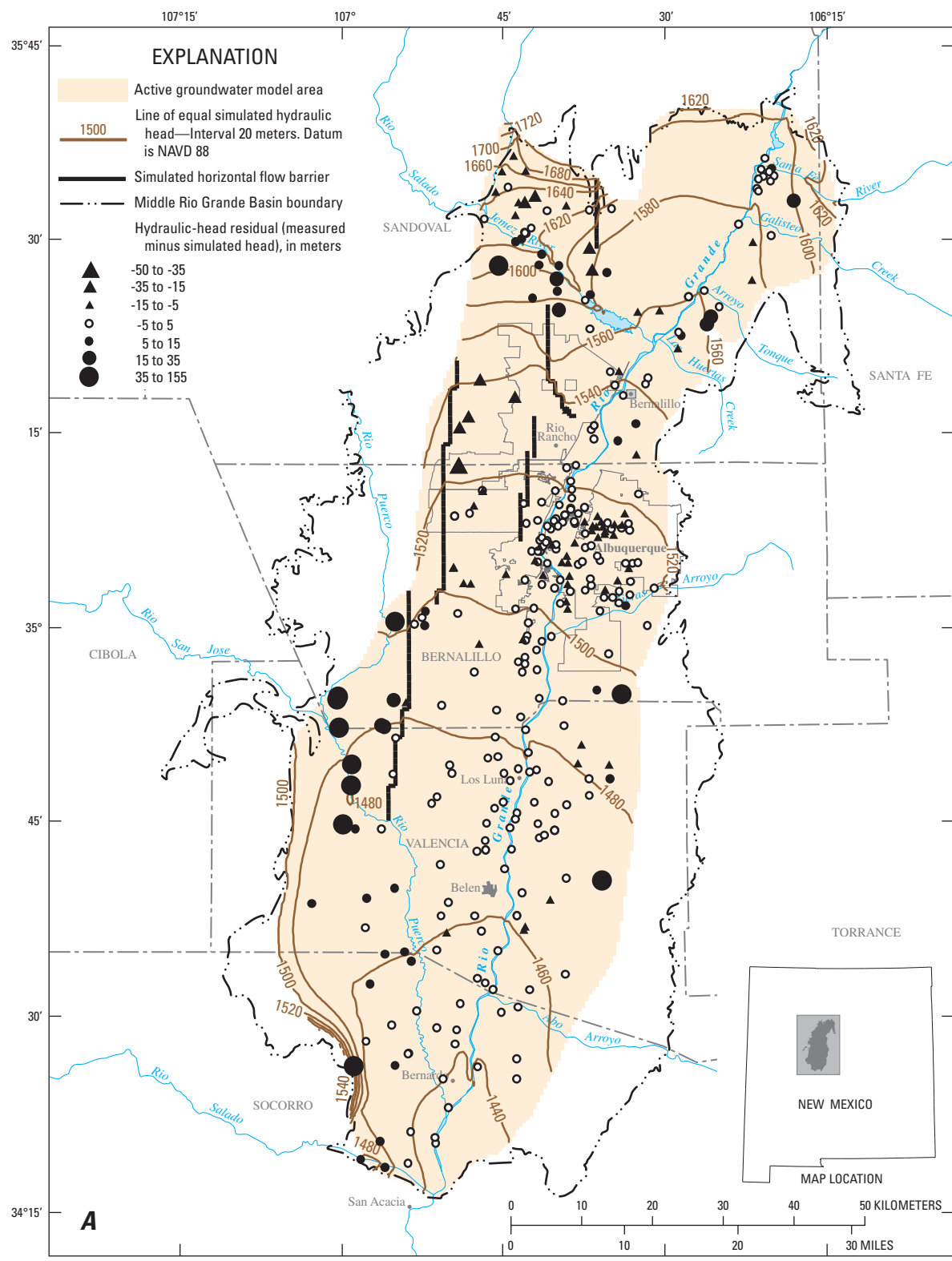
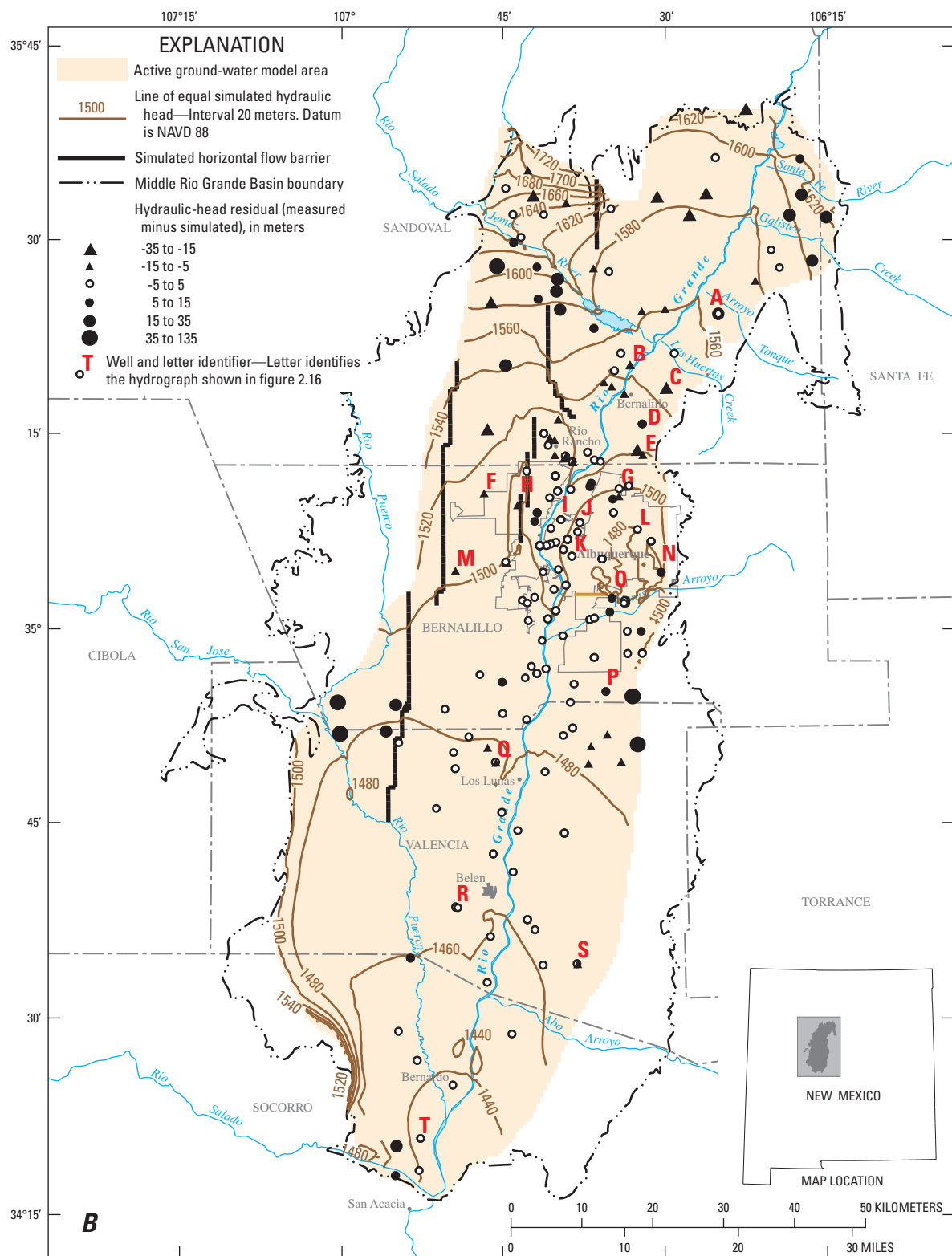


Figure 2.15A. Simulated steady-state water table and hydraulic-head residual at each steady-state observation well, Middle Rio Grande Basin, New Mexico.



Base modified from U.S. Geological Survey digital data, 1:24,000, 1999
Universal Transverse Mercator Zone 13N, North American Datum of 1983.

Figure 2.15B. Simulated March 2008 water table and maximum hydraulic-head residual for the period 1900-2008 at each transient observation well for the revised groundwater-flow model, Middle Rio Grande Basin, New Mexico.

2-46 Hydrogeologic Settings and Groundwater-Flow Simulations for Regional TANC Studies Begun in 2004

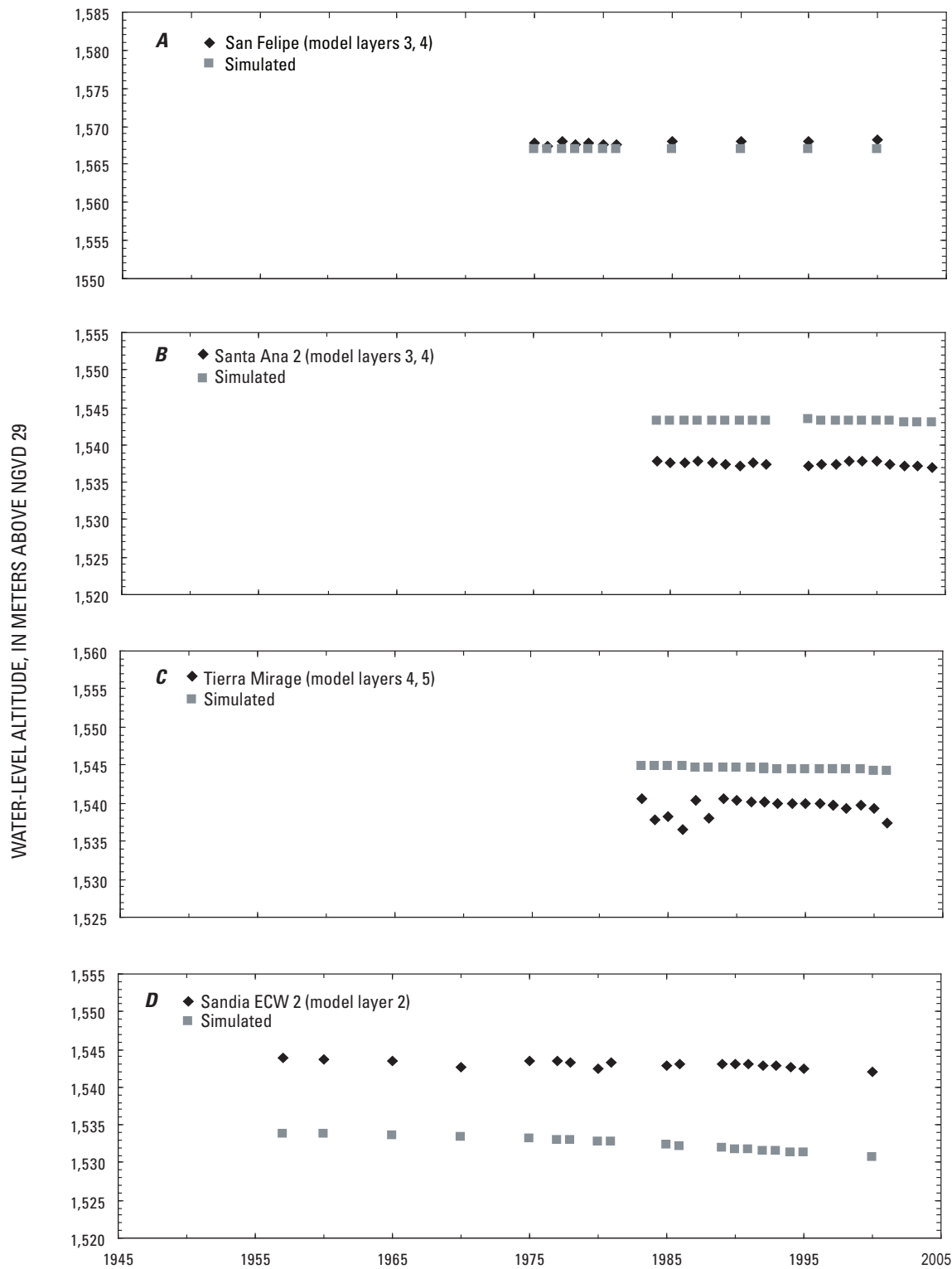


Figure 2.16A–D. Measured and simulated hydraulic heads for selected wells in the revised groundwater-flow model, Middle Rio Grande Basin, New Mexico. Well locations are shown in figure 2.15B. A, San Felipe, model layers 3 and 4; B, Santa Ana 2, model layers 3 and 4; C, Tierra Mirage, model layers 4 and 5; D, Sandia ECW 2, model layer 2.

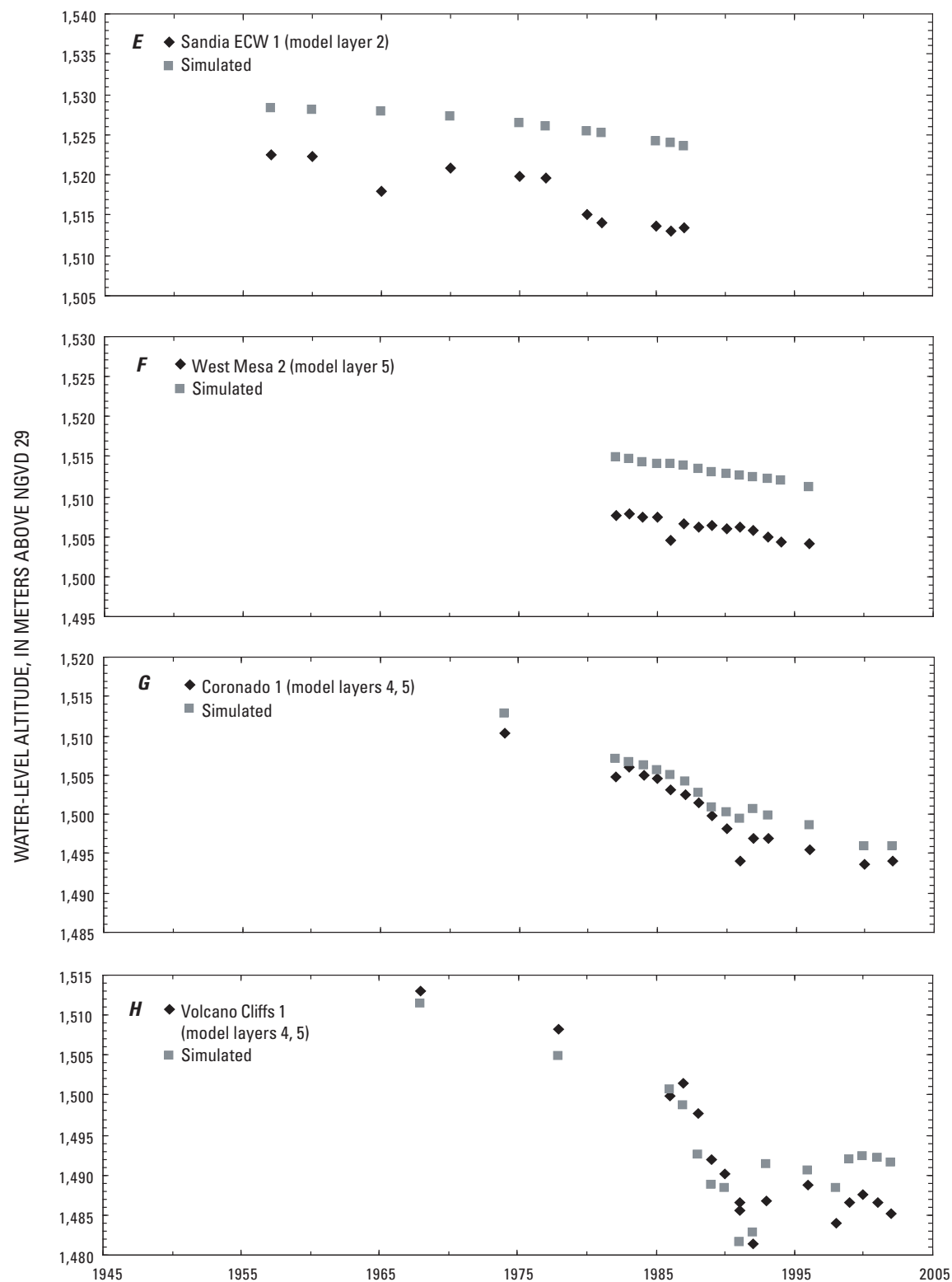


Figure 2.16E–H. Measured and simulated hydraulic heads for selected wells in the revised groundwater-flow model, Middle Rio Grande Basin, New Mexico. Well locations are shown in figure 2.15B. E, Sandia ECW 1, model layer 2; F, West Mesa 2, model layer 5; G, Coronado 1, model layers 4 and 5; H, Volcano Cliffs 1, model layers 4 and 5.

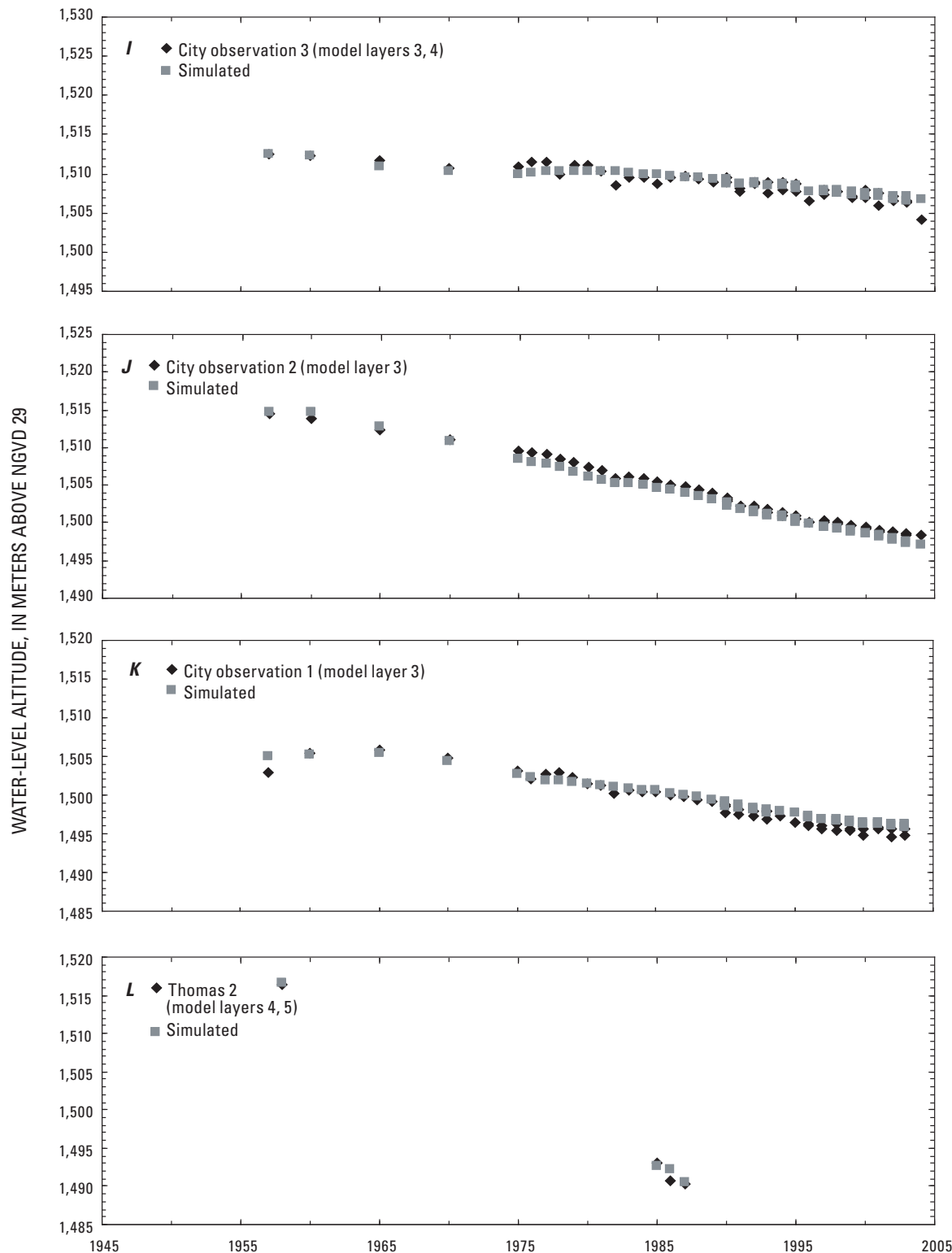


Figure 2.16I-L. Measured and simulated hydraulic heads for selected wells in the revised groundwater-flow model, Middle Rio Grande Basin, New Mexico. Well locations are shown in figure 2.15B. *I*, City Observation 3, model layers 3 and 4; *J*, City Observation 2, model layer 3; *K*, City Observation 1, model layer 3; *L*, Thomas 2, model layers 4 and 5.

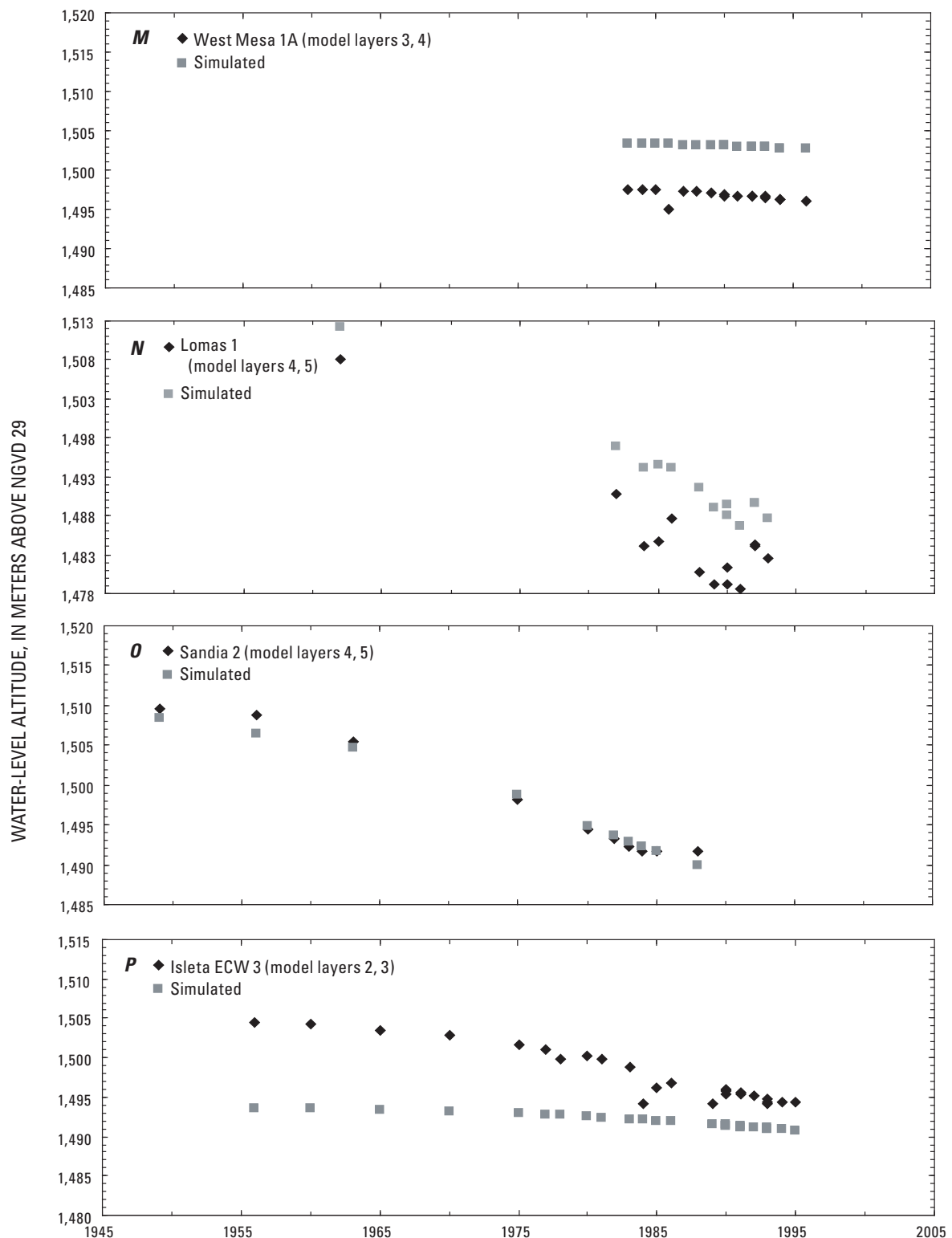


Figure 2.16M–P. Measured and simulated hydraulic heads for selected wells in the revised groundwater-flow model, Middle Rio Grande Basin, New Mexico. Well locations are shown in figure 2.15B. *M*, West Mesa 1A, model layers 3 and 4; *N*, Lomas 1, model layers 4 and 5; *O*, Sandia 2, model layers 4 and 5; *P*, Isleta ECW 3, model layers 2 and 3.

2-50 Hydrogeologic Settings and Groundwater-Flow Simulations for Regional TANC Studies Begun in 2004

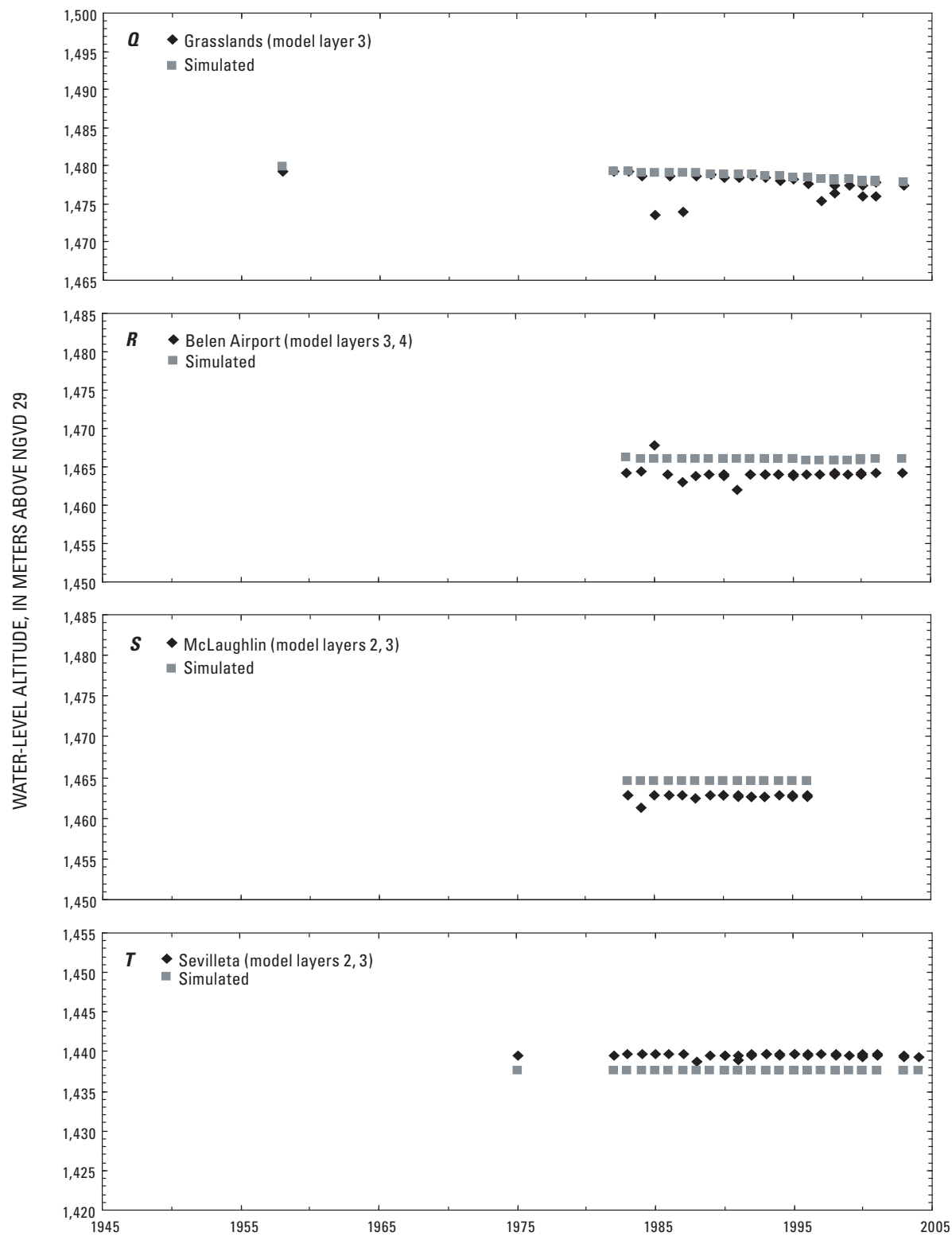


Figure 2.16Q–T. Measured and simulated hydraulic heads for selected wells in the revised groundwater-flow model, Middle Rio Grande Basin, New Mexico. Well locations are shown in figure 2.15B. *Q*, Grasslands, model layer 3; *R*, Belen Airport, model layers 3 and 4; *S*, McLaughlin, model layers 2 and 3; *T*, Sevilleta, model layers 2 and 3.

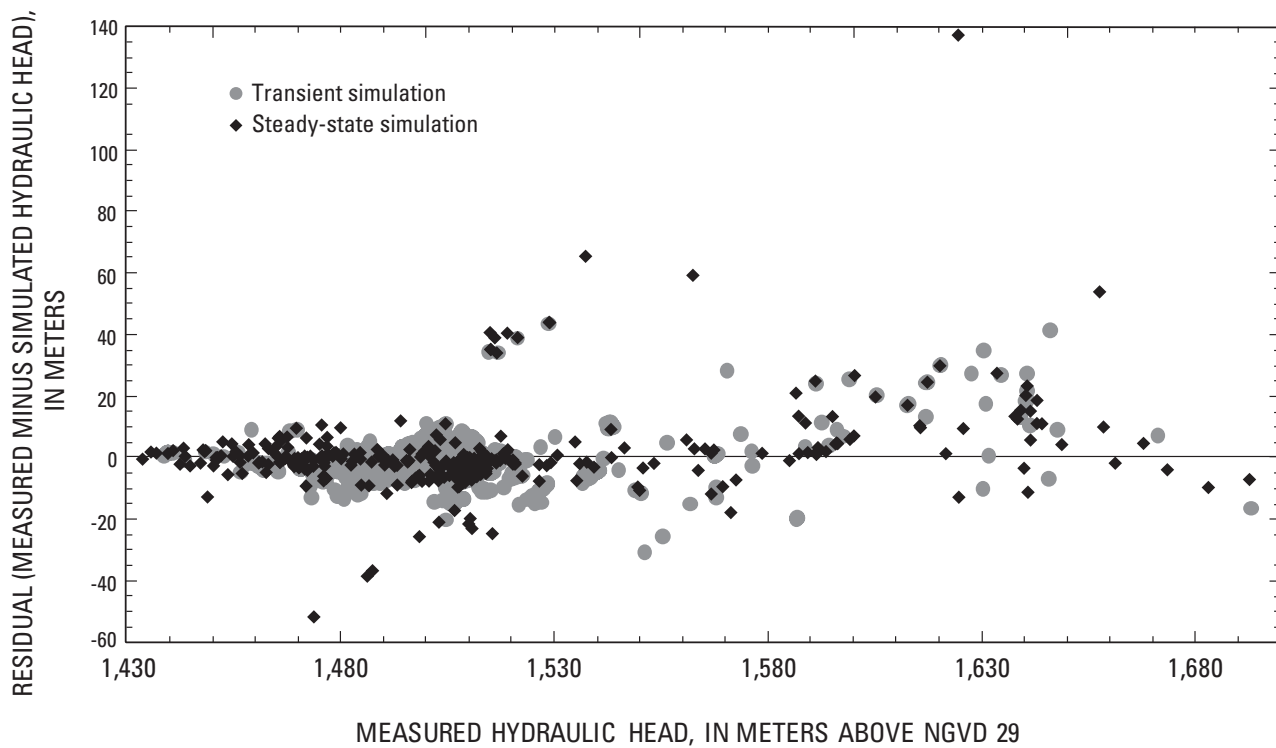


Figure 2.17 Comparison of residuals and measured hydraulic heads, steady-state and transient simulations of the revised groundwater-flow model, Middle Rio Grande Basin, New Mexico.

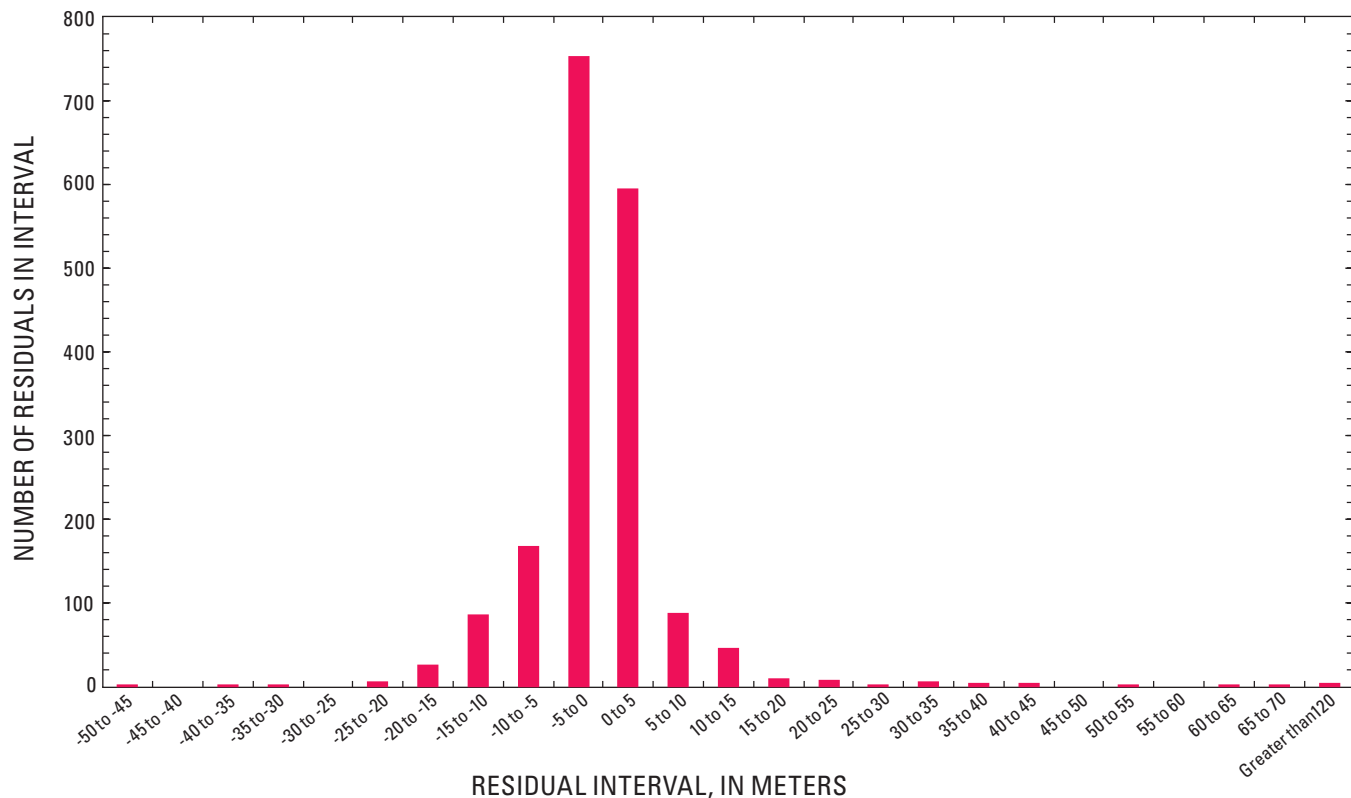


Figure 2.18 Hydraulic-head residuals from the steady-state and transient stress periods of the revised groundwater-flow model, Middle Rio Grande Basin, New Mexico. Residuals are calculated as measured minus observed heads.

structural model error possibly due to under representation of groundwater withdrawals (noted in the “Reported Groundwater Withdrawals” section), as well as error in the specification of the magnitude and spatial distribution of recharge, hydraulic conductivity, and aquifer storage properties.

Although simulated transient hydraulic-heads are within 5 m of historical measurements throughout most of the model domain (fig. 2.15B), measured heads are substantially higher than simulated heads near the basin margins, particularly to the west. (Likely causes of this model error are discussed above.)

Model-Computed Water Budgets

Net simulated inflow and outflow for the revised MRGB model was calculated by subtracting river leakage out of the groundwater system from the total inflows and outflows so that comparisons could be made with the original MRGB model (McAda and Barroll, 2002). The net inflow and outflow simulated with the revised MRGB model for the steady-state stress period representing predevelopment conditions was $152 \times 10^6 \text{ m}^3/\text{yr}$ (table 2.5), with a numerical discrepancy of 0.2 percent. Recharge from the Rio Grande and Jemez River account for 58 percent of the total net inflow, and subsurface, mountain-front, and tributary recharge account for the remaining 42 percent of the net inflow. The simulated net outflow is accounted for entirely by riparian evapotranspiration. Steady-state simulated river inflows and outflows totaled 106.4×10^6 and $18.3 \times 10^6 \text{ m}^3/\text{yr}$, respectively.

The average net inflow and outflow simulated with the revised MRGB model for the two transient stress periods representing the year ending October 31, 1999, was $583 \times 10^6 \text{ m}^3/\text{yr}$ (table 2.5), with a numerical discrepancy of 0.07 percent. The nearly four-fold simulated increase in total net inflow and outflow from 1900 (steady state) to 1999 resulted from development of surface-water and groundwater resources. By 1999, recharge from river, lake, reservoir, canal, and irrigation accounted for 75 percent of the total net inflow, whereas subsurface, mountain-front, and tributary recharge accounted for 11 percent. The remaining net inflow (14 percent) was simulated from septic-field seepage, leakage from sewer and water-distribution systems, and aquifer storage depletion. Outflow to drains, groundwater withdrawals, and riparian evapotranspiration account for 48, 33, and 19 percent, respectively, of the total net outflow. Although outflow to rivers was also simulated during the transient stress periods, this quantity was less than simulated inflow from rivers and is therefore not apparent in the *net* total.

For the year ending October 31, 1999, the simulated net inflow from the Rio Grande and outflow to drains for the revised MRGB model (table 2.5) are smaller by $126 \times 10^6 \text{ m}^3/\text{yr}$ and $140 \times 10^6 \text{ m}^3/\text{yr}$, respectively, than the flows simulated with the McAda and Barroll (2002) model (table 2.3). In contrast to this difference over the entire model domain, the seepage simulated from the Rio Grande in the sub-domain of the revised model between Bernalillo and the Rio Bravo Bridge

south of Albuquerque (fig. 2.5) is greater than both the seepage simulated by the McAda and Barroll (2002) model and the flow loss of $2.05 \times 10^5 \text{ m}^3/\text{d}$ measured by Veenhuis (2002). Whereas the river inflow simulated by the McAda and Barroll (2002) model along this reach model was 27 percent less than the Veenhuis (2002) observation, the inflow simulated by the revised model was 20 percent greater than the observation. This difference in simulated inflow results from the refined discretization of the revised model, which typically separates river and drain boundaries that coexisted in the same 1-km finite-difference cells in the McAda and Barroll (2002) model into separate 0.5-km cells. This additional simulated inflow from the river causes increased simulated outflow to nearby drains. The difference in simulated flow between layer 1 cells that contain river boundaries and underlying layer 2 cells in this reach of the Rio Grande (from Bernalillo to the Rio Bravo Bridge) south of Albuquerque is negligible (less than 0.1 percent) between the two models.

Areas Contributing Recharge to Public-Supply Wells

The revised MRGB model was used to estimate traveltimes distributions, areas contributing recharge, and zones of contribution under transient conditions for 59 public-supply wells in the greater Albuquerque area using the MODPATH (Pollock, 1994) particle-tracking post processor and methods outlined in Section 1 of this professional paper chapter. The model-computed areas contributing recharge are based on advective groundwater flow and do not account for mechanical dispersion. Advection-dispersion transport simulations would likely yield larger areas contributing recharge than advective particle-tracking simulations because the effects of dispersion caused by aquifer heterogeneity would be included.

In addition to heads and cell-to-cell flows from the groundwater-flow model, the MODPATH simulation requires effective porosity to calculate groundwater-flow velocities. For particle tracking based on a steady-state groundwater-flow model, the effective porosity affects only the simulated traveltimes. In contrast, for particle tracking based on a transient groundwater-flow model, both the location of flow paths and the traveltimes are affected by the value chosen for effective porosity.

To examine the effects of effective porosity on traveltimes and on the areas contributing recharge, particle tracking was performed using four values of effective porosity for layer 1: 0.02, 0.08, 0.2 and 0.35. The effective porosity was assumed to decrease with depth. For the lower two values of effective porosity, the value was decreased by 0.001 for each layer. For the higher two values of effective porosity, the value was decreased by 0.01 for each layer. No measurements of effective porosity are known to exist for the Santa Fe Group aquifer system. The effective porosity for a sand aquifer is probably closest to 0.35; however, use of a range of values accounts for groundwater-velocity variations resulting from

hydraulic-conductivity variations on a scale that cannot be incorporated in a regional-scale model.

Figure 2.19 shows the median simulated distribution of traveltimes of water to the 59 wells for the four simulated effective porosities. Particles were tracked backwards from the wells from a starting time of June 2005. The median simulated distribution of traveltimes was computed by using the median of the percentage of water in the wells with a traveltime less than the given year for each yearly increment based on all the simulated areas contributing recharge, and will be referred to hereafter as the distribution for the “typical” well. The distribution of these traveltimes for the typical well ranged from less than 10 years to more than 10,000 years; the shortest traveltimes coincide with the smallest effective porosity. Traveltimes of 100 years or less were observed for about 95 percent of the water entering the typical well when an effective porosity of 0.02 was simulated and 25 percent for an effective porosity of 0.08. For simulated effective porosities of 0.2 and

0.35, nearly all traveltimes to the typical well exceeded 400 years. These results indicate that for most public-supply wells in the greater Albuquerque area that contain tracers of young recharge, such as trichlorotrifluoroethane (CFC-113), either some percentage of the zones of contribution to these wells have effective porosities in the range of around 0.10 or smaller or the tracers arrive at these wells through some other fast pathways that are not adequately represented in the model.

The simulated traveltime distributions for water entering the public-supply wells were used with input histories of CFC-113 and ^{14}C to compute the concentrations of these tracers at the wells where there were corresponding measurements (37 wells for CFC-113, 13 wells for ^{14}C). To compute the concentrations of the CFC-113, the traveltime for each particle associated with a well was subtracted from the year when the well was sampled, and then that resulting year was matched against the input history for CFC-113. For ^{14}C , the initial activity was considered to be a value of 100 percent

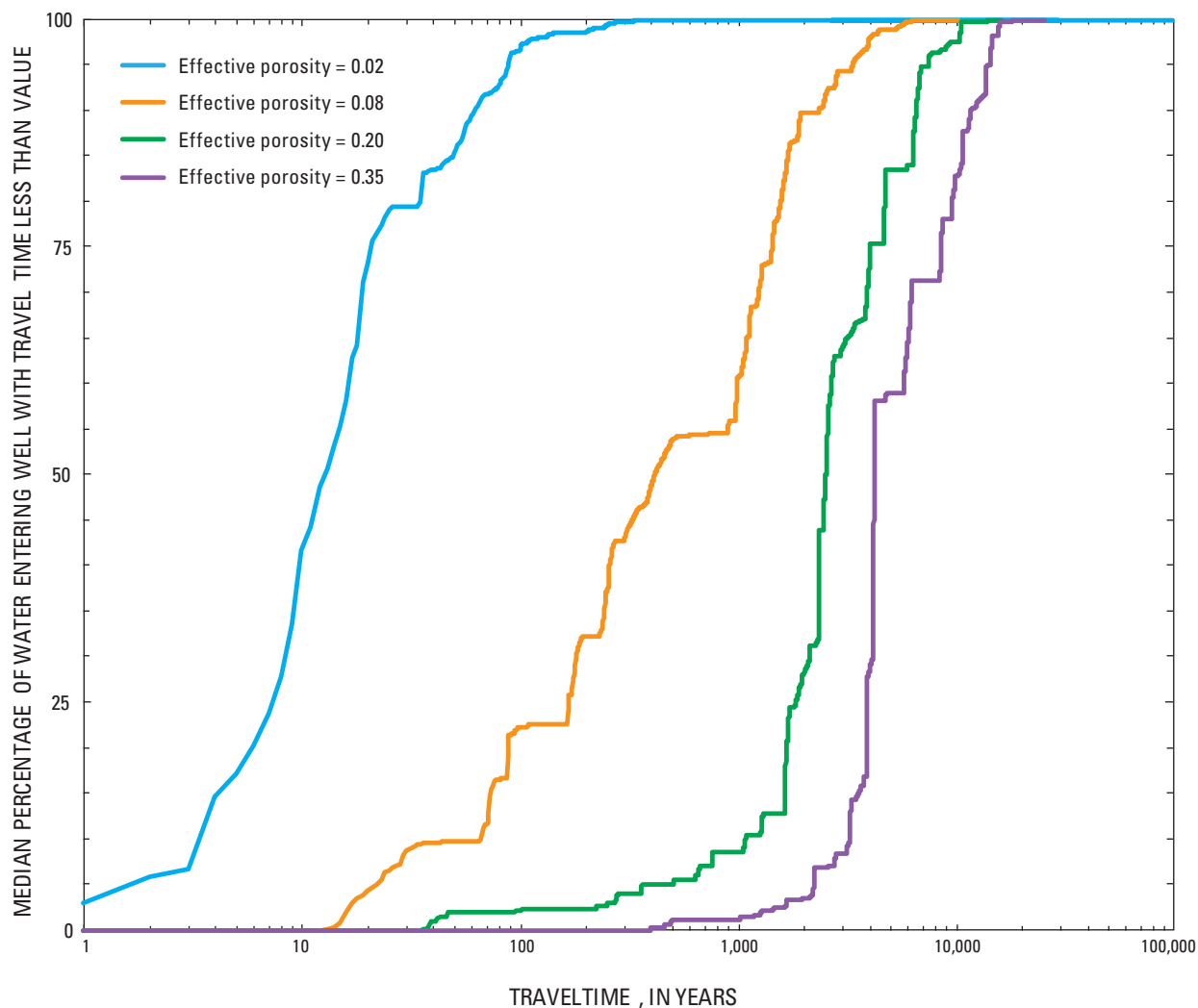


Figure 2.19. Median simulated distributions of traveltimes of groundwater to 59 public-supply wells under transient conditions with the revised groundwater-flow model, Middle Rio Grande Basin, New Mexico.

modern carbon. This value was decayed based on an exponential decay rate corresponding to a half life of 5,730 years and the traveltimes of each particle, and the resulting concentration also was expressed as percent modern carbon. A volume-weighted average of the individual tracer concentrations for all of the particles was computed as the concentration that would be measured in the well.

Figure 2.20 shows box plots of the measured tracer concentrations (^{14}C data from Plummer and others [2004a] and CFC-113 data from Plummer and others [2004a] and from wells sampled for the TANC study, as described in Section 1 of this professional paper chapter), as well as the simulated concentrations based on the four different effective porosities. The distribution for the measured CFC-113 concentrations is most similar to the distribution of simulated values using the effective porosity of 0.08. The percent modern carbon values of ^{14}C , in contrast, are best matched by an effective porosity of 0.35. The results of these comparisons indicate that no single effective porosity is sufficient to match the measured data. Different effective porosities yield different groundwater velocities and, in reality, there are likely a wide range of groundwater velocities in the aquifer due to variation in hydraulic conductivity and effective porosity that cannot be adequately represented in a regional model such as the one presented here. Most flow paths probably have a groundwater velocity best represented by an effective porosity near 0.35, although some flow paths through the system likely have groundwater velocities represented by an effective porosity as low as 0.02. The composite of different velocities is reflected in the wells where tracers introduced into the atmosphere since the 1940s are detected, although the age implied by ^{14}C is thousands of years.

By comparing figures 2.21A–D, one can see that the size of the zone of contribution and the size of the area contributing recharge where traveltime to the well is less than 100 years decrease with increasing effective porosities. Although most flow and recharge occurs through contribution zones and recharge areas delineated with the larger effective porosities, the larger contribution zones and recharge areas for traveltimes less than 100 years shown with an effective porosity of 0.02 are important in showing areas that might be able to contribute flow and anthropogenic contaminants relatively quickly to public-supply wells.

The simulated directions of flow and areas contributing recharge to wells vary based on the position of a well in the valley. The wells to the west of the Rio Grande generally have flow paths from the northwest with the main source of water being the Jemez River. This result is in contrast to previous investigations that determined the Jemez River was primarily a gaining stream (Craig, 1992) and that “infiltration from the Jemez River appears to be limited primarily to a relatively narrow and shallow area located directly along the river” (Plummer and others, 2004a). The wells on the east side, but close to the Rio Grande, generally have flow paths flowing from the northwest, north, and northeast with sources of water mainly from the Jemez River, Rio Grande, and subsurface flow along

the northern boundary. The wells in the far east of the valley generally have flow paths from the northeast with the main source of water being mountain-front recharge along the eastern side of the valley. An example of the pathlines representing each of these general flow patterns is shown in figure 2.21B in blue, green, and brown, respectively. The traveltimes of less than 100 years are generally from areas where either urban recharge or seepage from the Rio Grande is occurring.

Limitations and Appropriate Use of the Model

The revised groundwater-flow model for the MRGB was designed to evaluate the water budget under both steady-state and modern conditions from 1900 to 2008, approximately delineate areas contributing recharge to public-supply wells, and support future local data-collection and modeling efforts. Like any numerical groundwater model, the revised MRGB model is a simplified representation of the physical system, and it is intended to simulate the general characteristics of that system rather than detailed local attributes. In particular, the model of the MRGB was designed to be suitable for regional-scale, rather than local-scale, applications. In addition, the model calibration is nonunique, meaning that a different combination of model parameter values could produce a similar simulated hydraulic-head distribution. Limitations inherent to the model, assumptions and simplifications made during model development, and errors in the conceptual model of the physical characteristics of the system all constrain the appropriate use of the model.

Detailed simulation of shallow groundwater flow between the Rio Grande, various canals, and drains within the Rio Grande inner valley may be limited by the 500-m finite-difference-cell spacing. Although the simulated interaction between these features is improved over the 1,000-m finite-difference-cell spacing of the McAda and Barroll (2002) model, in which boundary conditions representing these features are often collocated in the same finite-difference cell, a finer spatial discretization would likely be necessary to adequately simulate flow between the Rio Grande and individual canals and drains.

Model-computed areas contributing recharge and traveltimes through zones of contribution to public-supply wells have multiple sources of uncertainty. For example, error in the model’s representation of the hydrologic system in the northern part of the MRGB might contribute to the simulation of infiltration from the Jemez River into the aquifer system, which is contrary to the interpretation of some previous investigations (Craig, 1992; Plummer and others, 2004a). If this simulated source of water from the Jemez River is not representative of actual conditions, the simulated zones of contribution from the northwest to wells on the west side of the Rio Grande may be in error. Other substantial sources of uncertainty are related to the long flow paths and residence times of groundwater in the MRGB. The groundwater-flow model was designed to simulate the regional groundwater system during the time period from 1900 to 2008, which is when

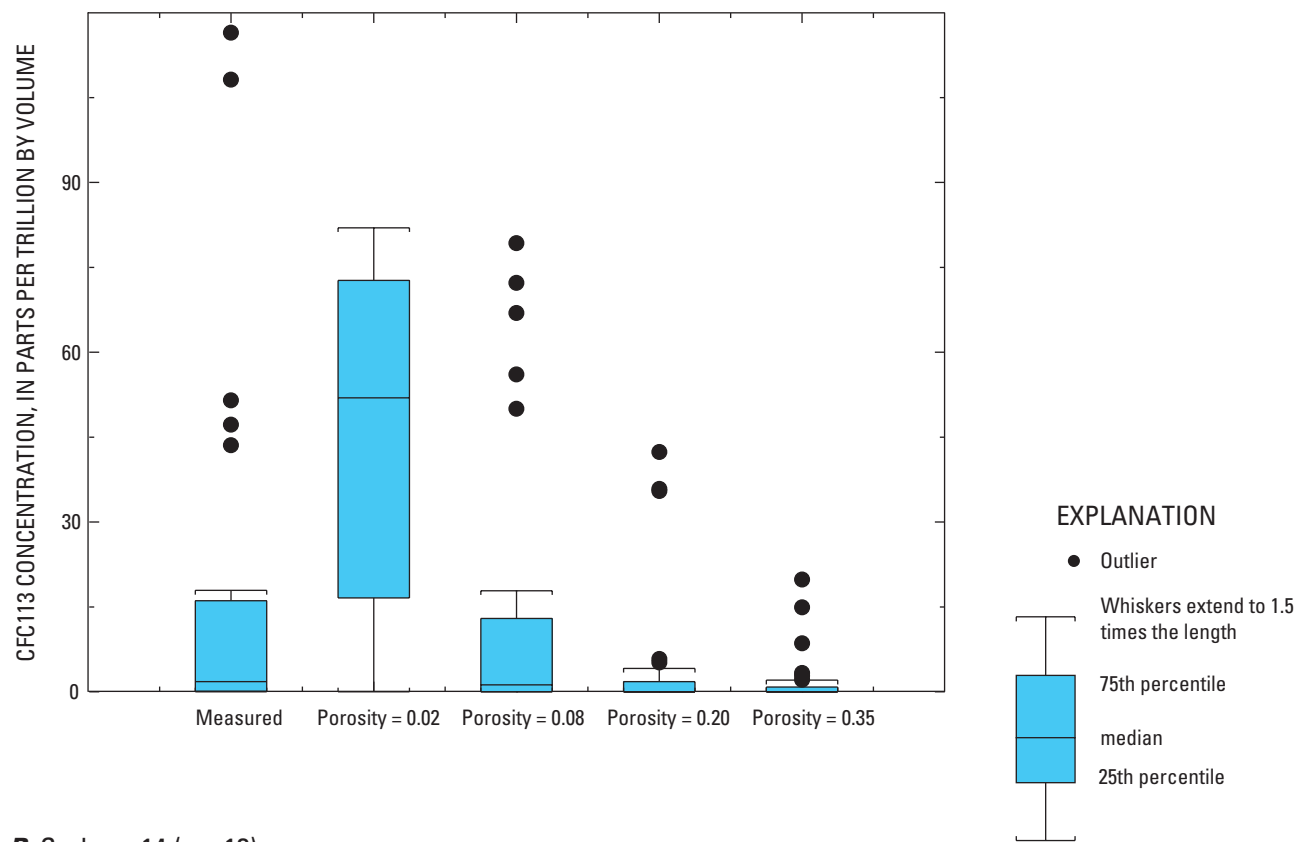
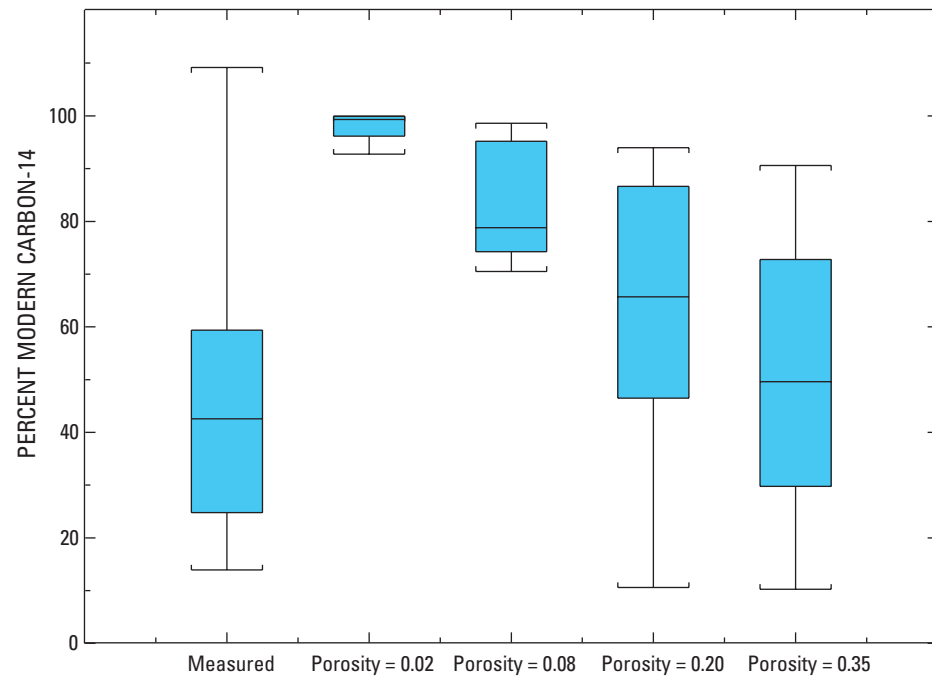
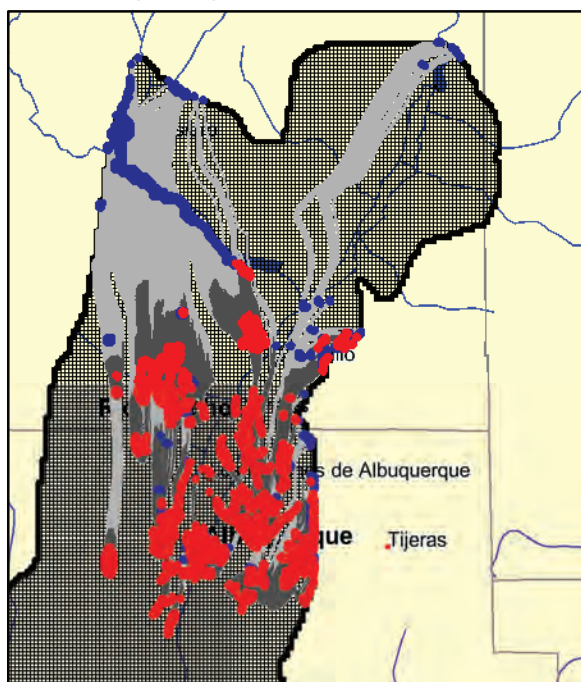
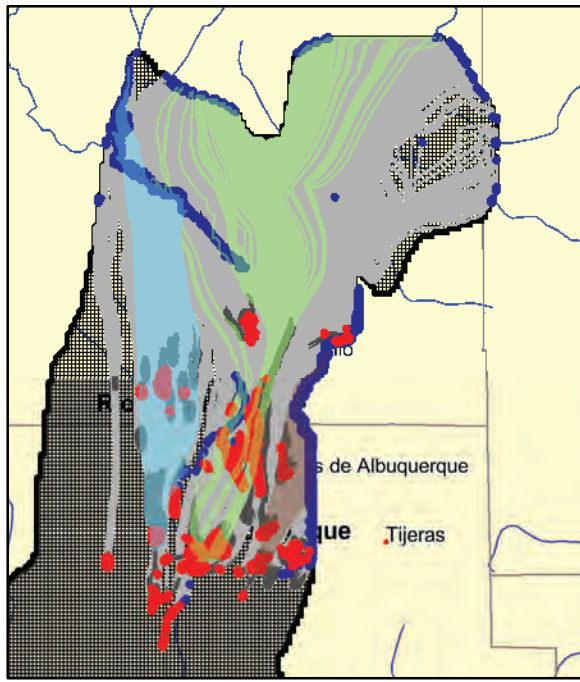
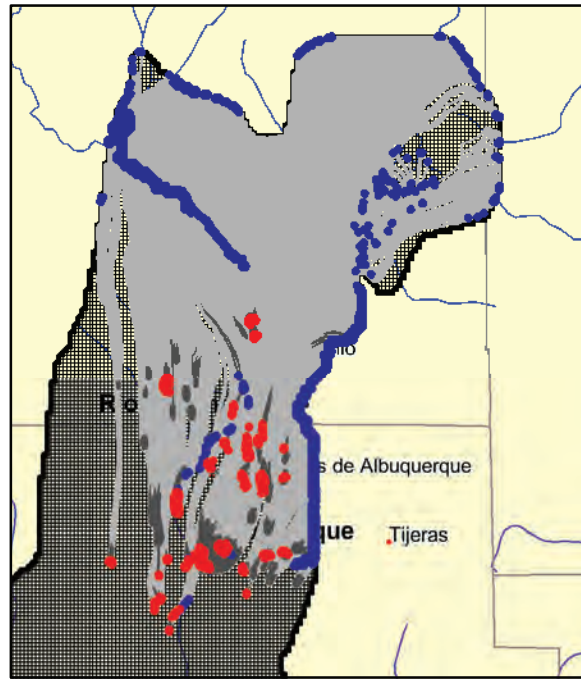
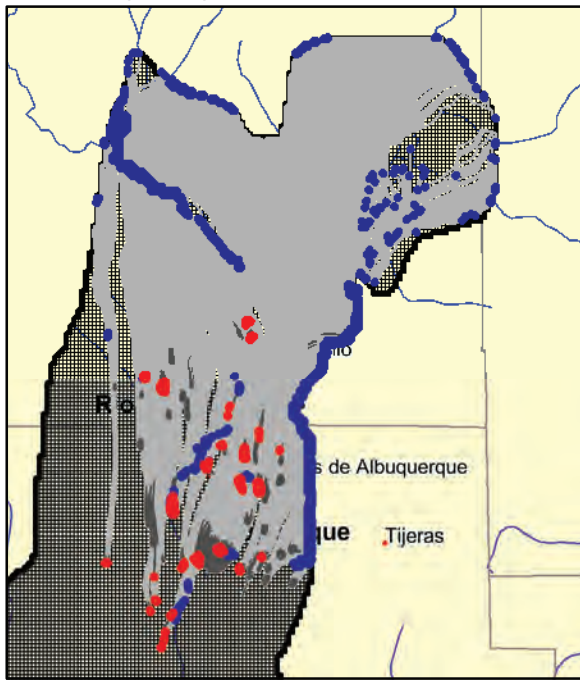
A CFC -113 (n = 37)**B Carbon -14 (n = 13)**

Figure 2.20. Distributions of measured and simulated A, trichlorotrifluoroethane (CFC-113) concentrations and B, carbon-14 values in public-supply wells simulated under transient conditions with the revised groundwater-flow model, Middle Rio Grande Basin, New Mexico. (Measured carbon-14 data from Plummer and others , 2004a, and CFC-113 data from Plummer and others, 2004a, and from wells sampled for the Transport of Anthropogenic and Natural Contaminants study, as described in Section 1 of this professional paper chapter)

A Effective porosity = 0.02**B** Effective porosity = 0.08**C** Effective porosity = 0.20**D** Effective porosity = 0.35**EXPLANATION**

Areas contributing recharge

- Traveltime less than 100 years
- Traveltime greater than 100 years

Zones of contribution (flow paths)

- Traveltime less than 100 years
- Traveltime greater than 100 years

For map **B** only

- Flow paths for an individual well
- Flow paths for an individual well
- Flow paths for an individual well

Figure 2.21. Areas contributing recharge and zones of contribution to 59 public-supply wells for effective porosities of *A*, 0.02, *B*, 0.08, *C*, 0.2, and *D*, 0.35 in the revised groundwater-flow model, regional study area, Middle Rio Grande Basin, New Mexico.

observations of important hydrologic characteristics—such as position of the Rio Grande and groundwater levels—were available or could be estimated. In contrast, as discussed in the “Groundwater Age” section, estimated residence times of groundwater to wells throughout most of the basin are thousands to tens of thousands of years. These long residence times are partly the result of recharge occurring primarily along basin margins and surface-water features, which can be located tens of kilometers from the public-supply wells to which the recharge contributes.

The comparison of simulated and measured tracer concentrations indicates the limitation of the model to correctly simulate the actual mix of traveltimes to wells, given the parameterization of effective porosity and hydraulic conductivity used in the model. The travelttime distribution for any given well should be considered to be some combination of the travelttime distributions from the various values of effective porosity used. However, the exact proportion of each is uncertain, depending on the actual heterogeneity of the aquifer materials existing in the zone of contribution to the wells.

Although inherent sources of uncertainty affect the accuracy of the areas contributing recharge and traveltimes through zones of contribution simulated with the revised MRGB model for groundwater that recharged the aquifer at any time, estimates of these characteristics for groundwater likely to have recharged more than about 100 years ago are especially uncertain. Backward particle tracking was conducted using the steady-state stress period (during which simulated hydrologic conditions are constant) to simulate all times prior to 1900. However, these simulated steady-state conditions could differ considerably from actual historical conditions. In particular, several thousands of years ago factors that could have resulted in substantially different groundwater-flow characteristics than those simulated include climatic changes that altered the quantity and distribution of recharge, which would cause changes to the hydraulic-head distribution and, consequently, both flow directions and velocities. Evidence that such climatic changes have occurred is provided by Plummer and others (2004a), who also used chemical and isotopic data to infer groundwater source areas, flowpaths, and traveltimes that in some cases differ considerably from those simulated with the model.

Although the simulation of contributing areas and traveltimes with the MRGB groundwater-flow model is limited by inherent uncertainty, the simulated results are useful, particularly for order-of-magnitude comparisons with other TANC study areas. For example, knowledge that, unlike most other TANC study areas, a substantial percentage of water contributed to wells in the MRGB regional study area was recharged more than 100 years ago (prior to most human development) provides valuable information for assessing relative vulnerability of the wells in the different study areas to contamination.

The revised MRGB groundwater-flow model, which uses previously specified boundary conditions and newly calibrated aquifer hydraulic conductivities, provides a representation of groundwater flow conditions for 1900 to 2008. The model is suitable for evaluating regional water budgets

and groundwater-flow paths in the study area from 1900 to 2008, but has limited utility in determining flow characteristics prior to this time period and may not be suitable for long-term predictive simulations. This regional model provides a tool to evaluate aquifer vulnerability at a regional scale, to facilitate order-of-magnitude comparisons of groundwater traveltime between regional aquifer systems, and to guide future detailed investigations in the study area.

References Cited

- Anderholm, S.K., 1988, Ground-water geochemistry of the Albuquerque-Belen Basin, Central New Mexico: U.S. Geological Survey Water-Resources Investigations Report 86-4094, 110 p.
- Anderholm, S.K., 1997, Water-quality assessment of the Rio Grande valley, Colorado, New Mexico, and Texas—shallow ground-water quality and land use in the Albuquerque area, central New Mexico, 1993: U.S. Geological Survey Water-Resources Investigations Report 97-4067, 73 p.
- Anderholm, S.K., 2001, Mountain-front recharge along the east side of the Albuquerque Basin, Central New Mexico (revised): U.S. Geological Survey Water-Resources Investigations Report 00-4010, 36 p.
- Banta, E.R., 2000, MODFLOW-2000, the U.S. Geological Survey modular ground-water model—documentation of packages for simulating evapotranspiration with a segmented function (ETS1) and drains with return flow (DRT1): U.S. Geological Survey Open-File Report 00-466, 127 p.
- Bartolino, J.R., and Cole, J.C., 2002, Ground-water resources of the Middle Rio Grande Basin, New Mexico: U.S. Geological Survey Circular 1222, 132 p.
- Bexfield, L.M., and Anderholm, S.K., 2000, Predevelopment water-level map of the Santa Fe Group aquifer system in the Middle Rio Grande Basin between Cochiti Lake and San Acacia, New Mexico: U.S. Geological Survey Water-Resources Investigations Report 00-4249, 1 sheet.
- Bexfield, L.M., and Anderholm, S.K., 2002a, Estimated water-level declines in the Santa Fe Group aquifer system in the Albuquerque area, central New Mexico, predevelopment to 2002: U.S. Geological Survey Water-Resources Investigations Report 02-4233, 1 sheet.
- Bexfield, L.M., and Anderholm, S.K., 2002b, Spatial patterns and temporal variability in water quality from City of Albuquerque drinking-water supply wells and piezometer nests, with implications for the ground-water flow system: U.S. Geological Survey Water-Resources Investigations Report 01-4244, 101 p.

2-58 Hydrogeologic Settings and Groundwater-Flow Simulations for Regional TANC Studies Begun in 2004

- Bexfield, L.M., and Plummer, L.N., 2003, Chapter 11—Occurrence of arsenic in ground water of the Middle Rio Grande Basin, central New Mexico, *in* Welch, A.H., and Stollenwerk, K.G., eds., Arsenic in ground water—Geochemistry and occurrence: Boston, Kluwer Academic Publishers, p. 295–327.
- Bjorklund, L.J., and Maxwell, B.W., 1961, Availability of ground water in the Albuquerque area, Bernalillo and Sandoval Counties, New Mexico: New Mexico State Engineer Technical Report 21, 117 p.
- Bureau of Reclamation, 1973, Progress report—Phreatophyte investigations—Bernardo evapotranspirometers: Albuquerque, Middle Rio Grande Project Office, 50 p.
- Camp Dresser & McKee, 1998, City of Albuquerque Water Conservation Program Evaluation: Sanitary Sewer Exfiltration Analysis: consulting report to the City of Albuquerque [variously paged].
- CH2MHill, 1999, City of Albuquerque Public Works Department water resources strategy implementation, diversion options task 2.1.1.1.3, Hydrogeologic field investigation report: Consultant's report prepared for the City of Albuquerque Public Works Department: [variously paged].
- City of Albuquerque, 2003, San Juan-Chama Diversion Project: accessed August 2003 at <http://www.cabq.gov/waterresources/sjc.html>.
- City of Albuquerque, 2009, Distribution system water loss: accessed May 2009 at <http://www.cabq.gov/progress/public-infrastructure/dcc-17/indicator-17-2>.
- Cole, J.C., 2001a, 3-D geologic modeling of regional hydrostratigraphic units in the Albuquerque segment of the Rio Grande Rift, *in* Cole, J.C., ed., U.S. Geological Survey Middle Rio Grande Basin Study—Proceedings of the Fourth Annual Workshop, Albuquerque, New Mexico, February 15–16, 2000: U.S. Geological Survey Open-File Report 00-488, p. 26–28.
- Cole, J.C., ed., 2001b, U.S. Geological Survey Middle Rio Grande Basin Study—Proceedings of the Fourth Annual Workshop, Albuquerque, New Mexico, February 15–16, 2000: U.S. Geological Survey Open-File Report 00-488, 57 p.
- Connell, S.D., 1997, Geology of Alameda quadrangle, Bernalillo and Sandoval Counties, New Mexico: Socorro, New Mexico Bureau of Mines and Mineral Resources Open-File Digital Map Series OF-DM-10, last modified September 16, 1999, 1 sheet.
- Connell, S.D., 2006, Preliminary geologic map of the Albuquerque-Rio Rancho metropolitan area and vicinity, Bernalillo and Sandoval Counties, New Mexico: New Mexico Bureau of Geology and Mineral Resources Open-File Report 496, 2 pls.
- Connell, S.D., Allen, B.D., and Hawley, J.W., 1998, Subsurface stratigraphy of the Santa Fe Group from borehole geophysical logs, Albuquerque area, New Mexico: New Mexico Geology, v. 20, no. 1, p. 2–7.
- Craig, S.D., 1992, Water Resources on the Pueblos of Jemez, Zia, and Santa Anna, Sandoval County, New Mexico: U.S. Geological Survey Water-Resources Investigations Report 89-4091, 122 p., 4 pls.
- DeWees, R.K., 2003, Water-level data for the Albuquerque Basin and adjacent areas, Central New Mexico, period of record through 2002: U.S. Geological Survey Open-File Report 03-321, 41 p.
- DeWees, R.K., 2006, Water-level data for the Albuquerque Basin and adjacent areas, Central New Mexico, period of record through 2004: U.S. Geological Survey Open-File Report 2006-1281, 40 p.
- Doherty, John, 2005, PEST: model-independent parameter estimation, user manual (5th ed.): Watermark Numerical Computing, Corinda, Australia, 336 p.
- Feller, Mark R., and Hester, David J., 2001, SLEUTH Urban Landscape Change 2050 Calibration and Prediction datasets covering (16) 1:24,000-scale quadrangles within the Albuquerque, New Mexico Metropolitan Statistical Area, distributed to the New Mexico Bureau of Geology and Mineral Resources.
- Fenneman, N.M., 1931, Physiography of the Western United States: New York, McGraw-Hill, 534 p.
- Grant, P.R., Jr., 1999, Subsurface geology and related hydrologic conditions, Santa Fe Embayment and contiguous areas, New Mexico, *in* Pazzaglia, F.J., and Lucas S.G., eds., Albuquerque Geology, New Mexico Geological Society Fiftieth Annual Field Conference, September 22–25, 1999: Socorro, New Mexico Geological Society, p. 425–435.
- Grauch, V.J.S., Gillespie, C.L., and Keller, G.R., 1999, Discussion of new gravity maps for the Albuquerque Basin area, *in* Pazzaglia, F.J., and Lucas, S.G., eds., Albuquerque Geology, New Mexico Geological Society Fiftieth Annual Field Conference, September 22–25, 1999: Socorro, New Mexico Geological Society, p. 119–124.

- Grauch, V.J.S., Hudson, M.R., Minor, S.A., 2001, Aeromagnetic expression of faults that offset basin fill, Albuquerque Basin, New Mexico: *Geophysics*, v. 66, no. 3, p. 707–720.
- Halford, K.J and Hanson, R.T., 2002, User guide for the drawdown-limited Multi-Node Well (MNW) package for the U.S. Geological Survey's modular three-dimensional finite-difference ground-water flow model, versions MODFLOW-96 and MODFLOW-2000: U.S. Geological Survey Open-File Report 02-293, 33 p.
- Harbaugh, A.W., 2005, MODFLOW-2005, the U.S. Geological Survey modular ground-water model—the Ground-Water Flow Process: U.S. Geological Survey Techniques and Methods 6-A16 [variously paged].
- Hawley, J.W., 1996, Hydrogeologic framework of potential recharge areas in the Albuquerque Basin, central New Mexico: New Mexico Bureau of Mines and Mineral Resources Open-File Report 402D, chap. 1, 68 p.
- Hawley, J.W., and Haase, C.S., 1992, Hydrogeologic framework of the northern Albuquerque Basin: Socorro, New Mexico Bureau of Mines and Mineral Resources Open-File Report 387 [variously paged].
- Hawley, J.W., and Haase, C.S., and Lozinsky, R.P., 1995, An underground view of the Albuquerque Basin, in Ortega-Klett, C.T., ed., The water future of Albuquerque and the Middle Rio Grande Basin: Proceedings of the 39th Annual New Mexico Water Conference, November 3–4, 1994: New Mexico Water Resources Research Institute WRRI Report no. 290, p. 37–55.
- Heywood, C.E., 1998, Piezometric-extensometric estimations of specific storage in the Albuquerque Basin, New Mexico, in Borchers, J.E., ed., Land subsidence case studies and current research: Proceedings of the Dr. Joseph F. Poland Symposium, Special Publication No. 8, Association of Engineering Geologists, Sacramento Section and Association of Engineering Geologists Subsidence Committee: Belmont, Calif., Star Publishing Company, p. 435–440.
- Heywood, C.E., 2001, Piezometric-extensometric test results, in Thorn, C.R., Analytical results of a long-term aquifer test conducted near the Rio Grande, Albuquerque, New Mexico: U.S. Geological Survey Water-Resources Investigations Report 00-4291, p. 8–11.
- Homer, C. Huang, C., Yang, L., B. Wylie B., and Coan, M., 2004, Development of a 2001 National Landcover Database for the United States: Photogrammetric Engineering and Remote Sensing, v. 70, no. 7, July 2004, p. 829–840, accessed Sept. 14, 2010, at <http://www.mrlc.gov/>.
- Kernodle, J.M., McAda, D.P., and Thorn, C.R., 1995, Simulation of ground-water flow in the Albuquerque Basin, central New Mexico, 1901–1994, with projections to 2020: U.S. Geological Survey Water-Resources Investigations Report 94-4251, 114 p.
- Kernodle, J.M., and Scott, W.B., 1986, Three-dimensional model simulation of steady-state ground-water flow in the Albuquerque-Belen Basin, New Mexico: U.S. Geological Survey Water-Resources Investigations Report 84-4353, 58 p.
- Kinkel, B., 1995, Estimates of consumptive use requirements for irrigated agriculture and riparian vegetation, v. I: Bureau of Reclamation Albuquerque Area Office, Middle Rio Grande Water Assessment Supporting Document no. 6, 31 p.
- Lee, W.T., 1907, Water resources of the Rio Grande valley and their development: U.S. Geological Survey Water-Supply Paper 188, 59 p.
- Logan, L.M., 1990, Geochemistry of the Albuquerque municipal area, Albuquerque, New Mexico: Socorro, New Mexico Institute of Mining and Technology, Independent study, 234 p.
- Lozinsky, R.P., 1994, Cenozoic stratigraphy, sandstone petrology, and depositional history of the Albuquerque basin, central New Mexico: Geological Society of American Special Paper 291, p. 73–82.
- McAda, D.P., 2001, Simulation of a long-term aquifer test conducted near the Rio Grande, Albuquerque, New Mexico: U.S. Geological Survey Water-Resources Investigations Report 99-4260, 66 p.
- McAda, D.P., and Barroll, Peggy, 2002, Simulation of ground-water flow in the Middle Rio Grande Basin between Cochiti and San Acacia, New Mexico: U.S. Geological Survey Water-Resources Investigations Report 02-4200, 81 p.
- Meeks, T.O., 1949, The occurrence of ground water in the Tijeras Soil Conservation District, Bernalillo County, New Mexico: U.S. Department of Agriculture Regional Bulletin 109, Geological Series I, Soil Conservation Service Region 6 [variously paged].
- New Mexico Environmental Finance Center, 2006, Review of leak and repair data, phase 1 report prepared for the Albuquerque Bernalillo County Water Utility Authority: 91 p.

2-60 Hydrogeologic Settings and Groundwater-Flow Simulations for Regional TANC Studies Begun in 2004

- Planert, Michael, and Williams, J.S., 1995, Ground water atlas of the United States—California and Nevada: U.S. Geological Survey Hydrologic Atlas 730-B, 28 p. (Also available at http://pubs.usgs.gov/ha/ha730/ch_b/index.html.)
- Plummer, L.N., Bexfield, L.M., Anderholm, S.K., Sanford, W.E., and Busenberg, Eurybiades, 2004a, Geochemical characterization of ground-water flow in the Santa Fe Group aquifer system, Middle Rio Grande Basin, New Mexico: U.S. Geological Survey Water-Resources Investigations Report 03-4131, 395 p.
- Plummer, L.N., Bexfield, L.M., Anderholm, S.K., Sanford, W.E., and Busenberg, Eurybiades, 2004b, Hydrochemical tracers in the Middle Rio Grande Basin, USA—1. Conceptualization of groundwater flow: *Hydrogeology Journal*, v. 12, no. 4, p.359–388.
- Plummer, L.N., Sanford, W.E., Bexfield, L.M., Anderholm, S.K., and Busenberg, Eurybiades, 2004c, Using chemical data and aquifer simulation to characterize recharge and groundwater flow in the Middle Rio Grande Basin, New Mexico, in Hogan, J.F., Phillips, F.M., and Scanlon, B.R., eds., *Groundwater recharge in a desert environment—the Southwestern United States*, Water Science and Applications Series, v. 9: Washington, D.C., American Geophysical Union, p. 185–216.
- Poeter, Eileen P., and Mary C. Hill, 2008, SIM_ADJUST—A computer code that adjusts simulated equivalents for observations or predictions: International Ground Water Modeling Center Report GWMI 2008–01, 28 p.
- Pollock, D.W., 1994, User's Guide for MODPATH/MODPATH-PLOT, version 3: A particle tracking post-processing package for MODFLOW, the U.S. Geological Survey finite-difference ground-water flow model: U.S. Geological Survey Open-File Report 94-464 [variously paged]. (Also available at <http://pubs.er.usgs.gov/publication/ofr94464>.)
- Reiter, M., 2001, Using precision temperature logs to estimate horizontal and vertical groundwater flow components: *Water Resources Research*, v. 37, no. 3, p. 663–674.
- Robinson, T.W., 1958, Phreatophytes: U.S. Geological Survey Water-Supply Paper 1423, 84 p.
- Robson, S.G., and Banta, E.R., 1995, Ground water atlas of the United States—Arizona, Colorado, New Mexico, and Utah: U.S. Geological Survey Hydrologic Atlas 730-C, 32 p. (Also available at http://pubs.usgs.gov/ha/ha730/ch_c/index.html.)
- Roelle, J.E., and Hagenbuck, W.W., 1994, Surface cover maps of the Rio Grande floodplain from Velarde to Elephant Butte Reservoir, New Mexico: U.S. Geological Survey, Fort Collins, Colo., 57 p.
- Sanford, W.E., Plummer, L.N., McAda, D.P., Bexfield, L.M., and Anderholm, S.K., 2004a, Hydrochemical tracers in the Middle Rio Grande Basin, USA—2. Calibration of a groundwater-flow model: *Hydrogeology Journal*, v. 12, no. 4, p. 389–407.
- Sanford, W.E., Plummer, L.N., McAda, D.P., Bexfield, L.M., and Anderholm, S.K., 2004b, Use of environmental tracers to estimate parameters for a predevelopment- ground-water-flow model of the Middle Rio Grande Basin, New Mexico: U.S. Geological Survey Water-Resources Investigations Report 03-4286, 102 p.
- Smith, G.A., and Kuhle, A.J., 1998, Hydrostratigraphic implications of new geological mapping in the Santo Domingo Basin, New Mexico: *New Mexico Geology*, v. 20, no. 1, p. 21–27.
- Stone, B.D., Allen, B.D., Mikolas, M., Hawley, J.W., Haneberg, W.C., Johnson, P.S., Allred, B., and Thorn, C.R., 1998, Preliminary lithostratigraphy, interpreted geophysical logs, and hydrogeologic characteristics of the 98th Street core hole, Albuquerque, New Mexico: U.S. Geological Survey Open-File Report 98-210, 82 p.
- Thomas, C.L., Stewart, A.E., and Constantz, J., 2000, Determination of infiltration and percolation rates along a reach of the Santa Fe River near La Bajada, New Mexico: U.S. Geological Survey Water-Resources Investigations Report 00-4141, 65 p.
- Thorn, C.R., McAda, D.P., and Kernodle, J.M., 1993, Geohydrologic framework and hydrologic conditions in the Albuquerque Basin, central New Mexico: U.S. Geological Survey Water-Resources Investigations Report 93-4149, 106 p.
- Thomas, C.L., and Thorn, C.R., 2000, Use of air-pressurized slug tests to estimate hydraulic conductivity at selected piezometers completed in the Santa Fe Group aquifer system, Albuquerque area, New Mexico: U.S. Geological Survey Water-Resources Investigations Report 00-4253, 19 p.
- Tiedeman, C.R., Kernodle, J.R., and McAda, D.P., 1998, Application of nonlinear-regression methods to a groundwater flow model of the Albuquerque Basin, New Mexico: U.S. Geological Survey Water-Resources Investigations Report 98-4172, 90 p.
- Titus, F.B., 1961, Ground-water geology of the Rio Grande trough in north-central New Mexico, with sections on the Jemez Caldera and Lucero Uplift, in Northrop, S.A., ed., *Guidebook of the Albuquerque country*: New Mexico Geological Society, 12th Field Conference, p. 186–192.

- Trainer, F.W., Rogers, R.J., and Sorey, M.L., 2000, Geothermal hydrology of Valles Caldera and the southwestern Jemez Mountains, New Mexico: U.S. Geological Survey Water-Resources Investigations Report 00-4067, 115 p.
- U.S. Census Bureau, 1970, Master reference file for 1970 census.
- U.S. Census Bureau, 1980, Master reference file for 1980 census.
- U.S. Census Bureau, 1990, Master reference file for 1990 census.
- U.S. Census Bureau, 2001a, Ranking tables in metropolitan areas—Population in 2000 and population change from 1990 to 2000 (PHC-T-3): accessed October 2006 at <http://www.census.gov/population/www/cen2000/phc-t3.html>
- U.S. Census Bureau, 2001b, Redistricting Census 2000 TIGER/Line files, accessed May 2006 at <http://rgisbeta.unm.edu/browsedata>
- U.S. Census Bureau, 2006, GCT-PH1. Population, housing units, area, and density: 2000 for New Mexico: accessed October 2006 at http://facffinder.census.gov/servlet/GCTTable?_bm=y&-context=gct&-ds_name=DEC_2000_SF1_U&-mt_name=DEC_2000_SF1_U_GCTPH1_ST7&-CONTEXT=gct&-tree_id=4001&-geo_id=04000US35&-format=ST-7|ST-7S&-_lang=en
- U.S. Environmental Protection Agency, 2005, South Valley, New Mexico: EPA ID# NMD 980745558: accessed October 2006 at <http://www.epa.gov/earth1r6/6sf/pdf/6sf/pdffiles/southval.pdf>.
- U.S. Environmental Protection Agency, 2006, National primary drinking water regulations:, accessed December 2006 at <http://www.epa.gov/safewater/contaminants/index.html>
- U.S. Geological Survey, Water Resources, 2010, National Water Information System, USGS surface water annual statistics for New Mexico, 1974–2009: U.S. Geological Survey database, accessed October 28, 2010, at URL http://waterdata.usgs.gov/nm/nwis/annual/?referred_module=sw&site_no=08330000&por_08330000_3=558903,00060,3,1942,2009&start_dt=1974&end_dt=2009&year_type=W&format=html_table&date_format=YYYY-MM-DD&rdb_compression=file&submitted_form=parameter_selection_list
- Veenhuis, J.E., 2002, Summary of flow loss between selected cross sections on the Rio Grande in and near Albuquerque, New Mexico: U.S. Geological Survey Water-Resources Investigations Report 93-4213, 17 p.
- Western Regional Climate Center, 2006a, Period of record monthly climate summary for Albuquerque WSFO Airport, New Mexico: accessed October 2006 at <http://www.wrcc.dri.edu/cgi-bin/cliMAIN.pl?nm0234>
- Western Regional Climate Center, 2006b, Period of record monthly climate summary for Sandia Crest, New Mexico: accessed October 2006 at <http://www.wrcc.dri.edu/cgi-bin/cliMAIN.pl?nm8011>
- Wilson, B.C., 1992, Water use by categories in New Mexico counties and river basins, and irrigated acreage in 1990: New Mexico State Engineer Technical Report 47, 141 p.
- Wilson, B.C., Lucero, A.A., Romero, J.T., and Romero, P.J., 2003, Water use by categories in New Mexico counties and river basins, and irrigated acreage in 2000: New Mexico State Engineer Office Technical Report 51, 164 p.